

**Chiral diphosphine ligands  
derived from  
1,4:3,6-dianhydro-D-mannitol:  
*synthesis, co-ordination  
to transition metals and  
catalytic applications.***

Thesis submitted for the degree of Doctor of  
Philosophy by:

**Cristina Carcedo Fernández**

Supervisor: Dr. Athanasia Dervisi  
Department of Chemistry  
Cardiff University  
June 2005

UMI Number: U584726

All rights reserved

INFORMATION TO ALL USERS

The quality of this reproduction is dependent upon the quality of the copy submitted.

In the unlikely event that the author did not send a complete manuscript and there are missing pages, these will be noted. Also, if material had to be removed, a note will indicate the deletion.



UMI U584726

Published by ProQuest LLC 2013. Copyright in the Dissertation held by the Author.  
Microform Edition © ProQuest LLC.

All rights reserved. This work is protected against  
unauthorized copying under Title 17, United States Code.



ProQuest LLC  
789 East Eisenhower Parkway  
P.O. Box 1346  
Ann Arbor, MI 48106-1346

## ACKNOWLEDGEMENTS

I would like to thank all those people who made this thesis possible and an enjoyable experience for me.

A special thanks goes to my supervisor Dr. Athanasia Dervisi for her encouragement and enthusiasm over the past three years. Also for giving me the chance to attend various national and international conferences, which in the case of Switzerland I will never forget (-17 °C...). I would also like to express my gratitude to Dr. Ian Fallis and Dr. Mike Coogan for their invaluable expertise and advice and also Dr. Liling Ooi and Dr. Abdul Malik for their effort with the X-ray crystallography data and Robert Jenkins for his help with the NMR data. I would like to thank Matthias Beller's group, St Andrew's University and Johnson Matthey for obtaining some results. Syntex (Johnson Matthey) are also greatly acknowledged for their financial support.

I would like to thank my lab mates, Despina and Simon who were very supportive and helpful. I would also like to thank my friends; Tomás, Benjamin, Javier, M<sup>a</sup> Angeles and little Teresa for all the fantastic lunches and dinners we have shared. To Monica and Emyr for their memorable teas together. To Ruth for sharing with me the trip to Switzerland and for being very helpful. To Maira and Elisenda for all their help and advice. To Pedro, Anabela, Ana Laura, Valente and little Cecilia for sharing with me all their cultural charms. To Marta for her on-line support. To Niels, Huw, Anne and little Tomos for being so special and to Thierry, Marie and little Amelié for being such a 'lovely' (with welsh accent) family.

A very special thanks goes to my boyfriend Rubén, to whom this thesis is dedicated. Thank you for being with me all these years and for giving me the opportunity to experience other cultures apart from the Burgos' one (la, le, li, lo, lu).

I wish to thank my 'welsh' family: the 'Mitchells and the 'Manjóns' for having always been there. And last but not least a big thanks to my family and Rubén's family. Their support and encouragement have always been very close even though they are very far (GRACIAS).

# INDEX

ABSTRACT	1
1. INTRODUCTION	
1.1 Phosphines	3
1.1.1 Steric Effects in Phosphine Ligands	5
1.1.2 Electronic Attributes of Phosphines	6
1.1.3 Bidentate phosphine ligands	7
1.2 Carbohydrate Phosphine Ligands	8
1.3 Isomannide: a sugar derived as a starting material	10
1.4 Chirality	11
1.5 Asymmetric catalysis	13
2 SYNTHESIS OF THE PHOSPHINE LIGAND: ddppm	
2.1 INTRODUCTION	18
2.2 DISCUSSION	21
2.2.1 Precursors for the synthesis of ddppm:	
a) 1,4:3,6-dianhydro-2,5-di-O-mesyl-D-mannitol:	21
b) 1,4:3,6-dianhydro-2,5-dichloride-D-iditol:	23
c) 1,4:3,6-dianhydro-2,5-dibromide-D-iditol:	23
2.2.2 Synthesis of Alkali Metal diphenylphosphide	26
2.2.3 Reactions of precursors with lithium diphenylphosphide	28
2.2.4 Synthesis of a preformed borane complex of lithium diphenylphosphide	30
2.2.5 Best method for the synthesis of ddppm	31
2.3 CONCLUSIONS	37
2.4 EXPERIMENTAL	37
3. Cu-, Pt- and Pd-ddppm complexes and their catalytic applications: carbonylation and allylic reactions	
3.1 INTRODUCTION	45
3.2 RESULTS AND DISCUSSTION	45
3.2.1 Synthesis and characterization of Copper complexes with ddppm	45
3.2.2 Synthesis and characterization of the platinum complex Pt(ddppm)Cl <sub>2</sub>	49
3.2.3 Synthesis and characterization of palladium complexes with ddppm	53

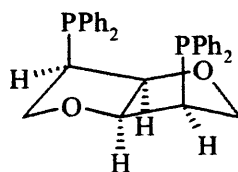


3.2.3.1	Synthesis of Pd(ddppm)Cl <sub>2</sub> .....	53
3.2.3.2	Synthesis of [Pd(ddppm)( $\eta^3$ -C <sub>3</sub> H <sub>5</sub> )]PF <sub>6</sub> .....	57
3.3	PALLADIUM CATALYZED REACTIONS.....	65
3.3.1	C-C coupling reactions: Sonagashira reaction.....	65
3.3.2	Carbonylation of Aryl-halide compounds.....	67
3.3.3	Hydroesterification of styrene.....	70
3.3.4	Catalytic carbonylation of benzylic substrates.....	74
3.3.5	Allylic alkylation and allylic amination reactions.....	77
3.4	CONCLUSIONS.....	84
3.5	EXPERIMENTAL.....	85
4	Rh- and Ru-ddppm complexes and their catalytic applications: hydrogenation and hydroformylation.	
4.1	INTRODUCTION.....	98
4.2	RESULTS AND DISCUSSION.....	99
4.2.1	Synthesis and characterization of rhodium complexes with ddppm.....	99
4.2.2	Synthesis and characterization of Ruthenium complexes with ddppm.....	103
4.2.3	Enantioselective hydrogenation reactions of olefins.....	106
4.2.4	Enantioselective hydrogenation reactions of ketones.....	113
4.2.5	Asymmetric hydroformylation.....	116
4.3	CONCLUSIONS.....	120
4.4	EXPERIMENTAL.....	121
5	Ir-ddppm complexes and their catalytic applications: enantioselective hydrogenation of imines.	
5.1	INTRODUCTION.....	132
5.2	RESULTS AND DISCUSSION.....	133
5.2.1	Synthesis and characterization of Iridium complexes with ddppm.....	133
5.2.2	Enantioselective hydrogenation of imines.....	137
5.2.3	Iridium-ddppm hydride complexes.....	147
5.3	CONCLUSIONS.....	150
5.4	EXPERIMENTAL.....	151

APPENDIX 1: Crystallographic data (CIF files) on CD at the back of the thesis.

## ABSTRACT

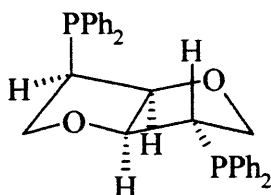
The synthesis of a new chiral diphosphine, 1,4:3,6-dianhydro-2,5-bis(diphenylphosphino)-D-mannitol (**ddppm**) is reported. **ddppm** is derived from the commercially available  $C_2$ -symmetric 1,4:3,6-dianhydro-D-mannitol (Isomannide). This new ligand exhibits a bend butterfly-like geometry with the two-phosphine groups on the concave side.



**ddppm**

The chelating ability of **ddppm** is demonstrated with the synthesis of several complexes with transition metals such as Cu, Pd, Pt, Rh, Ru and Ir. Some of these complexes have been successfully crystallized and tested in different catalytic reactions. These complexes have been characterized and their properties are reported. Their ability to catalyse a range of reactions is also discussed in detail.

Chapter 2 reports the synthesis of **ddppm**. This synthesis requires only two steps with the choice of the solvent being crucial for the formation of this ligand. **ddppg**, an epimer of **ddppm**, was also isolated as a by-product from the **ddppm** synthesis. This diphosphine is a non-chelating ligand unlike **ddppm**. Crystal structures of both isomers are shown in this chapter.



**ddppg**: 1,4:3,6-dianhydro-2,5-bis(diphenylphosphino)-D-glucitol

# *Chapter 1*

# 1. INTRODUCTION

The aims of this project are to synthesize transition metal complexes with a chiral bidentate phosphine derived from D-Isomannide and then use these complexes in homogenous catalysis. In the next sections, terms like phosphines, chirality and asymmetric catalysis are explained in some detail and examples of other carbohydrate phosphine ligands are presented. The structure and properties of the D-isomannide are discussed and some of its applications reported.

## 1.1 PHOSPHINES

Phosphines ( $\text{PR}_3$ ) are amongst one of the most important class of ligands. Together with other phosphorus-containing ligands and related compounds of arsenic and antimony, phosphines parallel the CO ligand in many ways. Like CO, phosphines are  $\sigma$  donors (via a hybrid orbital containing a lone pair on phosphorus) and  $\pi$  acceptors. For many years it was thought that empty 3d orbitals of phosphorus functioned as the acceptor orbitals<sup>1</sup>, as shown in Figure 1.1.

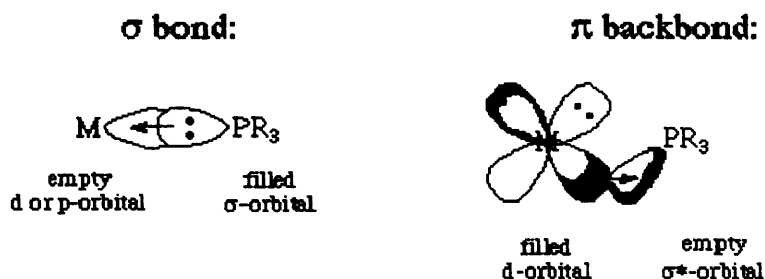
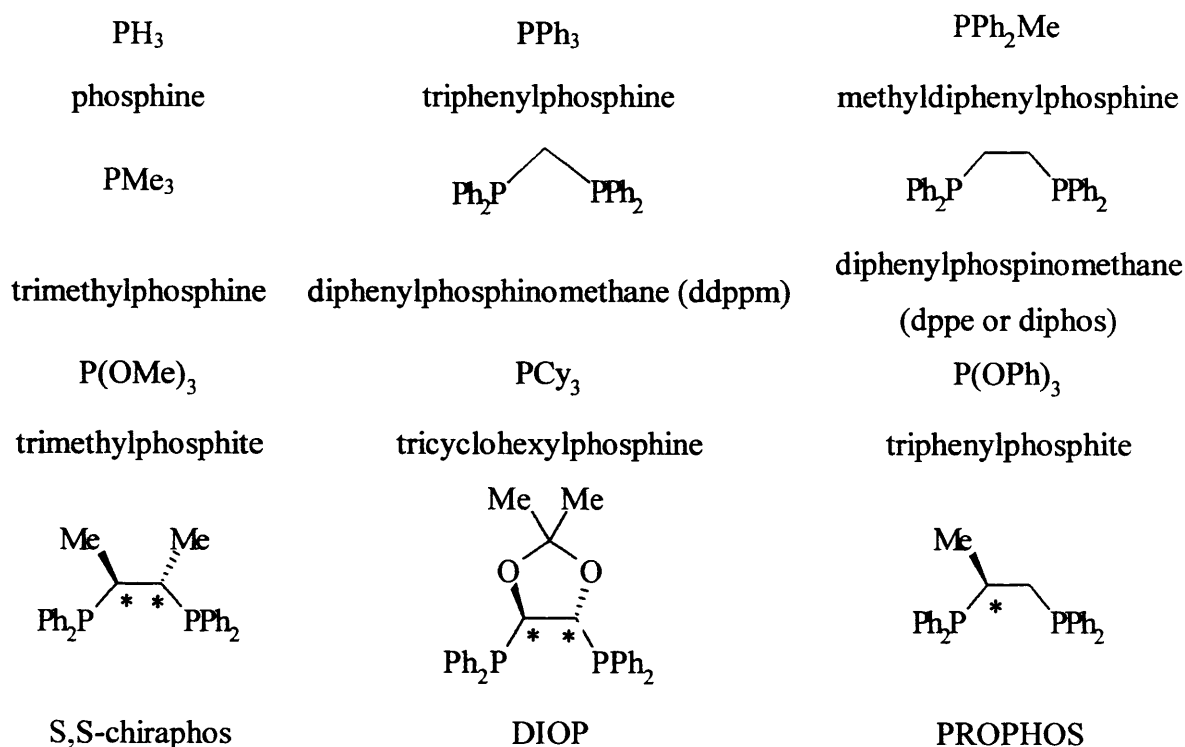


Figure 1.1: Bonding in phosphines

By this view, as the R groups attached to phosphorus become more electronegative, they withdraw electrons from phosphorus, making the phosphorus more positive and better able to accept electrons from the metal via a d orbital. The nature of R groups, therefore, determines the relative donor/acceptor ability of the ligand.  $\text{P}(\text{CH}_3)_3$  for example, is a strong  $\sigma$  donor due to the electron releasing.

Tertiary phosphine ligands have the general formula  $\text{PR}_3$  where R = alkyl, aryl, H, halide etc. Closely related are phosphite ligands which have the general formula  $\text{P}(\text{OR})_3$ . Both play an important role in the coordination chemistry of late transition elements. Furthermore, a variety of chiral phosphine transition metal complexes have been synthesized; these phosphine-metal complexes are stereogenic and can function as stereospecific catalysts. There are many examples of these kinds of ligands, some of which are shown in scheme 1.1:



**Scheme 1.1:** Examples of common phosphines and phosphites.

### 1.1.1 Steric Effects in Phosphine Ligands

The steric attributes of the phosphine ligand are easily controlled. This ability to control the bulk of the ligand permits one to tune the reactivity of the metal complex. The steric bulk can be measured using Tolman's cone angle<sup>2</sup> (Fig. 1.2). The cone containing the ligand and the metal as a vertex can be physically measured. The wider the angle of the cone the greater the steric influence of the ligand. A cone angle of 180 degrees would indicate that the ligand effectively covers one half of the coordination sphere of the metal complex:

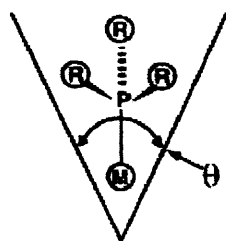


**Figure 1.2:** Tolman's cone angle

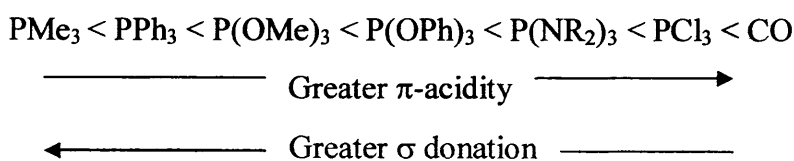
However if there is a great deal of steric congestion in a molecule, the cone angle may not be a realistic measure of the amount of space occupied by the substituents as two adjacent groups can mesh to relieve steric strain. Therefore, the solid angle was introduced to quantify steric effects in both organic and organometallic chemistry. Solid angles contain information about the shape of a substituent. In broad terms, if the cone angle represents a maximum measure of the steric influence of a substituent, the solid angle represents its minimum.<sup>3</sup>

### 1.1.2 Electronic Attributes of Phosphines

The bonding in phosphine ligands, like that of carbonyls can be thought of as having two important components. The primary component is sigma donation of the phosphine lone pair to an empty orbital on the metal. The second component is backdonation from a filled metal orbital to an empty orbital on the phosphine ligand. This empty phosphorus orbital has been described as being either a d-orbital or an antibonding sigma orbital; current consensus is that the latter is more appropriate given the relatively high energy of a phosphorous d-orbital (see Figure 1.1).

As electron-withdrawing (electronegative) groups are placed on the phosphorous atom, the sigma-donating capacity of the phosphine ligand tends to decrease. At the same time, the energy of the  $\pi$ -acceptor ( $\sigma^*$ ) on phosphorous is lowered in energy, providing an increase in backbonding ability. Therefore, phosphines can exhibit a range of sigma donor and  $\pi$ -acceptor capabilities and the electronic properties of a metal centre can be tuned by the substitution of electronically different but isosteric phosphines.

A rough ordering of the  $\pi$ -accepting or  $\sigma$ -donating capabilities of phosphines can be accomplished by synthesizing a series of complexes in which the only difference is the nature of the phosphine ligand. If these complexes contain a carbonyl ligand, then the CO stretching frequency can be used as an indicator of electron density at the metal (the lower the value of the CO stretching frequency, the greater the backbonding to the metal and thus the higher the electron density at the metal). Experiments such as this permit us to come up with the following empirical ordering:



### 1.1.3 Bidentate phosphine ligands

While Tolman's cone angle concept is commonly used for monodentate ligands, the extension to bidentate ligands appears to be less straightforward. Diphosphine ligands, however, offer more control over regio- and stereo- selectivity in many catalytic reactions. The main difference between mono- and bi-dentate ligands is the ligand backbone, a scaffolding which keeps two phosphorus donor atoms at a specific distance. The distance is ligand specific and, together with the flexibility of the backbone, an important characteristic of a ligand. A standardised bite angle, with defined M-P bond lengths and a 'metal' atom that does not prefer any specific P-M-P angle would appear to be the most convenient way of comparing bidentate ligands systematically.

The ligand bite angle is a property that can be calculated from a series of crystal structures or from molecular modelling. Systematic searches in the Cambridge Crystallographic database show that the P-M-P angles concentrate in narrow ranges for most transition metal complexes containing (P-P)M fragments. The ligand bite angle correlates with various spectroscopic properties of metal-diphosphine complexes and with the regio- or stereo- selectivity in a variety of catalytic reactions. In rhodium catalysed hydroformylation reactions, ligands with bite angles  $>100^\circ$  favour the formation of linear aldehydes. In many palladium catalysed reactions ligands such as dppf or dppp with bite angles around  $100^\circ$  give the best results in terms of activity and selectivity. In the case of palladium this can be explained by transition states between (four-co-ordinate) palladium (II) species with P-Pd-P angles around  $90^\circ$  and two or three-co-ordinate palladium(0) species with P-Pd-P angles of probably  $120\text{-}180^\circ$ . Although the hypothesis will have to be substantiated, there is an optimum bite angle for many catalytic systems.<sup>4</sup>



## 1.2 CARBOHYDRATE PHOSPHINE LIGANDS

Carbohydrates are naturally enantiomeric pure compounds which have an interesting stereochemical variety. Apart from their biological role, they are also significant chiral auxiliaries for enantioselective organic synthesis. The carbohydrate-metal interactions are of interest in metal-catalysed enantioselective synthesis. Modification of these ligands leads to high activity and selectivity in many metal-catalysed processes. Because homogeneous catalysis is one of the most important methods for preparing enantiomerically pure compounds carbohydrate derivatives have been increasingly used as chiral ligands in the last decade. Carbohydrates are readily available, highly functionalised compounds with several stereogenic centres and contain several weak donor sites. Since many of the catalytic precursors in homogeneous catalysis are coordination complexes of the platinum-group metals, the required ligands should have such donor atoms as N, S and P which can form stable complexes with almost all transition metals.

Bidentate phosphines are considered to be excellent ligands for transition metal asymmetric catalysis.<sup>5</sup> These chelating ligands are supposed to be superior because of the resulting rigid catalysts which favour effective chiral induction.<sup>6</sup>

In the beginning, diphosphines derived from carbohydrates were used in the metal-catalysed asymmetric hydrogenation of several prochiral olefins. Some examples are presented in the following Figure 1.3. In general, enantioselectivities were low to moderate. For example, enantioselectivities were best with ligands **3<sub>I</sub>** and **4<sub>I</sub>** in the Rh-hydrogenation of acetamidoacrylic acid and *Z*- $\alpha$ -acetamidocinnamic acid, 86% and 73% respectively.<sup>7</sup>

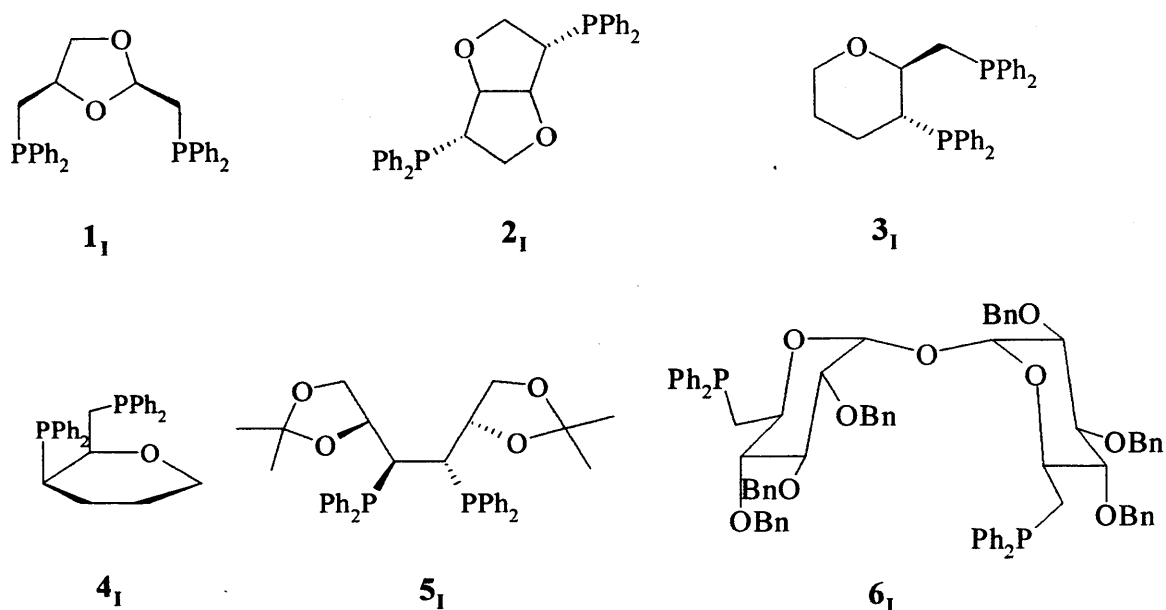
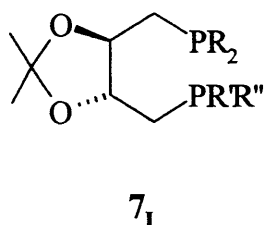


**Figure 1.3:** Diphosphines derived from carbohydrates.

One of the main limitations of using natural products as precursors of ligands is that often only one of the enantiomers (in the case of carbohydrates, the D-series) is readily available. However this limitation can be overcome by suitably adjusting the ligand structure. For example, the use of different derivatives of ligand  $7_I$  in the Rh- catalysed asymmetric hydrogenation of dehydroamino acids, itaconates and enamides led to similar enantioselectivities but a reversed absolute configuration to that obtained with the DIOP ligand.<sup>8</sup>



$\text{R}=\text{R}'=\text{R}''=\text{Ph}$ , **DIOP**  
 $\text{R}=\text{R}'=\text{Ph}$ ;  $\text{R}''=\text{Cy}$   
 $\text{R}=\text{R}'=\text{R}''=\text{Fc}$   
 $\text{R}=\text{Fc}$ ;  $\text{R}'=\text{R}''=\text{Cy}$   
 $\text{R}=\text{Fc}$ ;  $\text{R}'=\text{R}''=\text{Ph}$

### 1.3 ISOMANNIDE: A SUGAR DERIVED AS A STARTING MATERIAL.

1,4:3,6-Dianhydro-D-mannitol (D-Isomannide, Figure 1.4) can be prepared by dehydration of D-mannitol and was described for the first time in 1882 by Fauconnier<sup>9</sup> and its structure was elucidated in 1945 by Fletcher and Wiggins.<sup>10,11</sup> Unexpectedly, there are very few reports on its synthetic application as a significant commercially available chiral pool compound.

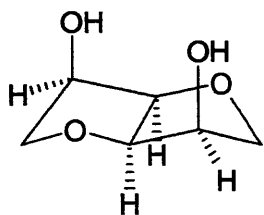


**Figure 1.4:** D-Isomannide: 1,4:3,6-Dianhydro-D-mannitol

An important structural characteristic of D-Isomannide is that its molecule consists of two fused furan rings, with the two-hydroxyl groups occupying the *endo* positions relative to the internal chiral cavity. Thanks to this feature, bis-P(III)-phosphorylated derivatives of D-Isomannide (figure 1.5) are of interest as bidentate ligands with the two chelating P(III) atoms located on a bulky chiral matrix.<sup>12</sup> As an example, monophosphite and diphosphite ligands derived from D-isomannide have been synthesized and used in Rh-catalyzed hydrogenation reactions giving high enantioselectivities.<sup>13</sup>

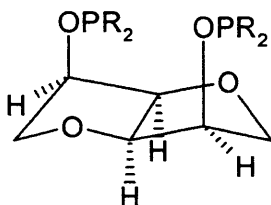


**Figure 1.5:** Bis-phosphorylated D-isomannide derivatives

D-isomannide has also been transformed into the corresponding *exo*-diphosphine (Figure 1.6), which was investigated as a homochiral ligand in the Rh-catalysed asymmetric hydrogenation of N-acyl- $\alpha$ -aminoacrylate esters, with rather poor enantioselectivity.<sup>14</sup>

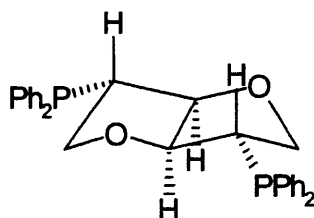


**Figure 1.6:** 1,4:3,6-dianhydro-2,5-dideoxy-2,5-bis(diphenylphosphino)-L-iditol (**ddppi**).

Furthermore, D-isomannide has been used successfully as a chiral auxiliary in the stereoselective synthesis of tertiary  $\alpha$ -hydroxy acids,<sup>15</sup> in aldehyde-alkene cyclizations via O-stannyl ketyl radicals,<sup>16</sup> and in asymmetric Diels-Alder reactions with novel homochiral bis-imine Cu(II)-catalysts.<sup>17</sup>

## 1.4 CHIRALITY

The bidentate phosphine ligand we want to synthesize is the isomer of the phosphine mentioned before, the *endo*-isomer of the diphosphine **ddppi** (Figure 1.6). Once this diphosphine is synthesized the transition metal complexes formed will be used in homogeneous catalysis.

As chirality plays a central role in asymmetric catalysis its meaning should be explained. A wide range of significant physical and biological functions are generated through precise molecular recognition which requires strict matching of chirality. For a long time access to highly enantiomerically pure compounds, at least in a practical sense,

was thought to be Nature's monopoly and was indeed accomplished by biological or biochemical transformations. Efficient creation of optically active organic molecules from pro-chiral compounds by chemical means, though it is challenging, has remained difficult, and only optical resolution and structural modification of naturally occurring chiral substances have provided complements in this respect. However, assiduous efforts made by synthetic chemists in the last two decades are converting the chemists' dream into reality. In order to maximize synthetic efficiency, 'multiplication of chirality', namely, stereoselective production of a large quantity of a chiral target compound utilizing a catalytic amount of chiral source, is obviously desirable. Enantioselective catalysis using chiral metal complexes, among various possibilities, provides one of the most general, flexible methods for this purpose.

Metallic elements possess a variety of catalytic activities, and permutation of organic ligands or auxiliaries directing the steric course of the reaction is practically unlimited. Accordingly, in principle, one can generate any dynamic properties at will through molecular architecture using accumulated chemical knowledge. To this end, creation of a single, highly reactive catalytic species possessing excellent chiral recognition ability is required. Besides the choice of central metals therefore, molecular design of the chiral modifiers is a particularly significant task. The efficient ligands must be gifted with a suitable functionality; an appropriate element of symmetry; substituents capable of differentiating space either sterically or electronically; skeletal rigidity or flexibility (depending on the nature of the reaction), etc.-all of which contribute to accomplish highly enantioselective catalysis.<sup>18</sup>

In 1966 Nozaki et al., explained the first example of asymmetric synthesis from chiral compounds catalysed by homogeneous chiral metal complexes. A chiral Schiff base-Cu(II) complex (Figure 1.7) was found to catalyse decomposition of ethyl diazoacetate in styrene to give *cis*- and *trans*-2-phenylcyclopropanecarboxylates in <10% ee.

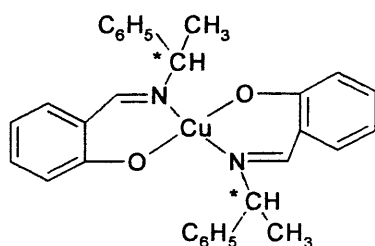


**Figure 1.7:** Cu prochiral catalyst

## 1.5 ASYMMETRIC CATALYSIS.

During the last 30 years, industrial organic chemistry has been based mainly on petroleum products, and most petrochemical processes use heterogeneous rather than homogeneous catalysts. This is principally because heterogeneous catalysts are generally more stable at higher temperatures and is less difficult to separate from the substrate phase. However, there is an increasing interest in homogeneous catalysts because they often show higher selectivity and greater catalytic activity, and they also provide greater control of temperature on the catalyst site. For some commercial processes it has been determined that these advantages of soluble catalysts balance the economic problems associated with catalyst recovery.

The ultimate application of high selectivities concerns the development of catalysts for the synthesis of chiral compounds with high degrees of enantioselectivity. The need for

chiral specificity in bioactive products reflects the fact that most enzymes have natural chirality. As a consequence, attempts to manipulate biological systems through therapeutic drugs or aroma enhancers often involve use of chemicals containing chiral centres. The desired biological activity is usually associated with only one of the two stereoisomers of a chiral compound. In the extreme case, exemplified by thalidomide, one optical isomer is therapeutic and the other has serious undesired biological consequences (teratogenicity). To improve product safety, the pharmaceutical industry is producing an increasing number of products in enantiomerically pure form and it is only a matter of time before legislation will require this as regular requirement.

In the past many attempts to effect, for example, asymmetric catalytic hydrogenation led to products with disappointingly low enantiomeric excesses (*ee*'s). This was undoubtedly a consequence of the complex nature of the surfaces of the heterogeneous catalyst, containing many types of reactive sites, that were used initially. Developments in organometallic chemistry and homogeneous catalysis have been instrumental in improving this situation beyond recognition. The discovery in the mid-1960s that L-3,4-dihydroxyphenylalanine (L-dopa) was effective in the treatment of Parkinson's disease created a sudden demand for this rather rare amino acid. This coincided with the discovery of Wilkinson's catalyst,  $\text{RhCl(PPh}_3)_3$ , which opened up the possibility of selective hydrogenation of unsaturated hydrocarbons under mild reaction conditions. These developments, coupled with interest in the development of synthetic routes to organophosphines containing an increasingly wide range of constituents, enabled access to the possibility of catalytic asymmetric hydrogenation, simply by the substitution of  $\text{PPh}_3$  with a chiral phosphine ligand.

Asymmetric induction can be achieved in many reactions catalysed by transition metal complexes but the first commercial application introduced in 1974, was in fact the Monsanto synthesis of L-dopa. This represented not only an attraction in industrial asymmetric synthesis, but also provided a great incentive for research into additional applications of homogeneous catalysis for the synthesis of fine chemicals. Even so, relatively few homogeneous enantioselective catalysts have been commercialized to date.<sup>19</sup> Representative examples of applications in fine chemicals manufacture are summarized in Table 1.1.

**Table 1.1:** Some commercial applications of homogenous catalysis in the manufacture of fine chemicals.

<i>Reaction</i>	<i>Catalyst</i>	<i>Product</i>	<i>Use</i>
Hydroformylation	Rh	Vitamin A	Natural product
Hydrocarboxylation	Pd	Ibuprofen	Pharmaceutical
Hydrogenation of enamides	Rh/DIPAMP	L-dopa	Pharmaceutical
		L-phenylalanine	Food additive
Isomerization of allylic amine	Rh/BINAP	L-menthol	Aroma and flavour chemical
Epoxidation of allylic alcohol	Ti(Opr <sup>t</sup> ) <sub>4</sub> /Bu <sup>t</sup> OOH di-iso-propyl tartrate	Disparlure	Insect attractant
		Glucidol	intermediate
Cyclopropanation	Cu/chiral base	Schiff Cilastatin	pharmaceutical

These are not exhaustive, but have been selected to illustrate both the range of catalytic reactions, e.g. hydroformylation, hydrogenation, isomerization, epoxidation and cyclopropanation, and their importance in key enabling reaction steps in the manufacture of specific products.



The essential feature for selective synthesis of one optical isomer of a chiral substance is an asymmetric site that will bind a pro-chiral olefin preferentially in one conformation. The recognition of the preferred conformation can be accomplished by the use of a chiral ligand coordinated to the metal, the ligand creating what is effectively a chiral hole within the coordination sphere. An important factor in the successful application of homogeneous asymmetric catalysts has been the design and development of a range of chiral, usually bidentate, phosphine ligands, especially those having  $C_2$ -symmetry, for use with different metal centres.

In the next chapter the synthesis of the new chiral diphosphine ligand with  $C_2$ -symmetry derived from the sugar: D-Isomannide is described.

---

<sup>1</sup> Gary O. Spessard, Gary L. Miessler, *Organometallic Chemistry*, St. Olaf College, Northfield, Minnesota, 1996.

<sup>2</sup> C. A. Tolman, *Chem. Rev.*, 1977, 77, 313.

<sup>3</sup> D. P. White, J.C. Anthony.; *J. Org. Chem.*, 1999, 64, 7707-7716.

<sup>4</sup> P. Dierkes, P.W.N. Leeuwen; *J. Chem. Soc., Dalton Trans.*, 1999, 1519-1529.

<sup>5</sup> (a) R. Noyori (Ed.), *Asymmetric Catalysis in Organic Synthesis*. Wiley, New York, 1994.  
(b) I. Ojima (Ed.), *Catalytic Asymmetric Synthesis*, Wiley, New York, 2000.

<sup>6</sup> (a) M.J. Burk, F. Bienewald, in: M. Beller, C. Bolm (Eds.), *Transition Metal for Organic Synthesis*, Wiley, New York, 1998. (b) W. N. Jacobsen, A. Pfaltz, H. Yamamoto (Eds.), *Comprehensive Asymmetric Catalysis*, Springer, Berlin, 1999.

<sup>7</sup> M. Dieguez, O. Pamies, A. Ruiz, Y. Diaz, S. Castillon and C. Claver, *Coord. Chem. Rev.*, 2004, 248, 2165-2192.

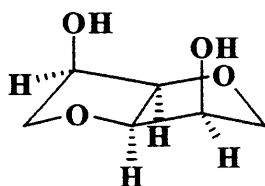
- 
- <sup>8</sup> M. Dieguez, O. Pamies and C. Claver, *Chem. Rev.* 2004, 104, 3189-3215.
- <sup>9</sup> A.C. R. Fauconnier, *Acad. Sci.* 1882, 95, 991; (b) A. Fauconnier, *Bull. Soc. Chim. Fr.* 1884, 41, 119.
- <sup>10</sup> R. C. Hockett, H. G. Fletcher, E. L. Sheffield, R. M. Goepp, S. J. Soltzberg, *J. Am. Chem. Soc.* 1946, 68, 930.
- <sup>11</sup> (a) L. F. Wiggins, *J. Chem. Soc.* 1945, 4; (b) L. F. Wiggins, R. Montgomery, *Nature* 1946, 157, 372; (c) R. Montgomery, L. F. Wiggins, *J. Am. Chem. Soc.* 1946, 68, 390.
- <sup>12</sup> (a) M. K. Grachev, N. O. Soboleva, G. I. Kurochkina, *Russian Journal of General Chemistry*, 2003, 73 (6), 903-908. (b) M.K. Grachev, G.I. Kurochkina, N.O. Soboleva, *Russian Journal of General Chemistry*, 2002, 72 (11), 1813-1819. (c) M. K. Crachev, K.L. Anfilov, A. R. Bekker, and E. E. Nifant'ev, *Russian journal of General Chemistry*, 1995, 65 (12), 1785-1789.
- <sup>13</sup> (a) M. T. Reetz and T. Neugebauer, *Angew. Chem. Int. Ed.* 1999, 38 (1-2), 179-181; (b) M. T. Reetz and G. Mehler, *Angew. Chem. Int. Ed.* 2000, 39 (21), 3889-3890.
- <sup>14</sup> J. Bakos, B. Heil, L. Markó, *J. Organomet. Chem.*, 1983, 253, 249-252.
- <sup>15</sup> A. Loupy and D. A. Monteux, *Tetrahedron*, 2002, 58, 1541-1549.
- <sup>16</sup> E. J. Enholm, F. Allais and S. Bareyt, *Tetrahedron: Asymmetry*, 2003, 14, 2871-2874.
- <sup>17</sup> G. de Coster, K. Vandyck, *Tetrahedron Asymmetry* 13 (2002), 1673-1679.
- <sup>18</sup> Noyori, R., *Chem. Soc. Rev.* 1989, 18, 187.
- <sup>19</sup> R. Whyman, *Applied Organometallic Chemistry and Catalysis*, Oxford University press, 2001.

# ***Chapter 2***

## 2 SYNTHESIS OF THE PHOSPHINE LIGAND: ddppm.

### 2.1 INTRODUCTION

Although D-isomannide **1** was first described in 1882 by Fauconnier<sup>1</sup> and its structure was elucidated in 1945 by Fletcher<sup>2</sup> and Wiggings<sup>3</sup>, reports on its synthetic applications as a commercially available chiral auxiliary are remarkably scarce. D-isomannide has been used successfully as a building block for (-)-*endo*- and (-)-*exo*-Brevicommin and (+)-Dodecanolide which are insect pheromones<sup>4</sup> and it has been employed as starting material for the synthesis of novel bicyclic dideoxynucleosides, which are potential antiviral agents.<sup>5</sup>



**1:** D-Isomannide: 1,4:3,6-dianhydro-D-mannitol

Synthetic applications of D-Isomannide have been so far limited even more for *endo* derivatives. This is probably due to difficulties encountered in S<sub>N</sub>2 type substitutions of leaving groups in the *exo* positions of the two cis fused tetrahydrofuran rings, which lead to the relatively hindered *endo* products (the *endo* and *exo* prefixes here refer to the bend V-shape of the two fused furan rings).

An *endo*-diimine isomannide derivative (Figure 2.1) has been previously reported and used in catalytic asymmetric Diels-Alder reactions. The synthesis of this compound was readily accessible from its diamine, which is prepared from D-isomannide in five steps.<sup>6</sup>

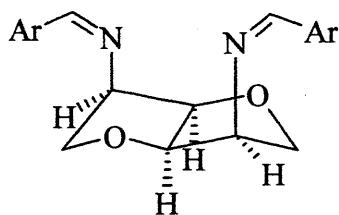


**Figure 2.1:** *endo*-diimine isomannide derivative.

Monophosphite and diphosphite ligands derived from D-isomannide (Figure. 2.2) have also been synthesized and used in Rh-catalyzed hydrogenation reactions giving high enantioselectivities.<sup>7</sup>

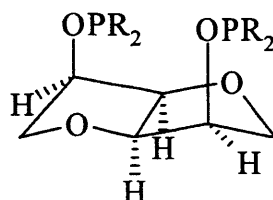
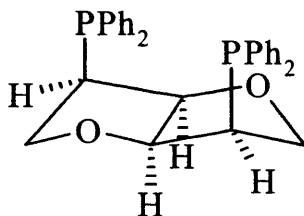


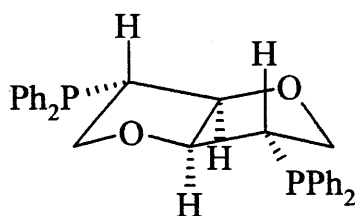
**Figure 2.2:** Bis-Phosphorylated D-isomannide derivatives

One of our main aims was to synthesize the *endo*-diphosphine derived from D-Isomannide (**ddppm**). This diphosphine with the two phosphine groups in position *endo* is interesting because it can be an efficient bidentate ligand residing in a chiral matrix with distinct geometric parameters specified between chelating P(III) atoms.



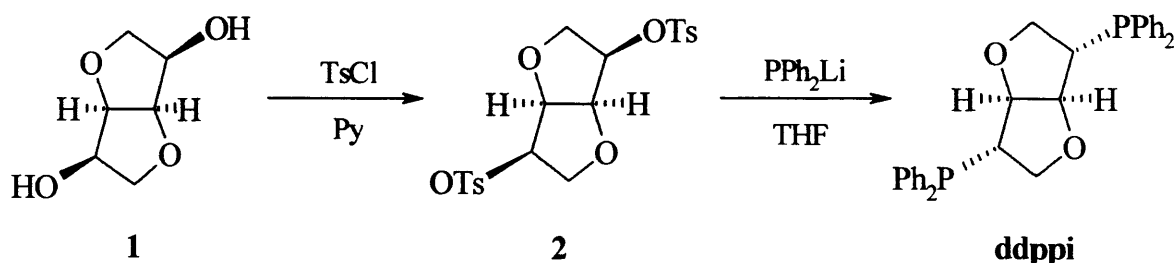
**ddppm:** 1,4:3,6-dianhydro-2,5-dideoxy-2,5-bis(diphenylphosphino)-D-mannitol

The corresponding *exo*-diphosphine (**ddppi**) with the two phosphine groups outside the concave side, has been previously reported.<sup>8</sup> **ddppi** stands for the name of 1,4:3,6-dianhydro-2,5-dideoxy-2,5-bis(diphenylphosphino)-L-idoitol and it is a non-chelating ligand. It has been used as a catalyst in various asymmetric reactions including hydrogenation of  $\alpha$ -acylamido cinnamate esters with moderate enantioselectivities and asymmetric carbonylation.<sup>9</sup> Among these applications it has also been used for copolymerisation of carbon monoxide with functional olefins<sup>10</sup> and asymmetric hydroesterification of styrene.<sup>11</sup>



**ddppi**: 1,4:3,6-dianhydro-2,5-dideoxy-2,5-bis(diphenylphosphino)-L-idoitol.

**ddppi** was synthesised in two simple steps. Treatment of D-isomannide **1** with *p*-toluenesulfonyl chloride in dry pyridine afforded 1,4:3,6-dianhydro-2,5-di-*o*-(*p*-toluenesulfonyl)-D-mannitol **2**. Nucleophilic displacement of the *p*-toluene sulfonate groups of **2** with lithium diphenylphosphide in tetrahydrofuran gave **ddppi** with good yield (see Scheme 2.1).



**Scheme 2.1:** Conditions and reagents: (a) TsCl, Pyridine, 0°C, 4 h; (b) LiPPh<sub>2</sub>, THF.

To synthesize its isomer, **ddppm**, several attempts have been tried. In the next section, the synthesis of some precursors with different leaving groups and the reactions to synthesize this diphosphine are discussed.

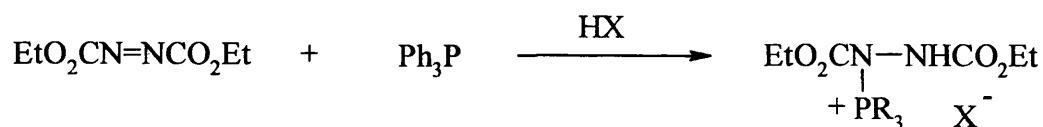
## 2.2 DISCUSSION

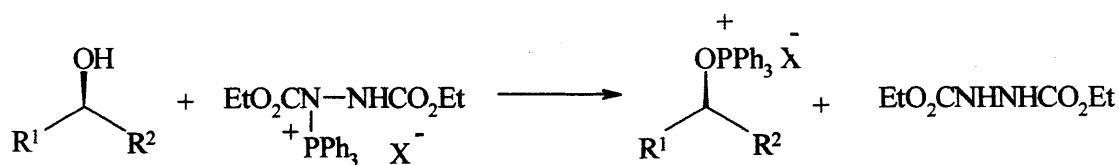
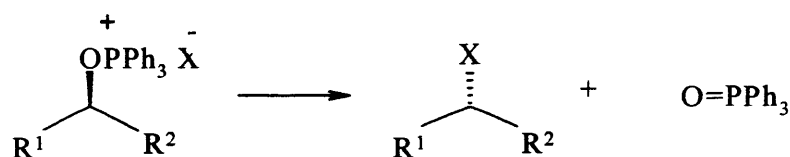
### 2.2.1 Precursors for the synthesis of ddppm:

#### a) 1,4:3,6-dianhydro-2,5-di-O-mesyl-D-mannitol:

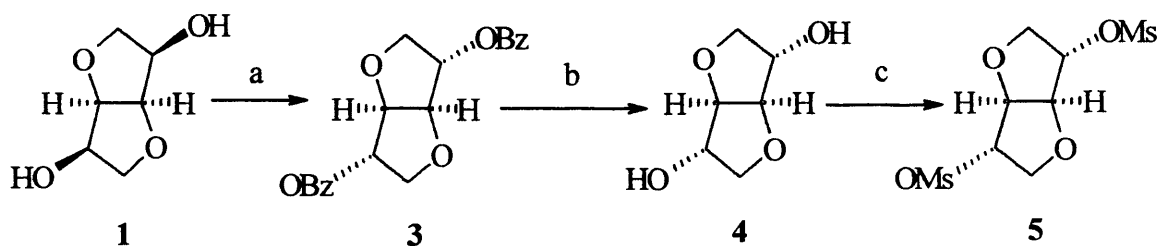
First of all, the Mitsunobu reaction was tried in order to synthesize the precursor 1,4:3,6-dianhydro-2,5-di-O-mesyl-D-mannitol. Mitsunobu<sup>12</sup> in his 1981 review proposed that the dehydration reactions of alcohols using diethyl azodicarboxylate (DEAD) and triphenylphosphine (Ph<sub>3</sub>P) proceed in three steps: (a) reaction of Ph<sub>3</sub>P in the presence of the acid component to form a salt wherein a phosphorus-nitrogen bond is formed; (b) reaction of the DEAD-Ph<sub>3</sub>P adduct with the alcohol to form an activated oxyphosphonium ion intermediate; and (c) displacement via a S<sub>N</sub>2 process to form the inverted product and the phosphine oxide. The mechanism of each step is discussed in following Scheme 2.2:

#### Step a: Adduct Formation



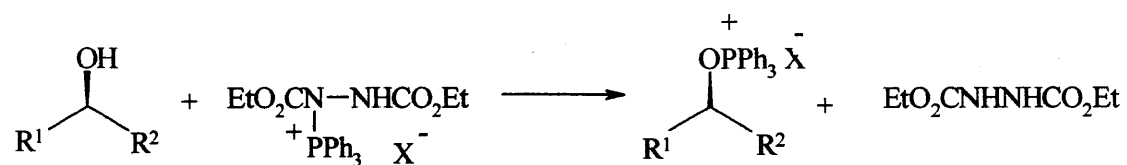
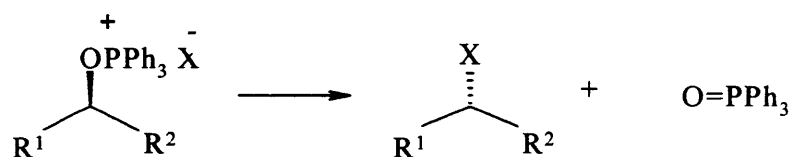
**Step b: Alcohol Activation****Step c: S<sub>N</sub>2 Reaction****Scheme 2.2:** Intermediates formed in Mitsunobu reaction.

Mitsunobu inversion of D-isomannide **1** and subsequent cleavage of the dibenzoate ester **3** afforded 1,4:3,6-dianhydro-L-iditol **4**, which was easily transformed into 1,4:3,6-dianhydro-2,5-di-O-mesyl-L-iditol **5** with mesyl chloride in pyridine at  $-10^\circ\text{C}$ . (See Scheme 2.3).

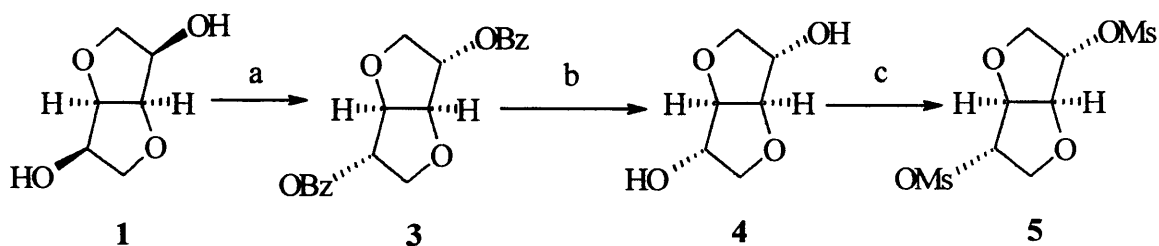


**Scheme 2.3:** Conditions and reagents: (a) DIAD, Ph<sub>3</sub>P, PhCOOH, THF, 25 °C; (b) NaOH, MeOH, 80 °C, 24 h; (c) MsCl, pyridine,  $-10^\circ\text{C}$ , 24 h.



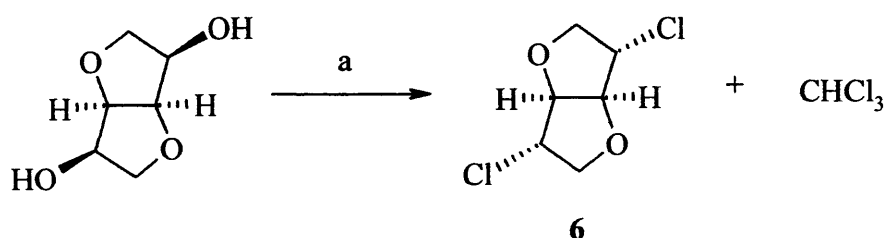
**Step b: Alcohol Activation****Step c: S<sub>N</sub>2 Reaction****Scheme 2.2:** Intermediates formed in Mitsunobu reaction.

Mitsunobu inversion of D-isomannide **1** and subsequent cleavage of the dibenzoate ester **3** afforded 1,4:3,6-dianhydro-L-iditol **4**, which was easily transformed into 1,4:3,6-dianhydro-2,5-di-O-mesyl-L-iditol **5** with mesyl chloride in pyridine at  $-10^\circ\text{C}$ . (See Scheme 2.3).

**Scheme 2.3:** Conditions and reagents: (a) DIAD, Ph<sub>3</sub>P, PhCOOH, THF, 25 °C; (b) NaOH, MeOH, 80 °C, 24 h; (c) MsCl, pyridine,  $-10^\circ\text{C}$ , 24 h.

**b) 1,4:3,6-dianhydro-2,5-dichloride-D-itol:**

Halides from D-isomannide **1** have been studied since 1945 obtaining very poor yield<sup>3,4</sup>. New methods were tried in order to improve the yield of these compounds. D-isomannide **1** was transformed into 1,4:3,6-dianhydro-2,5-dichloride-D-itol **6** following a S<sub>N</sub>2 mechanism (see Scheme 2.4). D-Isommanide **1** was reacted with triphenylphosphine and carbon tetrachloride.<sup>13</sup> The mixture was refluxed for 6 h affording 1,4:3,6-dianhydro-2,5-dichloride-D-itol **6**.

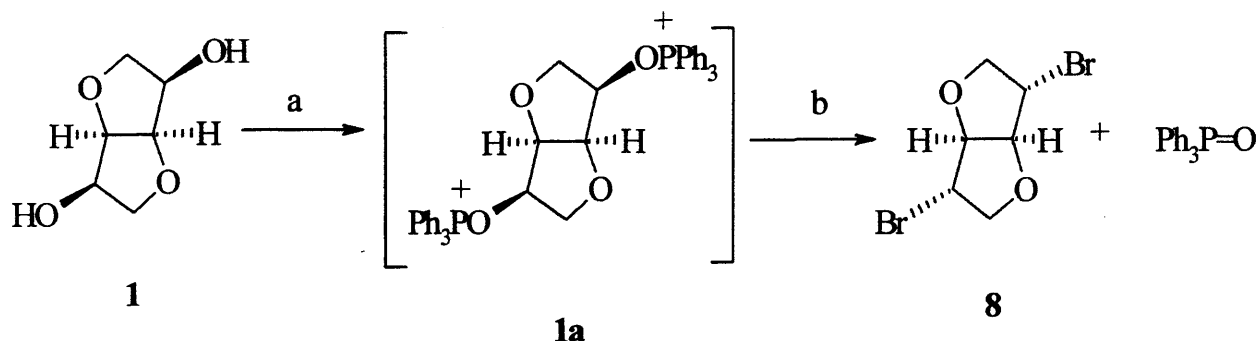


**Scheme 2.4:** Conditions and reagents: (a) PPh<sub>3</sub>, CCl<sub>4</sub>, DMF, Δ, 6 h.

**c) 1,4:3,6-dianhydro-2,5-dibromide-D-itol:**

The second halide to be synthesised was with a better leaving group than **6**. The procedure followed was the same as for the synthesis of **6** but with carbon tetrabromide instead of carbon tetrachloride. In this case, a problem arose when the compound and bromoform were going to be separated by chromatographic column. Both compounds were eluting together therefore the separation was not possible. Because of this, another procedure was followed. D-isomannide **1** was converted in quantitative yield to the corresponding *exo*-dibromide **8** after reaction with two equivalents of bromine, triphenylphosphine and imidazole in refluxing acetonitrile.<sup>14</sup> When this reaction is carried out at room temperature the isolated product was the bis-alkoxyphosphonium

salt **1a**, which upon heating converts to 1,4:3,6-dianhydro-2,5-dibromide-D-iditol **8** and triphenylphosphine oxide (Scheme 2.5).



**Scheme 2.5:** Conditions and reagents: (a) 2 eqv.  $\text{Br}_2$  /  $\text{PPh}_2$  / imidazole in  $\text{CH}_3\text{CN}$ , reflux, 3 days; (b) 2 eqv.  $\text{LiPPh}_2$ ,  $\text{Et}_2\text{O}$ , 3 h.

The course of the reaction was conveniently followed by the disappearance of the  $^{31}\text{P}$  NMR signal at  $\delta$  65 ppm attributed to **1a**. Alkoxyphosphonium salts are postulated intermediates in  $\text{S}_{\text{N}}2$  displacements of alcohols in the presence of phosphines, such as their conversion to halides and the Mitsunobu reaction, but in general are not stable enough to isolate. However in the course of  $\text{S}_{\text{N}}2$  displacements of carbohydrates, alkoxyphosphonium salts have been isolated as stable intermediates.<sup>15</sup> The unwillingness of these substrates to undergo further substitution was attributed to unfavourable dipolar interactions with the charged nucleophiles (e.g.  $\text{Br}^-$ ). Compound **1a** is the first structurally characterised alkoxyphosphonium salt of this type (Figure 2.3). The isomannide backbone of **1a** adopts an *exo-exo* envelope conformation which places the two  $\text{OPPh}_3$  groups at pseudo-axial positions. The P-O bond lengths [1.577(4), 1.572(4) Å] have intermediate values to P-O single bonds adjacent to primary and tertiary carbons.<sup>16</sup> (See Tables 2.1 and 2.2)

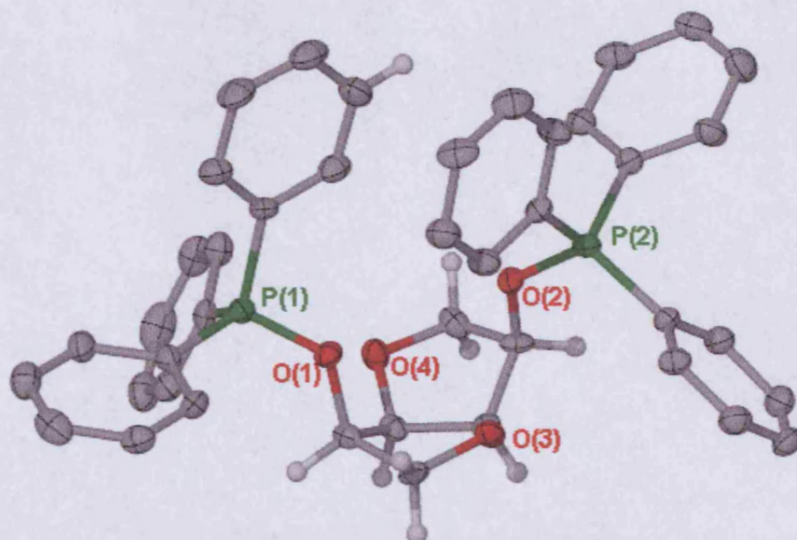


**Figure 2.3:** Crystal structure of the alkoxyphosphonium salt **1a**.

**Table 2.1:** Crystallographic data for the alkoxyphosphonium salt **1a**.

Formula	$C_{42} H_{38} O_4 P_2, 2Br, 3(CH_3OH)$
Mol wt	924.61
Data collection T,K	150(2)
Diffractometer	Bruker-Nonius KappaCCD
Cryst syst	Monoclinic
Space group	P2(1)
a, Å	9.3604(2)
b, Å	23.4811(5)
c, Å	9.7168(2) Å
V, Å <sup>3</sup>	2125.89(8)
Z	2
$\rho$ , mg m <sup>-3</sup>	1.444
$\mu$ , mm <sup>-1</sup>	2.032
$\theta$ range, deg	$3.01 < \theta < 27.49$
no. of indep data	9299 [R(int) = 0.0766]
no. of obsd rflns ( $n_\sigma$ )	16969
Final R indices [ $I > 2\sigma(I)$ ]	R1 = 0.0609, wR2 = 0.1466
R indices (all data)	R1 = 0.0772, wR2 = 0.1534
GOF	1.049
Largest diff. peak and hole	1.153 and -0.704 e.Å <sup>-3</sup>

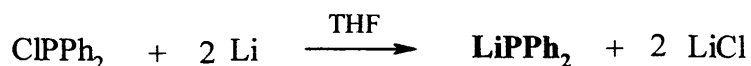
**Table 2.2:** Selected bond lengths (Å) and angles (deg) for the alkoxyphosphonium salt **1a**.

P(1)-O(1)	1.577(4)	O(1)-P(1)-C(19)	109.5(2)
P(1)-C(19)	1.772(6)	O(1)-P(1)-C(13)	102.2(2)
P(1)-C(13)	1.784(6)	C(19)-P(1)-C(13)	110.2(3)
P(1)-C(7)	1.789(6)	O(1)-P(1)-C(7)	112.1(2)
P(2)-O(2)	1.572(4)	C(19)-P(1)-C(7)	108.8(3)
P(2)-C(37)	1.763(5)	C(13)-P(1)-C(7)	113.9(3)
P(2)-C(25)	1.787(5)	O(2)-P(2)-C(37)	112.9(2)
P(2)-C(31)	1.791(5)	O(2)-P(2)-C(25)	108.1(2)
O(1)-C(1)	1.460(6)	C(37)-P(2)-C(25)	108.0(3)
O(2)-C(6)	1.462(6)	O(2)-P(2)-C(31)	102.9(2)
O(3)-C(3)	1.437(7)	C(37)-P(2)-C(31)	114.3(3)
O(3)-C(4)	1.443(7)	C(25)-P(2)-C(31)	110.4(3)
O(4)-C(2)	1.416(7)	C(1)-O(1)-P(1)	124.1(3)
O(4)-C(5)	1.459(7)	C(6)-O(2)-P(2)	124.5(3)

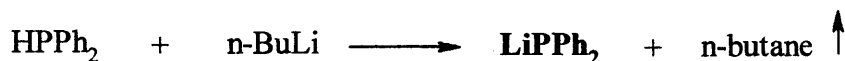
### 2.2.2 Synthesis of Alkali Metal diphenylphosphide.

A number of variants of literature procedures were essayed in order to optimise the yield in the final stage, which involves the reaction between diphenylphosphide anion and the precursor (dimesylate or dihalide). Alkali Metal diphenylphosphide was prepared:

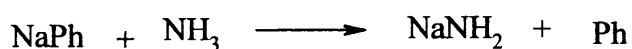
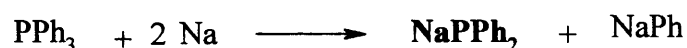
- a) By using lithium metal as the metalating agent.<sup>17</sup> Chlorodiphenylphosphine was reacted with two equivalents of lithium in tetrahydrofuran. A slight molar excess of the metal was used. Under these conditions tetradiphenyldiphosphine (PPh<sub>2</sub>-PPh<sub>2</sub>) can be formed as a by-product.



- b) By reaction of diphenylphosphine with molar equivalents of n-butyl lithium.<sup>18</sup> In this reaction butane is liberated and the yellow solution is ready to use for the next step.

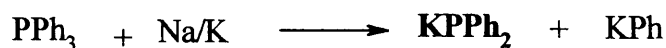


- c) By reaction of sodium diphenylphosphide in liquid ammonia.<sup>19</sup> Triphenylphosphine was slowly added to a solution of sodium in liquid ammonia. The solution changes colour from blue to red orange. After that, cautiously ammonium bromide was added to the reaction mixture in order to destroy  $\text{NaNH}_2$ . The solution was stirred for some minutes and it is ready for the addition of the halide.



- d) By reaction of sodium potassium alloy and triphenylphosphine in dioxan at reflux.<sup>20</sup>

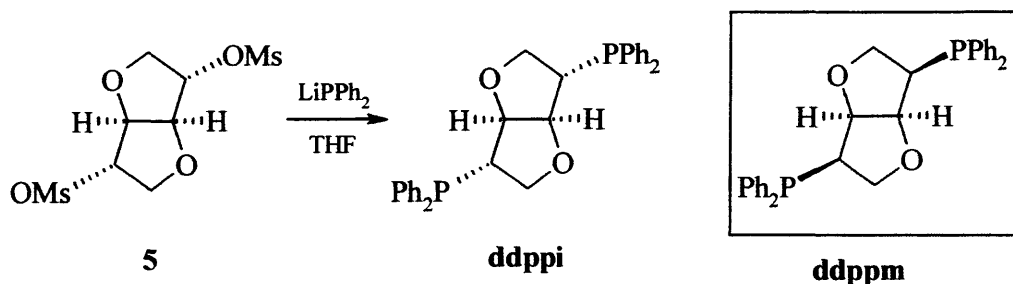
The use of the alloy instead of only potassium permits quantitative cleavage of triphenylphosphine under very much milder conditions.



All the reactions were achieved, however when these compounds are reacted with the different precursors (mesylate or halide) some problems started to arise.

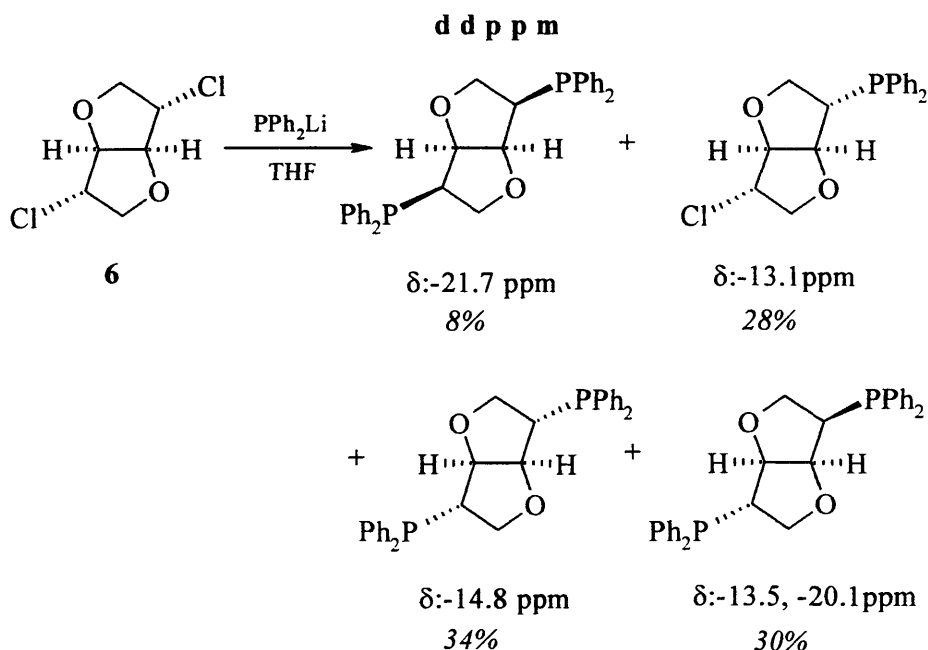
### 2.2.3 Reactions of precursors with lithium diphenylphosphide

- a) When *exo*-dimesylate **5** was reacted with lithium diphenylphosphide in THF, **ddppi** was obtained (*exo-exo* diphosphine) instead of the desired **ddppm** (*endo-endo* diphosphine) (see Scheme 2.6). The phosphorus NMR shows a main peak at  $-14.45$  ppm which corresponds with the phosphine **ddppi**.<sup>8</sup>



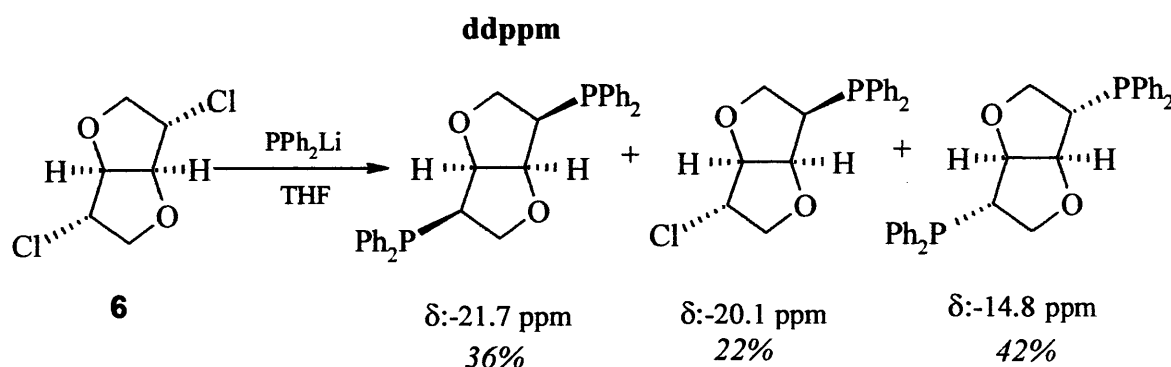
**Scheme 2.6:** Reaction of the *exo*-dimesylate **5** with  $\text{LiPPh}_2$  in THF.

- b) The second attempt was the reaction of the *exo*-dichloride **6** with lithium diphenylphosphide in THF. When lithium diphenylphosphide was formed from diphenylphosphine and *n*-butyl lithium, the result of this reaction is a mixture of different phosphines as shown in the scheme 2.7:



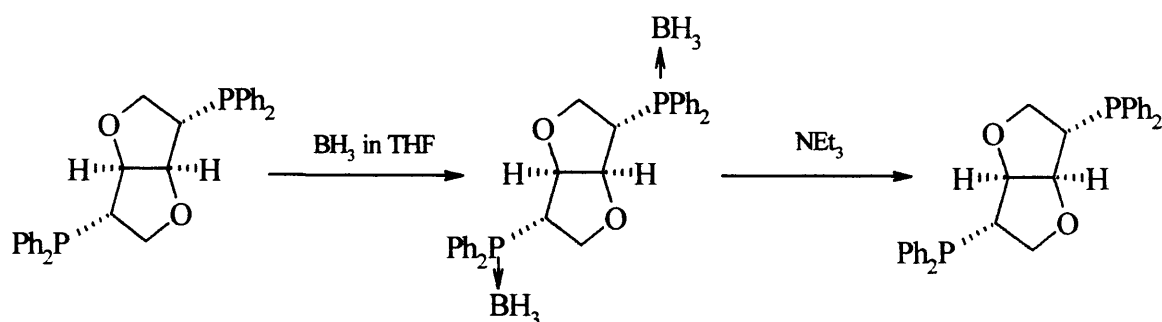
**Scheme 2.7:**  $^{31}\text{P}$  NMR chemical shifts of the different phosphines and abundance.

If we prepare lithium diphenylphosphide from chlorodiphenylphosphine and lithium, **ddppm** was synthesised in greater proportion (36% yield, see Scheme 2.8) although various amounts of tetradiphenylphosphine ( $\text{PPh}_2\text{-PPh}_2$ ) were also obtained.  $\text{PPh}_2\text{-PPh}_2$  has a chemical shift in the phosphorus NMR around  $-14.5$  ppm which is close to the chemical shift of the phosphine **ddppi**.



**Scheme 2.8:**  $^{31}\text{P}$  NMR chemical shifts of the different phosphines and abundance.

In order to separate this mixture of phosphines by chromatographic column, a borane complex was formed with a solution of  $\text{BH}_3$  in THF (1M).<sup>21</sup> Removal of the borane group was accomplished with triethylamine to give the free phosphines. This reaction gave very low yields (see Scheme 2.9).

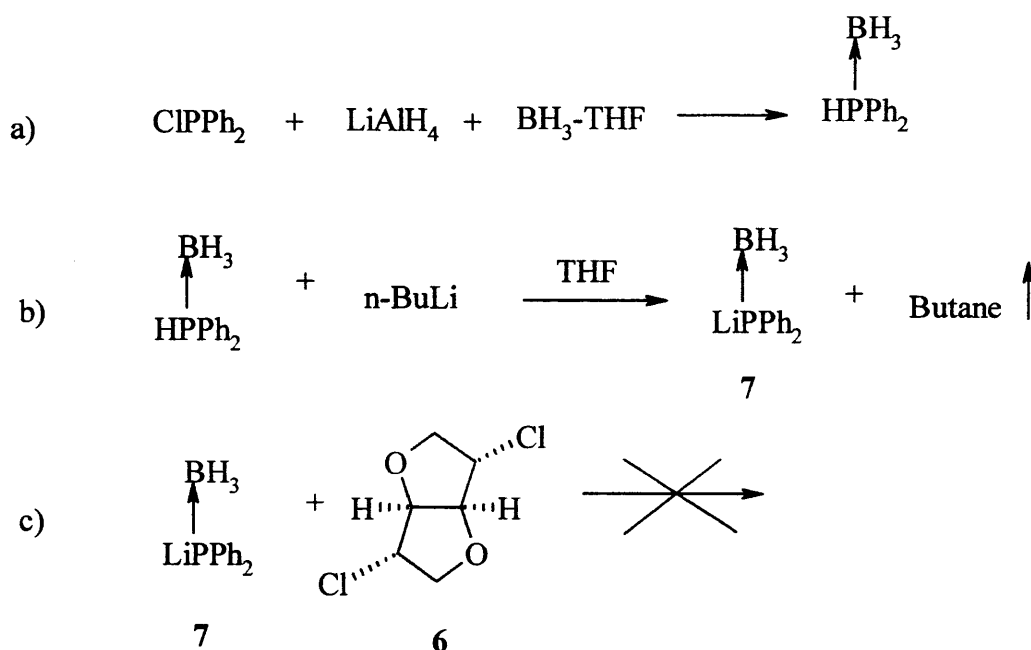


**Scheme 2.9:**  $\text{BH}_3$  as P-Protective group for isolation and purification procedures.



### 2.2.4 Synthesis of a preformed borane complex of lithium diphenylphosphide.

It is known that the *exo* groups of 1,4:3,6 dianhydrohexitols are reluctant to undergo  $S_N2$  displacements due to steric constraints, in many cases leading to elimination and racemisation by-products. To avoid formation of elimination products as was the case for the *endo* diimine isomannide derivative<sup>6</sup> the *exo*-dichloride **6** is reacted with a preformed borane complex of  $LiPPh_2$  **7** which is less basic and not air sensitive<sup>22</sup> to synthesize **ddppm** (see Scheme 2.10):



**Scheme 2.10:** Different steps for the reaction with borane complex **7**.

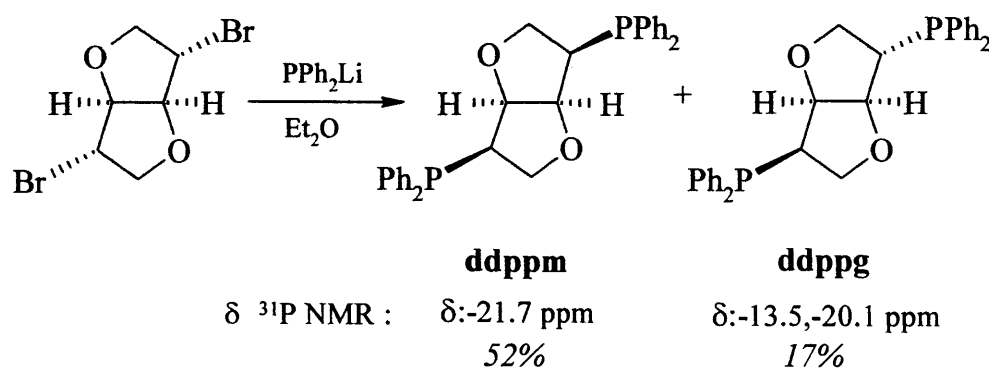
In this case the product was not formed because the borane complex **7** was very bulky and less nucleophilic than lithium diphenylphosphide, so the  $S_N2$  displacement of the chloride of **6** did not have effect.

### 2.2.5 Best method for the synthesis of **ddppm**.

The last attempt to form **ddppm** was done in ether and using lithium diphenylphosphide synthesized from diphenylphosphine and *n*-butyl lithium. This synthesis involves an  $S_N2$  displacement of the *exo*-dibromide **8** by the  $-PPh_2$  nucleophile. No elimination by-products were observed in the last step of the **ddppm** synthesis and the epimer 1,4:3,6-dianhydro-2,5-dideoxy-2,5-bis(diphenylphosphino)-D-glucitol (**ddppg**) was also isolated (see Figures 2.4 and 2.5).

The two isomers were separated as colourless, air stable crystals by fractional crystallisation from ethanol in 52% (**ddppm**) and 17% (**ddppg**) yields, respectively (Scheme 2.11). This time, a borane complex was not necessary to be done, and subsequently the additional step of the chromatographic column was avoided.

The  $^{31}P$  NMR spectrum in  $d^1$ -chloroform for **ddppm** shows a singlet at  $\delta$  -21.4. The corresponding spectrum for **ddppg** consists of two singlets at  $\delta$  -22.2 and -13.1 ppm for the *endo* and *exo* phosphorus atoms respectively. Therefore, there is no coupling observed between the two phosphine groups.



**Scheme 2.11:** Conditions and reagents:  $LiPPh_2$ ,  $Et_2O$ , 3h.

The  $^1\text{H}$  NMR spectrum of **ddppm** has three signals corresponding to the protons of the backbone. The multiplets resonate at  $\delta$  2.94, 3.88 and 4.52 ppm (see Figure 2.4).

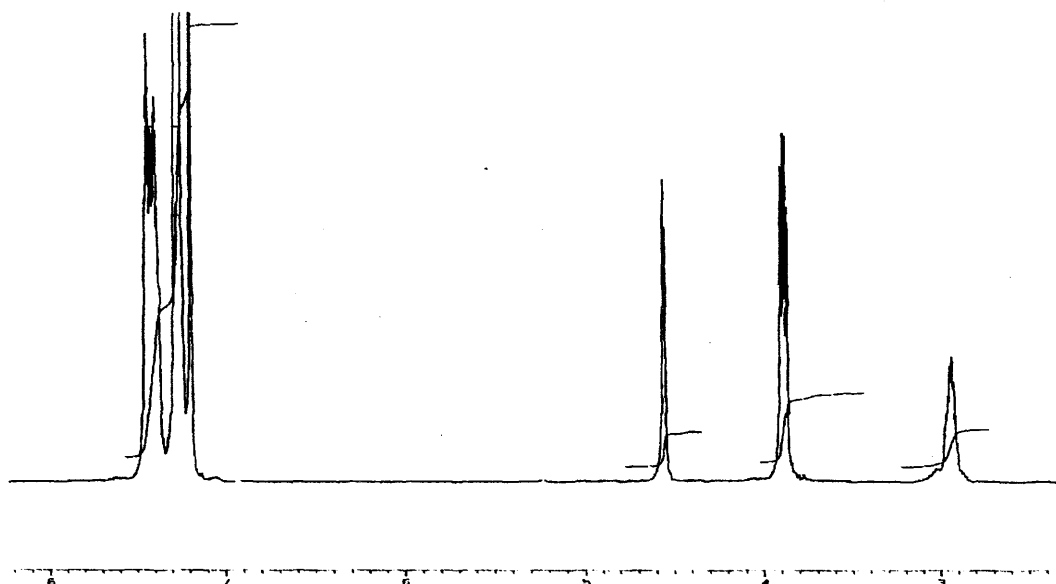


**Figure 2.4:**  $^1\text{H}$  NMR spectrum of **ddppm**.

The  $^1\text{H}$  NMR spectrum of **ddppg** has eight signals corresponding to the protons of the backbone. This implies that the complex is asymmetrical unlike **ddppm**. The multiplets resonate at  $\delta$  2.88, 3.02, 3.58, 3.75, 3.83, 4.09, 4.44 and 4.75 ppm (see Figure 2.5).

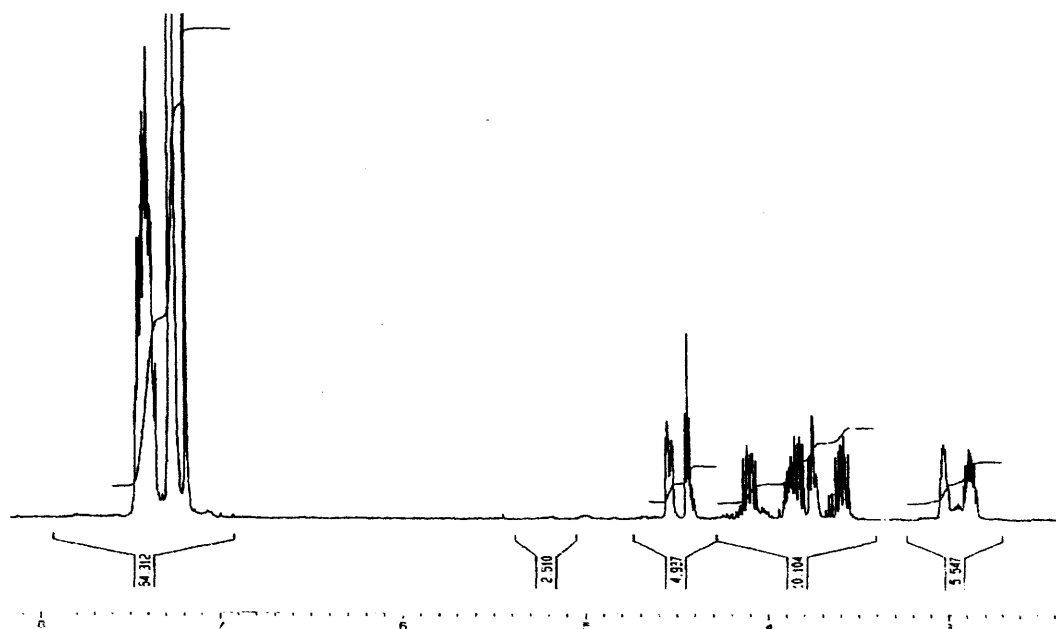
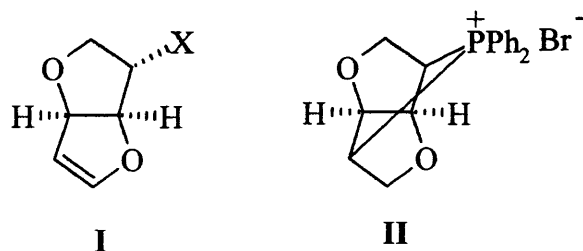


**Figure 2.5:**  $^1\text{H}$  NMR spectrum of **ddppg**.

Formation of the minor isomer may arise from the hydrophosphination of elimination intermediates such as **1<sub>II</sub>** (where X = PPh<sub>2</sub>) by HPPH<sub>2</sub> leading to **ddppg** as the more thermodynamically stable product. Alternatively, **ddppg** may be formed by attack of -PPh<sub>2</sub> to the bridged phosphonium salt intermediate **2<sub>II</sub>**. From reactions with ammonia a bridged secondary amine analogous to intermediate **2<sub>II</sub>** has been reported previously.<sup>23</sup> As we have seen, the choice of solvent is crucial in the formation of **ddppm**. In THF the di-*endo* ligand was hardly detected and **ddppg** was a minor product. The major products formed were the mono- and di-*exo* phosphines. This preferential formation of *exo* phosphine derivatives favours a competing mechanism via phosphide-promoted elimination to yield intermediate **1<sub>II</sub>** and HPPH<sub>2</sub> followed by hydrophosphination, see Scheme 2.12.<sup>24</sup>



**Scheme 2.12:** Intermediates in the synthesis of the phosphine **ddppm**.

The crystal structure of **ddppm** confirms its absolute stereochemistry and shows the two fused tetrahydrofuran rings adopting an *endo-endo* envelope conformation with the two phosphine groups at pseudo-equatorial positions pointing away from the central vault (Figure 2.6). If we look at the backbone, both CH<sub>2</sub> groups look into the cavity.

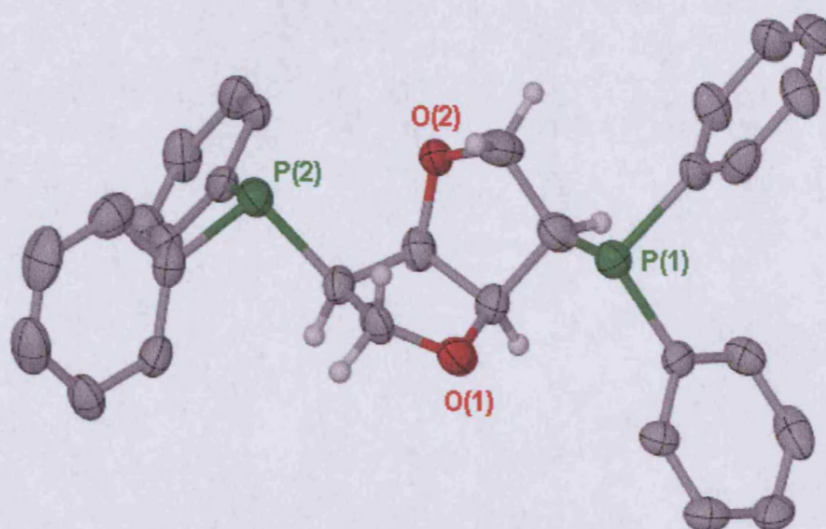


**Figure 2.6:** Ellipsoid plot of the molecular structure of **ddppm**.

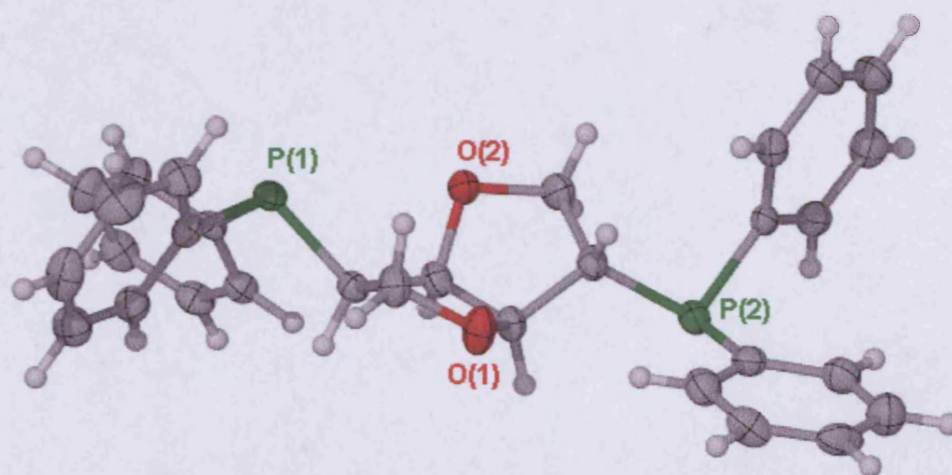
**Table 2.3:** Crystallographic data for **ddppm**.

Formula	C <sub>30</sub> H <sub>28</sub> O <sub>2</sub> P <sub>2</sub>
Mol wt	482.46
Data collection T,K	150(2)
Cryst syst	Orthorhombic
Space group	P2(1)2(1)2(1)
a, Å	11.5522(9)
b, Å	14.0034(11)
c, Å	15.4518(14)
V, Å <sup>3</sup>	2499.6(4)
Z	4
no. of indep data	4278 [R(int) = 0.2142]
no. of obsd rflns (n <sub>o</sub> )	24363
Final R indices [I>2sigma(I)]	R1 = 0.0731, wR2 = 0.1400
R indices (all data)	R1 = 0.1324, wR2 = 0.1602
GOF	0.985
Largest diff. peak and hole	0.594 and -0.270 e.Å <sup>-3</sup>

**Table 2.4:** Selected bond lengths (Å) and angles (deg) for **ddppm**.

P(1)-C(5)	1.832(6)	C(5)-P(1)-C(7)	101.5(3)
P(1)-C(7)	1.833(6)	C(5)-P(1)-C(13)	101.9(3)
P(1)-C(13)	1.856(6)	C(7)-P(1)-C(13)	100.7(3)
P(2)-C(19)	1.830(6)	C(19)-P(2)-C(25)	102.5(3)
P(2)-C(25)	1.842(6)	C(19)-P(2)-C(2)	101.4(3)
P(2)-C(2)	1.865(6)	C(25)-P(2)-C(2)	98.2(3)
O(1)-C(3)	1.397(7)	C(3)-O(1)-C(4)	109.2(4)
O(1)-C(4)	1.430(7)	C(6)-O(2)-C(1)	110.6(5)
O(2)-C(6)	1.375(7)	O(2)-C(1)-C(2)	114.2(5)
O(2)-C(1)	1.402(7)	O(2)-C(1)-C(4)	107.6(5)
C(1)-C(2)	1.534(8)	C(1)-C(2)-P(2)	113.5(4)
C(1)-C(4)	1.540(8)	C(3)-C(2)-P(2)	114.1(4)
C(2)-C(3)	1.537(8)	O(1)-C(3)-C(2)	106.6(5)
C(4)-C(5)	1.537(7)	O(1)-C(4)-C(5)	114.2(5)
C(5)-C(6)	1.538(8)	O(1)-C(4)-C(1)	107.2(4)

On the contrary **ddppg** as shown in Figure 2.7 is a non-chelating ligand. It has the two phosphine groups in pseudo-equatorial positions and looking at the backbone we can observed that one of the CH<sub>2</sub> group is pointing into the cavity and the other out of the cavity.

**Figure 2.7:** Ellipsoid plot of the molecular structure of **ddppg**.

**Table 2.5:** Crystallographic data for **ddppg**.

Formula	C <sub>30</sub> H <sub>28</sub> O <sub>2</sub> P <sub>2</sub>
Mol wt	482.46
Cryst syst	Orthorhombic
Space group	P2(1)2(1)2(1)
a, Å	9.3120(4)
b, Å	10.1516(4)
c, Å	26.5195(14)
V, Å <sup>3</sup>	2506.9(2)
Z	4
no. of indep data	4394 [R(int) = 0.0812]
no. of obsd rflns (n <sub>o</sub> )	13050
Final R indices [I > 2σ(I)]	R1 = 0.0588, wR2 = 0.1249
R indices (all data)	R1 = 0.0844, wR2 = 0.1368
GOF	1.006
Largest diff. peak and hole	0.756 and -0.230 e.Å <sup>-3</sup>

**Table 2.6:** Selected bond lengths (Å) and angles (deg) for **ddppg**

P(1) C(7)	1.840(4)	C(7) P(1) C(2)	103.21(17)
P(1) C(13)	1.841(4)	C(13) P(1) C(2)	99.39(17)
P(1) C(2)	1.853(4)	C(25) P(2) C(19)	100.87(18)
P(2) C(25)	1.841(4)	C(25) P(2) C(5)	100.67(18)
P(2) C(19)	1.843(4)	C(19) P(2) C(5)	102.75(19)
P(2) C(5)	1.846(4)	C(1) O(1) C(4)	110.1(3)
O(1) C(1)	1.422(5)	C(6) O(2) C(3)	104.1(3)
O(1) C(4)	1.435(5)	O(1) C(1) C(2)	105.9(3)
O(2) C(6)	1.428(5)	C(3) C(2) P(1)	115.3(3)
O(2) C(3)	1.441(5)	C(1) C(2) P(1)	111.1(3)
C(1) C(2)	1.535(5)	O(2) C(3) C(2)	110.3(3)
C(2) C(3)	1.527(6)	O(2) C(3) C(4)	105.3(3)
C(3) C(4)	1.533(6)	O(1) C(4) C(5)	113.8(3)
C(4) C(5)	1.530(5)	O(1) C(4) C(3)	106.7(3)
C(5) C(6)	1.531(6)	C(4) C(5) P(2)	114.9(3)
C(7) C(8)	1.394(5)	C(6) C(5) P(2)	110.8(3)
C(8) C(9)	1.384(6)	O(2) C(6) C(5)	105.8(3)

## 2.3 CONCLUSIONS

Improved methods have been developed for the preparation of halides derived from D-Isomannide (1,4:3,6-dianhydro-2,5-dideoxy-2,5-dichloro-L-iditol, **7** and 1,4:3,6-dianhydro-2,5-dideoxy-2,5-dibromo-L-iditol, **8**) have been developed. From the reaction leading to dibromide (**8**), the bisalkoxyphosphonium salt, **1a**, was isolated as a by-product.

The *exo*-dihalides **7** and **8** were used in the synthesis of the *endo*-diphosphine, **ddppm**. *Endo* derivatives of D-Isomannide are very hard to synthesize due to the difficulties found in S<sub>N</sub>2 type substitutions of leaving groups in the *exo* positions of the two *cis* fused tetrahydrofuran rings.

After several attempts to synthesize **ddppm**, the best yields were obtained from the reaction of 1,4:3,6-dianhydro-2,5-dideoxy-2,5-dibromo-L-iditol, **8** with lithium diphenylphosphide in ether. A mixture of two different isomers, **ddppm** (52%) and **ddppg** (17%) was obtained. **ddppg** unlike **ddppm** is a non-chelating ligand. The choice of the solvent is crucial in the formation of **ddppm** from the above reaction, since in THF the major product obtained was the **ddppm** diastereoisomer, **ddppi**.

The chelating ability of the **ddppm** ligand will be discussed in the following chapters, where complexes with late transition metals and their catalytic applications are reported.

## 2.4 EXPERIMENTAL

**General considerations:** All manipulations were performed using standard Schlenk techniques under an argon atmosphere, except where otherwise noted. Solvents of analytical grade and deuterated solvents for NMR measurements were distilled from the appropriate drying agents under N<sub>2</sub> immediately prior to use following standard literature



methods.<sup>25</sup> NMR spectra were obtained on Bruker Avance AMX 400 or Jeol Eclipse 300 spectrometers and referenced to external TMS. Mass spectra were obtained in ES (Electrospray) mode from the EPSRC Mass Spectrometry Service, Swansea University unless otherwise reported.

**1,4:3,6-dianhydro-2,5-di-O-tosyl-L-iditol, 2:** To a solution of Isomannide (10 g, 0.068 mol) in 100 ml of dry pyridine cooled in a ice bath was added 27 g (0.21 mol) of recrystallized p-toluenesulphonyl chloride. The mixture was stirred at 0°C for 4 h. The solution was kept overnight at +5°C. The solution was then added to 500 ml of a mixture of ice and water with stirring. The precipitated was filtered off and dissolved in 150 ml of CHCl<sub>3</sub>. The CHCl<sub>3</sub> solution was washed successively with 1 N hydrochloric acid, then with water, and dried over MgSO<sub>4</sub>. The solvent was removed under reduced pressure, and the residue was recrystallized from EtOH to yield 26.4 g (85 %) of pure *endo*-ditosylate **2**: m.p. 83°C; <sup>1</sup>H NMR (CDCl<sub>3</sub>, 400MHz) δ 2.28 (s, 6H), 3.65 (m, 2H), 3.83 (m, 2H), 4.40 (s, 2H), 4.78 (m, 2H), 7.27 (d, *J* 8.2 Hz, 4H) and 7.73 (d, *J* 8.4 Hz, 4H).<sup>8</sup>

**1,4:3,6-dianhydro-2,5-di-benzoate-L-iditol, 3:** To a solution of D-isomannide (5g, 34mmol) and triphenylphosphine (18g, 69mmol) in THF (80ml) was added drop wise a solution of benzoic acid (8.4g, 69mmol) and DIAD (13ml, 69mmol) in THF (80ml) over a period of 2h at ambient temperature. The mixture was stirred for 15h. Then, additional benzoic acid (1.35ml, 6.9mmol) and DIAD (0.843g, 6.9mmol) in THF were added and the mixture was further stirred for 3h. The reaction was concentrated in vacuum and petroleum ether to form a solid. This solid was dissolved in the minimum amount of CH<sub>2</sub>Cl<sub>2</sub> and it was subjected to column chromatography (85:15 Petroleum Ether and Ethyl Acetate). The solid formed was the dibenzoate ester **3** and it can be crystallized in ethanol (11.63g, 96%

yield).  $^1\text{H}$  NMR ( $\text{CDCl}_3$ , 400MHz)  $\delta$  4.06 (s, 4H), 4.86 (s, 2H), 5.44 (s, 2H), 7.38 (m, 4H), 7.51 (m, 2H), 7.96 (m, 4H).<sup>6</sup>

**1,4:3,6-dianhydro -L-iditol, 4:** 1 g (2.82 mmol) of dibenzoate-L-iditol **3** was dissolved in methanol and 590 mg (14.75 mmol) of sodium hydroxide were dissolved in the minimum amount of distilled water. The two solutions were mixed in a sealed tube and refluxed for 1 day. After that time, a white precipitate appeared and it was filtered. The filtrate was concentrated and HCl (14.75 mmol) was added drop wise and the solution is left in an ice bath. A solid crystallized (benzoic acid) and it was filtered. The filtrate is evaporated affording 1, 4:3, 6-dianhydro -L-iditol **4**. (2.26 g, 55% yield).  $^1\text{H}$  NMR ( $\text{CDCl}_3$ , 400MHz)  $\delta$  3.78 (m, 4H), 4.23 (d,  $J$  2.7 Hz, 2H), 4.34 (m, 2H).<sup>6</sup>

**1,4:3,6-dianhydro-2,5-di-O-mesyl-L-iditol, 5:** To a solution of **4** (2.2g, 15 mmol) in pyridine (2 ml, 25 mmol) was added mesyl chloride (6ml, 75 mmol) at  $-10^\circ\text{C}$ . It was stirred for 1 day. After that time the reaction mixture was diluted with ice water and then 10 ml of HCl solution (10% conc.) was also added. The water solution was extracted three times with chloroform and the organic layer was washed with a solution of  $\text{NaHCO}_3$  and then with NaCl. Then, the organic layer was dried over  $\text{MgSO}_4$  and evaporated obtaining a liquid which becomes solid with. This solid was crystallized in hot ethanol (0.75 g, 17% yield).  $^1\text{H}$  NMR ( $\text{CDCl}_3$ , 400MHz)  $\delta$  3.03 (s, 6H), 3.87 (dd,  $J$  3.2 Hz,  $J$  11.2 Hz, 2H), 4.04 (d,  $J$  11.2 Hz, 2H), 4.77 (s, 2H), 5.02 (d,  $J$  2.7 Hz, 2H).<sup>6</sup>

**1,4:3,6-dianhydro-2,5-dideoxy-2,5-dichloro-L-iditol, 6:** A dry, 250 ml two necked flask was equipped with a magnetic stirring bar and reflux condenser (to which is attached a Drierite-filled drying tube) and charged with 100 ml of carbon tetrachloride and 8.47 g of D-

isomannide. Some ml of DMF was added to help dissolve the alcohol. To this solution was added 39.7 g of  $\text{Ph}_3\text{P}$  and the stirred reaction mixture was heated under reflux for one day. The mixture was allowed to cool to room temperature and petroleum ether (80 ml) was added and stirring was continued for some more minutes. The precipitate formed was filtered and washed with more petroleum ether. The solvent was evaporated and the solution was subjected to a column chromatography. (9:1 petroleum ether and ether). (6.49g, 61 % yield).  $^1\text{H}$  NMR ( $\text{CDCl}_3$ , 400MHz)  $\delta$  3.99 (m, 4H), 4.30 (d,  $J$  3.2 Hz, 2H), 4.81 (s, 2H).<sup>13</sup>

**1,4:3,6-dianhydro-2,5-dideoxy-2,5-dibromo-L-idoitol, 8:** A 500 ml flask is charged with 23g (86 mmol) of triphenylphosphine under argon followed by 150 ml of dry acetonitrile. In the formed solution bromine (90 mmol) is added drop wise at 0°C. Subsequently an acetonitrile solution of imidazole (5.6 g, 82 mmol) and isomannide (6 g, 41 mmol) is transferred to the flask. The reaction mixture is refluxed for 5 days. Any precipitate formed at this point is filtered and the filtrate evaporated to dryness. Addition of petroleum ether (90 ml) and diethyl ether (10 ml) forms a slurry which is filtered through silica. The silica column is washed with another 100 ml of a 9/1 mixture of petroleum ether and diethyl ether. The combined washings are evaporated to dryness to afford 8. 1,4:3,6-dianhydro-2,5-dideoxy-2,5-dibromo-L-idoitol can be obtained as colourless crystals after recrystallisation from hot ethanol, yield 9.25g (83% yield).  $^1\text{H}$  NMR ( $\text{CDCl}_3$ , 400MHz)  $\delta$  4.15 (m, 4H), 4.32 (d,  $J$  = 3.3 Hz, 2H), 4.98 (s, 2H).<sup>13</sup>

When the same reaction is carried out without reflux the **alkoxyphosphonium salt 1a** is formed exclusively. Data for 1a:  $^1\text{H}$  NMR ( $\text{CDCl}_3$ , 400MHz) 4.20 (m, 4H,  $\text{CH}_2$ ), 4.32 (d, 2H, endo  $\text{CHPh}_2$ ), 5.28 (m, 2H, CCH), 7.73-7.82 (m, 30H);  $^{31}\text{P}$  NMR ( $\text{CDCl}_3$ , 121MHz)  $\delta$  64.95 (s).

**Synthesis of the phosphines: *ddppm* and *ddppg*:** Diphenylphosphine (3.3 ml, 19.1 mmol) was syringed into ether (30 ml) at 0°C and subsequently 11.2 ml of *n*-BuLi (1.71 M) were added. After 30 minutes an ether solution of **2** (2.6g, 9.6 mmol) was added drop wise and the yellow solution was left to reach ambient temperature and stirred until the solution turns colourless and a heavy white precipitate formed. Water (15 ml) was then added and the ether layer collected, subsequently the water layer was washed with ether (2 x 20 ml) and the ethereal extracts collected.

Evaporation of ether under vacuum afforded a mixture of **ddppm** and **ddppg** as a white air stable solid. The ligand was separated by fractional crystallization from hot ethanol to afford colourless needles of **ddppm** (0.67g, 52%).

Data for **ddppm**: (Found: C, 73.82; H, 5.57.  $C_{30}H_{28}O_2P_2$  requires C, 74.68; H, 5.85%);  $^1H$  NMR ( $CDCl_3$ , 400MHz)  $\delta$  2.94 (m, 2H,  $CHPh_2$ ), 3.88 (m, 4H,  $CH_2$ ), 4.52 (m, 2H, CCH), 7.2-7.4 (m, 20H);  $^{31}P$  NMR ( $CDCl_3$ , 121MHz) -21.4;  $^{13}C$  NMR ( $CDCl_3$ , 100 MHz) 45.78 (d,  $^2J_{CP}$  11.5 Hz, 2C,  $CH_2$ ), 73.04 (d,  $^1J_{CP}$  26.5 Hz, 2C, CHP), 86.12 (m, 2C, HCCH), 128.63 (s, 4C, Ar), 128.65 (m, 4C, Ar), 129.03 (m, 4C, Ar), 133.04 (d,  $J_{CP}$  19.6 Hz, 4C, Ar), 133.51 (d,  $J_{CP}$  21.4 Hz, 4C, Ar), 136.69 (d,  $J_{CP}$  13.3 Hz, 2C, Ar), 137.44 (d  $J_{CP}$  15.0 Hz, 2C, Ar); MS (accurate mass, ES+) calculated mass for  $[M+H]^+$ : 483.1637, measured: 483.1636.

Data for **ddppg**: (Found: C, 73.82; H, 5.75.  $C_{30}H_{28}O_2P_2$  requires C, 74.68; H, 5.85%);  $^1H$  NMR ( $CDCl_3$ , 400MHz)  $\delta$  2.88 (m, 1H, *exo*  $CHPh_2$ ), 3.02 (m, 1H, *endo*  $CHPh_2$ ), 3.58 (m, 1H,  $CH_2$ ), 3.75 (m, 1H,  $CH_2$ ), 3.83 (m, 1H,  $CH_2$ ), 4.09 (m, 1H,  $CH_2$ ), 4.44 (m, 1H, CCH), 4.75 (m, 1H, CCH), 7.15-7.45 (m, 20H);  $^{31}P$  NMR ( $CDCl_3$ , 121MHz)  $\delta$  -13.1 (s), -22.2 (s).  $^{13}C$  NMR ( $CDCl_3$ , 100 MHz) 44.94 (m, 2C,  $CH_2$ ), 71.25 (d,  $^1J_{CP}$  26.6 Hz, 1C, CHP), 72.37 (d, 1C,  $^1J_{CP}$  23.6 Hz, CHP), 85.56 (m, 1C, HCCH), 88.52 (dd, 1C,  $^2J_{CP}$  24.8

Hz,  $^3J_{\text{CP}}$  3.5 Hz, HCCH), 128.5-129.5 (m, 12C, Ar), 132.7-133.9 (m, 8C, Ar), 136.5-137.4 (m, 4C, Ar).

---

<sup>1</sup> (a) A. C. R. Fauconnier, 1882, 95, 991; (b) A. Fauconnier, *Bull. Soc. Chim. Fr.* 1884, 41, 119

<sup>2</sup> R. C. Hockett, H. G. Jr. Fletcher, E. L. Sheffield, R. M. Goepp, S. Soltzberg, *J. Am. Chem. Soc.* 1946, 68, 930.

<sup>3</sup> (a) L. F. Wiggins, *J. Chem. Soc.* 1945, 4; (b) L. F. Wiggins, R. Montgomery, *Nature* 1946, 157, 372; (c) R. Montgomery, L. F. Wiggins, *J. Am. Chem. Soc.* 1946, 68, 390.

<sup>4</sup> V. Cerè, C. Mazzini, C. Paolucci, S. Policino, A. Fava, *J. Org. Chem.* 1993, 58, 4567-4571.

<sup>5</sup> Q. Chao, J. Zhang, L. Pickering, T. S. Jahnke, V. Nair, *Tetrahedron* 1998, 54, 3113-31124.

<sup>6</sup> G. De Coster, K. Vandyck, E. Van der Eycken, J. Van der Eycken, M. Elseviers, H. Roper, *Tetrahedron Asymmetry*, 2002, 13, 1673-1679.

<sup>7</sup> (a) M. K. Grachev, N.O. Soboleva, G.I. Kurochkina, *Russian Journal of General Chemistry*, Vol. 73, No 6, 2003, 903-908. (b) M. K. Grachev, G. I. Kurochkina, N.O. Soboleva, *Russian Journal of General Chemistry*, Vol 72, No. 11, 2002, 1813-1819. (c) M. K. Crachev, K. L. Anfilov, A. R. Bekker, and E. E. Nifant'ev, *Russian journal of General Chemistry*, Vol. 65, No. 12, 1995, 1785-1789.

<sup>8</sup> J. Bakos, B. Heil and L. Marko; *J. Organomet. Chem.*, 1983, 253, 249-252.

<sup>9</sup> B. Xie, C. Xia, L. Chun-Gu, *Tetrahedron Lett.* 1998, 39 (40), 7365-7368.

<sup>23</sup> A. C. Cope and T. V. Shen, *J. Am. Chem. Soc.*, 1956, **78**, 3177.

<sup>24</sup> T. Bunlaksananusorn and P. Knochel, *Tetrahedron Lett.*, 2002, **43**, 5817.

<sup>25</sup> D. D. Perrin and W. F. A. Amarego, *Purification of Laboratory Chemicals*, Pergamon, Oxford, 1988.

# *Chapter 3*

### 3. Cu-, Pt- and Pd-ddppm complexes and their catalytic applications: carbonylation and allylic reactions.

#### 3.1 INTRODUCTION

In this chapter the syntheses of **ddppm** copper, platinum and palladium complexes is discussed. The Pd complexes have been tested in different catalytic reactions such as C-C coupling reactions, carbonylation of aryl-halide compounds, hydroesterification of styrene and allylic substitutions.

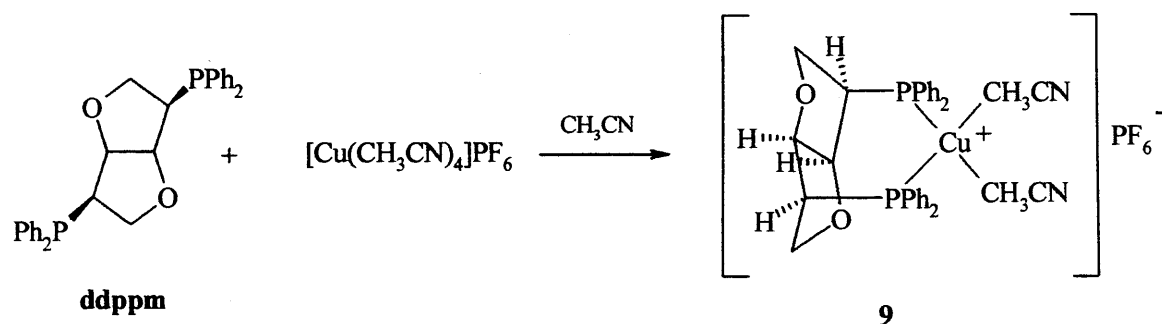
#### 3.2 RESULTS AND DISCUSSTION

##### 3.2.1 Synthesis and characterization of Copper complexes with **ddppm**.

Copper(I) compounds of bidentate phosphines have been shown to be potent anti-tumour agents, particularly against leukemia, reticulum cell sarcoma, and melanoma.<sup>1</sup> Recently, catalytic enantioselective Aza Diels-Alder reaction (ADAR) has attracted interest due to the powerful strategy for the construction of six-membered nitrogen heterocycles, which are key units in medicinal chemistry. Copper (I) complexes of BINAP and phosphino-oxazolines have been used in this asymmetric process.<sup>2</sup>

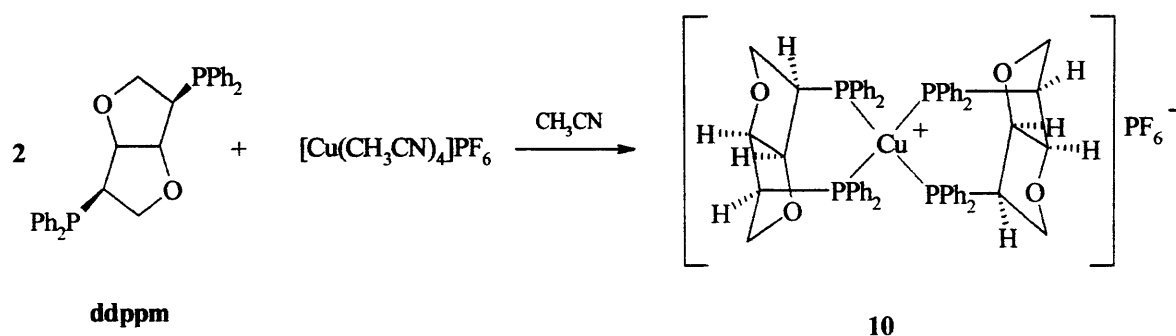
The aim in this section is to present the synthesis of copper (I) complexes with the chiral diphosphine **ddppm**. The  $[\text{Cu}(\text{ddppm})(\text{CH}_3\text{CN})_2]\text{PF}_6$  (**9**) and  $[\text{Cu}(\text{ddppm})_2]\text{PF}_6$  (**10**) complexes have been prepared. Complex **9** was isolated from the reaction of  $[\text{Cu}(\text{CH}_3\text{CN})_4]\text{PF}_6$  with **ddppm** in 1:1 ratio in acetonitrile at 50°C under a nitrogen atmosphere as a white solid, Scheme 3.1.





**Scheme 3.1:** Synthesis of the copper (I) complex **9**.

Furthermore, complex **10** was prepared in the same fashion as **9**, using a 1:2 ratio of the Cu precursor to **ddppm**, Scheme 3.2.



**Scheme 3.2:** Synthesis of the copper (I) complex **10**.

These Cu(I)-ddppm complexes have not been successfully crystallographically characterized however their identity was determined by NMR and mass spectrometry techniques. NMR spectra were recorded in  $d^3$ -acetonitrile at ambient temperature. The  $^{31}\text{P}\{^1\text{H}\}$  NMR spectra of complexes **9** and **10** reveal broad singlets at -11.1 and -14.6 ppm respectively, shifted to higher frequency in comparison to free **ddppm** ( $\delta$ : -21.4 ppm). Broad signals are due to quadrupole coupling between the NMR active copper nuclei ( $^{63}\text{Cu}$  and  $^{65}\text{Cu}$ ,  $I = 3/2$ ) and phosphorus ( $I = 1/2$ ).

The  $^{13}\text{C}$  NMR spectra of these complexes reveal some differences in comparison to the free **ddppm** and their data are shown in Table 3.1.

**Table 3.1:**  $^{13}\text{C}$  NMR chemical shifts (ppm) from free phosphine **ddppm** and Cu(I)-**ddppm** complexes **9** and **10**.

	Complex <b>9</b>	Complex <b>10</b>	Free phosphine
$\text{CH}_2$	42.79	39.93	45.78
$\text{CHP}$	72.98	73.91	73.04
$\text{HCCH}$	85.98	85.93	86.12
	128.72	128.71	128.63
$\text{C arom.}$	129.91	130.01	129.03
	133.27	133.13	133.04

The  $^1\text{H}$  NMR spectrum of complex **9** has four signals corresponding to the protons of the backbone of the phosphine **ddppm**. This implies that the complex is  $C_2$ -symmetrical, i.e. the four protons from one furan ring are identical to the four protons in the other furan ring. The multiplets resonate at  $\delta$  3.53, 3.65, 3.88 and 5.16 ppm (see Figure 3.1). In comparison, the free phosphine **ddppm** reveals three signals in the  $^1\text{H}$  NMR spectrum at 2.94, 3.88 and 4.52 ppm, where all  $\text{CH}_2$  protons are equivalent.

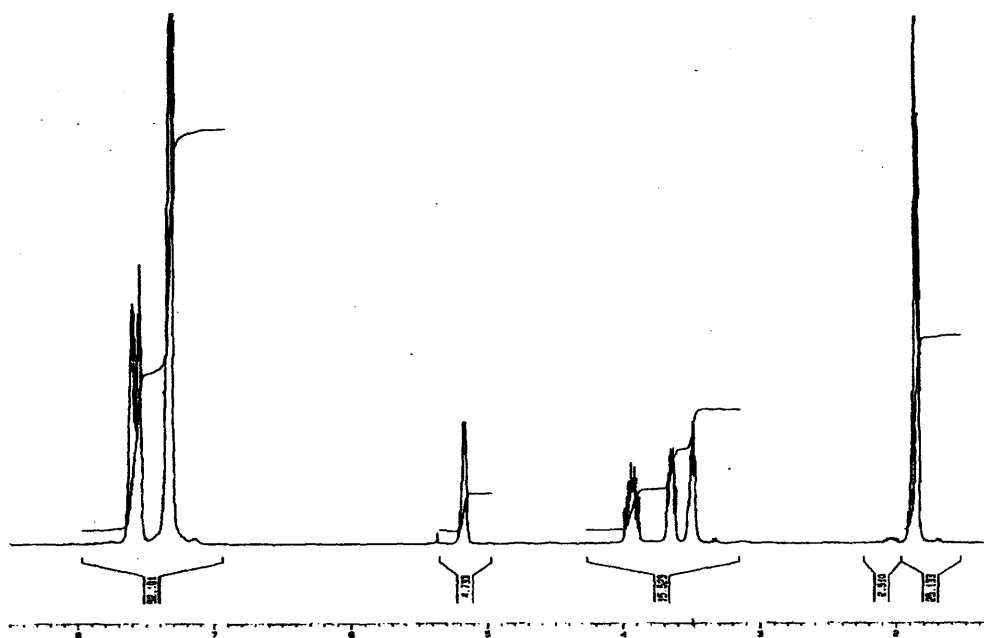


**Figure 3.1:**  $^1\text{H}$  NMR spectrum of  $[\text{Cu}(\text{ddppm})(\text{CH}_3\text{CN})_2]\text{PF}_6$ , **9** recorded in  $d^3\text{-CH}_3\text{CN}$ .

For complex **10**, the signals appear at lower frequency than in complex **9**. Their chemical shifts are at 3.20, 3.59, 3.75 and 4.76 ppm, therefore, this complex is also  $C_2$ -symmetric (see Figure 3.2).

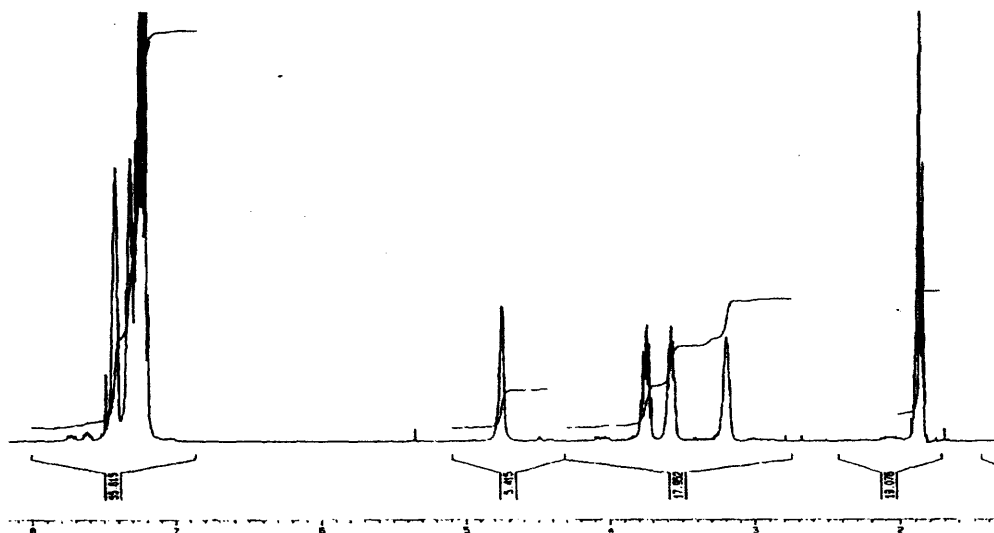
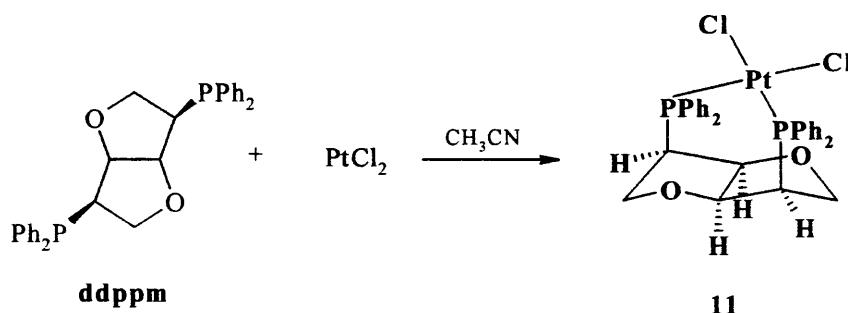


**Figure 3.2:**  $^1\text{H}$  NMR spectrum of  $[\text{Cu}(\text{ddppm})_2]\text{PF}_6$  **10** recorded in  $d^3\text{-CH}_3\text{CN}$ .

The Mass spectra (Low Resolution Electrospray) for complexes **9** and **10** do not show their molecular peak ion. The highest ion observed in both cases is at  $m/z$  545, corresponding to the  $[\text{Cu}(\text{ddppm})]^+$  cation.

### 3.2.2 Synthesis and characterization of the platinum complex $\text{Pt}(\text{ddppm})\text{Cl}_2$ (**11**).

Platinum complexes with phosphine ligands have been found to be active catalysts in a variety of enantioselective reactions, such as hydroformylation reactions.<sup>6</sup> **ddppm** and platinum dichloride were reacted in 1:1 ratio in hot acetonitrile to afford the complex  $\text{Pt}(\text{ddppm})\text{Cl}_2$  (**11**) as a white air stable solid, Scheme 3.3.



**Scheme 3.3:** Synthesis of  $\text{Pt}(\text{ddppm})\text{Cl}_2$ , **11**.

The NMR spectra of platinum complex **11** were recorded in  $d^1$ -chloroform at ambient temperature. The  $^{31}\text{P} \{^1\text{H}\}$  NMR spectrum of  $[\text{Pt}(\text{ddppm})\text{Cl}_2]$  shows a sharp peak at  $\delta$  8.47 ppm. This peak is flanked by platinum satellites resulting in a characteristic 1:4:1 pattern with a  $^1J(^{31}\text{P}, ^{195}\text{Pt})$  coupling constant of 3746 Hz, in agreement with a cis P arrangement.<sup>3</sup> This  $^1J(\text{PtP})$  value is comparable with other  $\text{Pt}(\text{II})$  complexes of chelating diphosphines e.g. 1,8-bis(diphenylphosphino)naphthalene,  $^1J(\text{PtP})$  3656 Hz.<sup>4</sup>

The  $^1\text{H}$  NMR spectrum of complex **11** illustrates four signals corresponding to the protons of the backbone of **ddppm**. This complex like the Cu(I)-**ddppm** complexes is symmetrical and the chemical shifts are at 3.37, 3.77, 4.14 and 5.04 ppm.

This platinum complex has been successfully crystallized and pale yellow crystals suitable for an X-ray structural analysis were obtained after recrystallisation by diffusion of ether in a chloroform solution of **11**. Crystallographic and experimental data are given in Table 3.2. A plot of the molecular structure is shown in Figure 3.3 and selected geometric data are presented in Table 3.3.

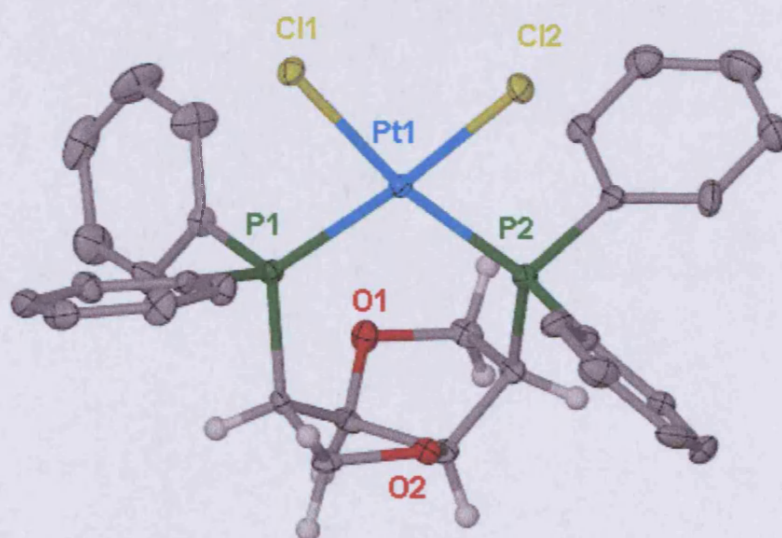


**Figure 3.3:** X-Seed <sup>5</sup> ellipsoid plot at 50% probability of the molecular structure of **11**. (Top view with reference to the coordination plane).

**Table 3.2:** Crystallographic data for Pt(ddppm)Cl<sub>2</sub>, **11**.

Formula	C33 H31 Cl11 O2 P2 Pt
Mol wt	1106.56
Crystal system	Orthorhombic
Space group	P 212121
a, Å	13.6098(2)
b, Å	17.0958(3)
c, Å	17.6043(4)
V, Å <sup>3</sup>	4096.00(13)
Z	4
Independent reflections	11665 [R(int) = 0.0872]
Reflections collected	23535
Final R indices [I > 2σ(I)]	R1 = 0.0620, wR2 = 0.1281
R indices (all data)	R1 = 0.0902, wR2 = 0.1456
GOF	1.070
Largest diff. peak and hole	1.127 and -2.715 e.Å <sup>-3</sup>

**Table 3.3:** Selected bond lengths (Å) and angles (deg) for Pt(ddppm)Cl<sub>2</sub>, **11**.

Cl(1)-Pt(1)	2.355(2)	P(2)-Pt(1)-P(1)	103.52(9)
Cl(2)-Pt(1)	2.350(2)	C(4)-C(1)-P(1)	112.5(6)
P(1)-Pt(1)	2.262(2)	C(2)-C(1)-P(1)	112.2(6)
P(2)-Pt(1)	2.261(2)	C(1)-P(1)-Pt(1)	121.5(3)
C(1)-P(1)	1.857(9)	C(13)-P(2)-C(7)	105.8(4)
C(2)-O(2)	1.415(11)	C(7)-P(2)-C(6)	103.8(4)
C(3)-O(2)	1.448(10)	C(7)-P(2)-Pt(1)	113.2(3)
C(4)-O(1)	1.414(11)	C(6)-P(2)-Pt(1)	122.2(3)
C(5)-O(1)	1.448(11)	P(2)-Pt(1)-Cl(2)	83.64(8)
C(6)-P(2)	1.836(9)	P(1)-Pt(1)-Cl(2)	171.93(9)
C(13)-P(2)	1.804(9)	P(2)-Pt(1)-Cl(1)	169.64(9)
C(7)-P(2)	1.809(9)	P(1)-Pt(1)-Cl(1)	86.78(9)
C(25)-P(1)	1.828(8)	Cl(2)-Pt(1)-Cl(1)	86.15(8)
C(19)-P(1)	1.846(9)		

The phosphorous and chloride atoms coordinated to platinum exhibit a distorted square planar arrangement. The mean bond lengths in the coordination plane are 2.35 Å for the Pt-Cl bonds and 2.26 Å for the Pt-P bonds similar to other examples of platinum diphosphine complexes. However, the bite angle ( $P_1$ -Pt- $P_2$ ) of this complex is 103.5° which is quite large for a square planar complex. For comparison the bite angles of a ferrocenyl diphosphine and dppe are 95.37° and 86.66°, respectively.<sup>6,7</sup> A distorted tetrahedral arrangement is observed around the phosphorus atoms imposed from the sterics of the backbone. It is also observed that the phenyl rings have intermediate positions between pseudo-axial and pseudo-equatorial positions (see Figure 3.4).

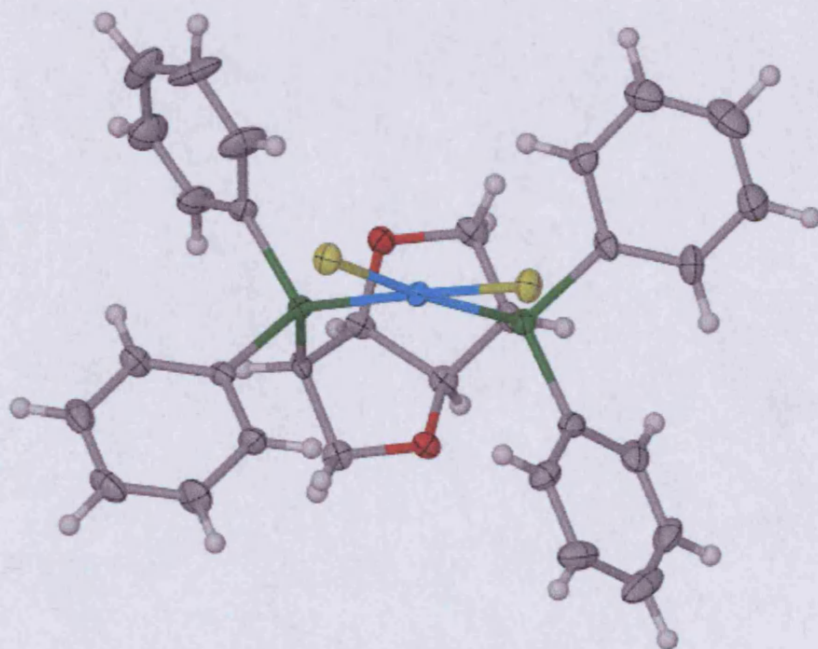


**Figure 3.4:** Side view of Pt(ddppm)Cl<sub>2</sub>, **11** with reference to the coordination plane.

### 3.2.3 Synthesis and characterization of palladium complexes with ddppm.

Palladium(II) complexes have been synthesized from different palladium precursors.

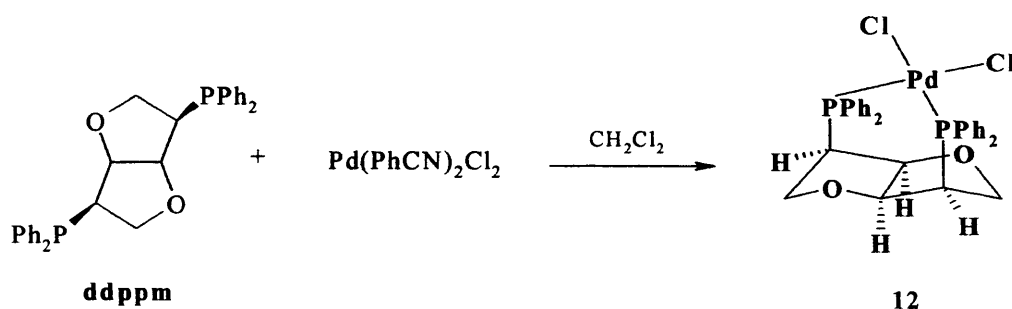
The syntheses of these compounds is discussed in the following sections:

#### 3.2.3.1 Synthesis of Pd(ddppm)Cl<sub>2</sub>, **12**

**ddppm** and palladium bis-benzonitrile dichloride were reacted in 1:1 ratio in dichloromethane to afford the square planar palladium complex Pd(ddppm)Cl<sub>2</sub> (**12**), see Scheme 3.4.

The NMR spectra of palladium complex **12** were recorded in d<sup>3</sup>-acetonitrile at ambient temperature. The <sup>31</sup>P{<sup>1</sup>H} NMR spectrum of [Pd(ddppm)Cl<sub>2</sub>] shows a singlet at δ 25.6 ppm.

The <sup>1</sup>H NMR spectrum of complex **12** illustrates four unresolved multiplets corresponding to the protons of the backbone of the phosphine **ddppm**. Chemical shifts for complex **12** are at δ 3.27, 3.79, 4.01 and 5.04 ppm, quite similar to the platinum complex **11**.



**Scheme 3.4:** Synthesis of Pd(ddppm)Cl<sub>2</sub>, **12**.



$\text{Pd}(\text{ddppm})\text{Br}_2$  and  $\text{Pd}(\text{ddppm})\text{I}_2$  were also synthesized and characterized by  $^{31}\text{P}\{^1\text{H}\}$  NMR, see Table 3.4.  $\text{Pd}(\text{ddppm})\text{Br}_2$  was prepared from  $\text{Pd}(\text{COD})\text{Br}_2$  following the same procedure as with complex **12**. However,  $\text{Pd}(\text{ddppm})\text{I}_2$  was synthesized from complex **12**. This complex was reacted with an excess of tetrabutylammonium iodide ( $\text{NBu}_4\text{I}$ ) in dichloromethane, after stirring the mixture for one hour, the solvent was evaporated and  $\text{NBu}_4\text{I}$  was extracted with methanol in which the complex  $\text{Pd}(\text{ddppm})\text{I}_2$ , **12** precipitates.

**Table 3.4:**  $^{31}\text{P}\{^1\text{H}\}$  chemical shifts of the palladium-ddppm halide complexes.

$^{31}\text{P}\{^1\text{H}\}$	$\text{Pd}(\text{ddppm})\text{Cl}_2$	$\text{Pd}(\text{ddppm})\text{Br}_2$	$\text{Pd}(\text{ddppm})\text{I}_2$
$\delta$ (ppm)	25.6	24.5	16.1

$\text{Pd}(\text{ddppm})\text{Cl}_2$  (**12**) has been structurally characterized; crystallographic and experimental data are given in Table 3.5. A plot of the molecular structure is shown in Figure 3.5 and selected geometric data are presented in Table 3.7.

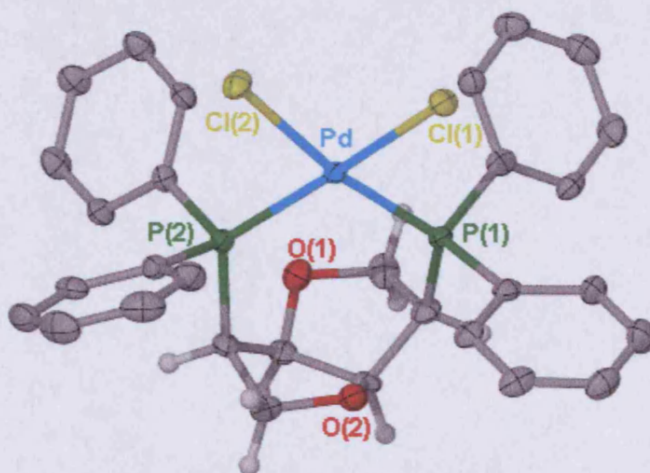


**Figure 3.5:** X-Seed <sup>5</sup> ellipsoid plot at 50% probability of the molecular structure **12**. (Top view with reference to the coordination plane).

**Table 3.5:** Crystallographic data for Pd(ddppm)Cl<sub>2</sub>, **12**.

Formula	C33 H31 Cl11 O2 P2 Pd
Mol wt	659.76
Crystal system	Monoclinic
Space group	P2(1)
a, Å	10.2360(3)
b, Å	12.9870(5)
c, Å	11.1880(3)
V, Å <sup>3</sup>	1388.11(8)
Z	2
Independent reflections	5736 [R(int) = 0.0879]
Reflections collected	15846
Final R indices [I>2sigma(I)]	R1 = 0.0406, wR2 = 0.0865
R indices (all data)	R1 = 0.0517, wR2 = 0.0916
GOF	1.019
Largest diff. peak and hole	0.593 and -0.736 e.Å <sup>-3</sup>

**Table 3.6:** Selected bond lengths (Å) and angles (deg) Pd(ddppm)Cl<sub>2</sub>, **12**.

Pd(1)-P(1)	2.2693(12)	P(1)-Pd(1)-P(2)	101.71(4)
Pd(1)-P(2)	2.2733(11)	P(1)-Pd(1)-Cl(1)	83.77(4)
Pd(1)-Cl(1)	2.3460(11)	P(2)-Pd(1)-Cl(1)	172.70(5)
Pd(1)-Cl(2)	2.3645(12)	P(1)-Pd(1)-Cl(2)	170.52(5)
P(1)-C(7)	1.820(5)	P(2)-Pd(1)-Cl(2)	85.29(4)
P(1)-C(13)	1.832(5)	Cl(1)-Pd(1)-Cl(2)	89.84(4)
P(1)-C(1)	1.854(5)	C(7)-P(1)-Pd(1)	109.72(16)
P(2)-C(19)	1.826(4)	C(13)-P(1)-Pd(1)	109.98(16)
P(2)-C(25)	1.841(5)	C(1)-P(1)-Pd(1)	124.26(17)
P(2)-C(6)	1.849(5)	C(19)-P(2)-Pd(1)	111.60(16)
O(1)-C(2)	1.422(6)	C(25)-P(2)-Pd(1)	108.28(15)
O(1)-C(3)	1.426(6)	C(6)-P(2)-Pd(1)	124.33(16)
O(2)-C(4)	1.423(6)		
O(2)-C(5)	1.426(6)		

The phosphorous and chloride atoms coordinated to palladium exhibit a distorted square planar arrangement. The mean bond lengths in the coordination plane are 2.35 Å for the Pd-Cl bonds and 2.25 Å for the Pd-P bonds similar to other examples of palladium diphosphine complexes.<sup>8</sup> As in the platinum complex **11**, a distorted tetrahedral arrangement is observed around the phosphorus atoms imposed from the sterics of the backbone. A line drawing of **12** (Figure 3.6) shows the two phosphine groups at intermediate positions between a pseudoaxial and pseudoequatorial conformation.

Pd(ddppm)Br<sub>2</sub> (**12b**) was also structurally characterized. A plot of the molecular structure is shown in Figure 3.6. Experimental data and geometric data are very similar to complex **12** and they are included in the CD of the thesis.

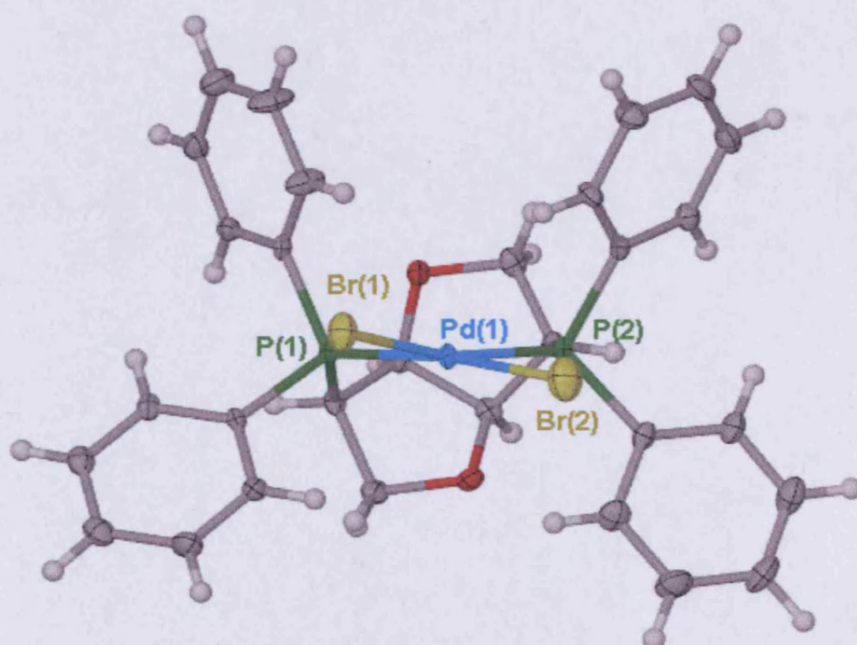


**Figure 3.6:** Side view of Pd(ddppm)Br<sub>2</sub>, **12b** with reference to the coordination plane.

The bite angle ( $P_1-Pd-P_2$ ) of complexes **12a** and **12b** are  $101.7^\circ$  and  $100.3^\circ$  respectively, which are smaller than in the platinum complex **11** ( $103.5^\circ$ ) but still large for a square planar complex. The ligand 11,12-bis(2,3,4,5-tetramethylphospholylmethyl)-9,10-dihydro-9,10-ethano-anthracene which also forms a seven-membered chelate palladium complex has a bite angle of  $99.75^\circ$ .<sup>8</sup> Figure 3.4 shows the drawing of this palladium dichloride complex.

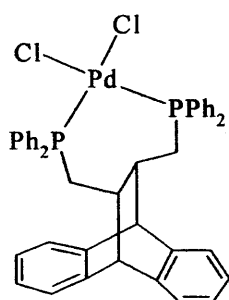


**Figure 3.7:** [*cis*-11,12-bis(diphenylphosphinomethyl)-9,10-dihydro-9,10-ethano-anthracene} $\}PdCl_2]$ .

### 3.2.3.2 Synthesis of $[Pd(ddppm)(\eta^3-C_3H_5)]PF_6$ , **13**.

The palladium allyl complex  $[Pd(ddppm)(\eta^3-C_3H_5)]PF_6$ , **13** has been synthesized in two steps. First, two equivalents of **ddppm** were reacted with one equivalent of palladium allyl chloride dimer in dichloromethane, subsequently the solvent was evaporated and the solid dissolved in acetonitrile. Potassium hexafluorophosphate was then added in order to exchange the anion chloride for a hexafluorophosphate anion, Scheme 3.5. The pale yellow solid obtained is moderately air-stable though it slowly decomposes.

**ddppm**-complexes synthesized so far were symmetrical consequently their  $^1\text{H}$  NMR and  $^{13}\text{C}\{^1\text{H}\}$  NMR spectra showed four and three signals for the **ddppm** backbone respectively. In complex **13** the  $C_2$  symmetry is lifted and all the backbone protons and carbons become non-equivalent. As a result their  $^1\text{H}$  NMR and  $^{13}\text{C}\{^1\text{H}\}$  NMR spectra shows eight and six signals for the **ddppm** backbone, respectively.

In the  $^1\text{H}$  NMR a multiplet at 5.86 ppm ( $J = 7\text{Hz}$ ) is assigned to the central allylic hydrogen, two broad signals at 4.21 and 4.48 ppm are assigned to *syn*-hydrogen atoms ( $\text{H}^1$ ,  $\text{H}^2$ ) and the signals at 3.58 ppm and 2.95 ppm assigned to *anti*-hydrogen atoms ( $\text{H}^3$ ,  $\text{H}^4$ ), see Figures 3.9 and 3.10. Resonances were assigned according to 2D-NMR data obtained for complex **13** (Figure 3.11).

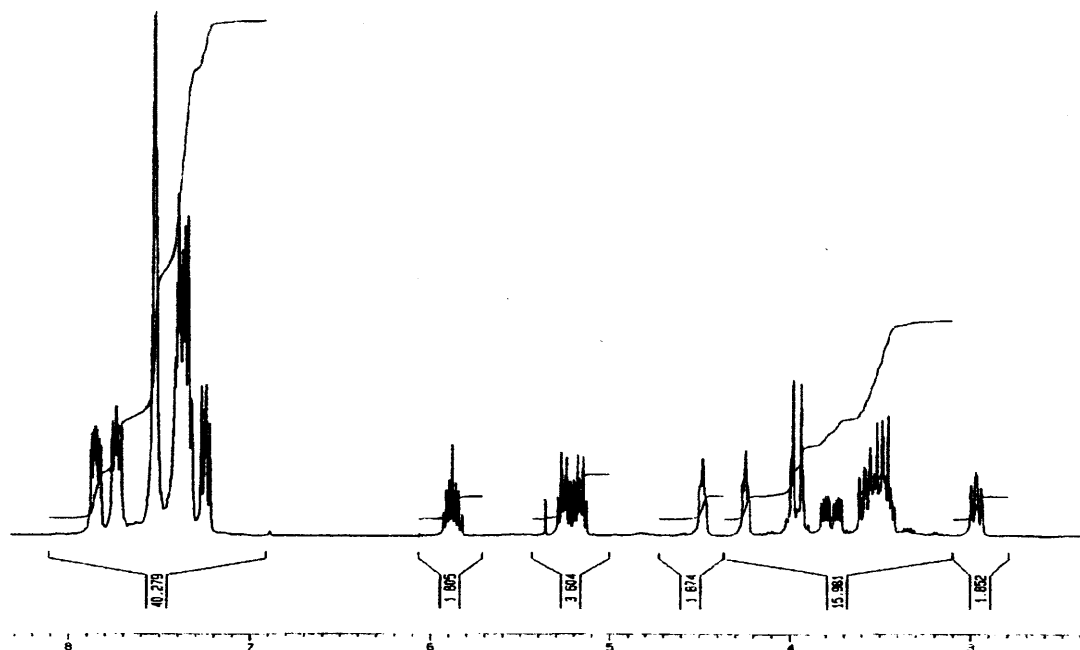
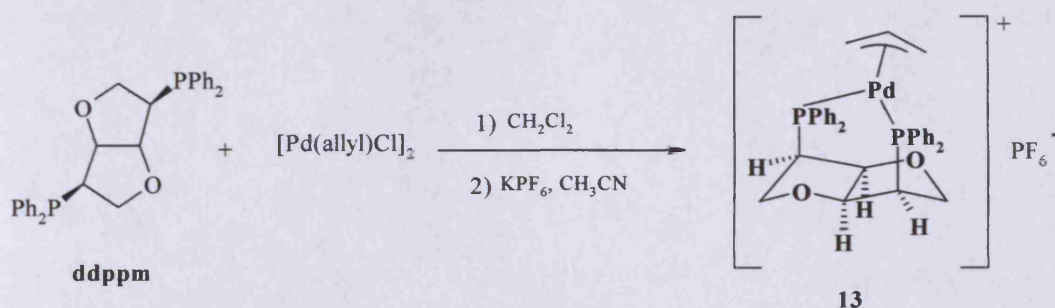


**Figure 3.9:**  $^1\text{H}$  NMR of  $[\text{Pd}(\text{ddppm})(\eta^3\text{-C}_3\text{H}_5)]\text{PF}_6$ , **13**.





**Scheme 3.5:** Synthesis of  $[\text{Pd}(\text{ddppm})(\eta^3\text{-C}_3\text{H}_5)]\text{PF}_6$ , **13**.

Although  $[\text{Pd}(\text{ddppm})(\eta^3\text{-C}_3\text{H}_5)]\text{PF}_6$  (**13**) has a  $C_2$  symmetry in the solid state, Figure 3.8, the NMR data shows that in solution this  $C_2$  symmetry is not observed.

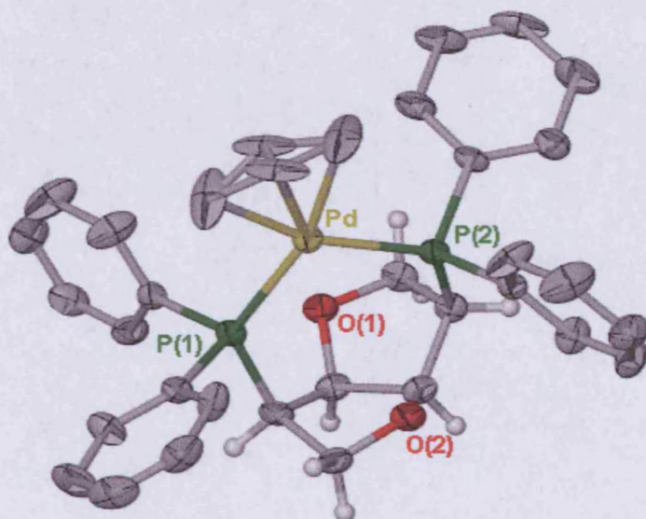


**Figure 3.8:** X-Seed<sup>5</sup> ellipsoid plot at 50% probability of the molecular structure **13**. (Top view with reference to the coordinate plane)

$^3\text{P}\{^1\text{H}\}$  NMR spectra recorded in  $d^3$ -acetonitrile at ambient temperature shows two sets of doublets at 22.3 ppm ( $^2J_{\text{PP}} = 45$  Hz) and 23.3 ppm ( $^2J_{\text{PP}} = 45$  Hz) due to the two non-equivalent phosphorus atoms. The magnitude of the coupling constant  $J_{\text{PP}}$  is similar to other Pd allyl diphosphine complexes such as  $[(\text{Pd}(\text{diop})(\eta^3\text{-C}_3\text{H}_5)]\text{BF}_4$  ( $^2J_{\text{PP}} = 44$  Hz).<sup>9</sup>

$^{13}\text{C}\{^1\text{H}\}$  NMR spectrum shows three signals in the allylic region that can be assigned to the three carbon atoms of the  $\text{C}_3\text{H}_5$  ligand, central  $\text{C}^2$  at 122.4 ppm and terminal carbons  $\text{C}^1$  and  $\text{C}^3$  as doublets at 77.7 ppm and 75.9 ppm both of which are coupled to the *trans* P atoms ( $J_{\text{CP}} = 28$  Hz).

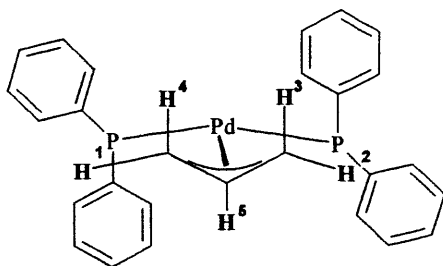


**Figure 3.10:** Structural fragment showing the protons of the allyl group of complex **13**.

$^1\text{H}$  2D-NOESY (Nuclear Overhauser Effect Spectroscopy) and  $^1\text{H}$  2D-COSY (Correlated Spectroscopy) were also done in order to assign the complete spectral data for complex **13** showing the interaction between the protons of the allyl group.

The COSY spectrum verifies that the central proton  $\text{H}^5$  at 5.86 ppm couples with all the terminal allylic protons ( $\text{H}^1$ ,  $\text{H}^2$ ,  $\text{H}^3$  and  $\text{H}^4$ ), see Figure 3.11 (circle peaks). It is also observed in this 2-D experiment a W-coupling ( $^4J$ ) between the two *syn*-protons ( $\text{H}^1$ ,  $\text{H}^2$ ), (see Fig. 3.11 square selection) and there is no evidence of coupling between the two-*syn* and *anti* protons ( $\text{H}^1/\text{H}^4$  or  $\text{H}^2/\text{H}^3$ ) ( $^2J_{\text{geminal}} \sim 0$ ).

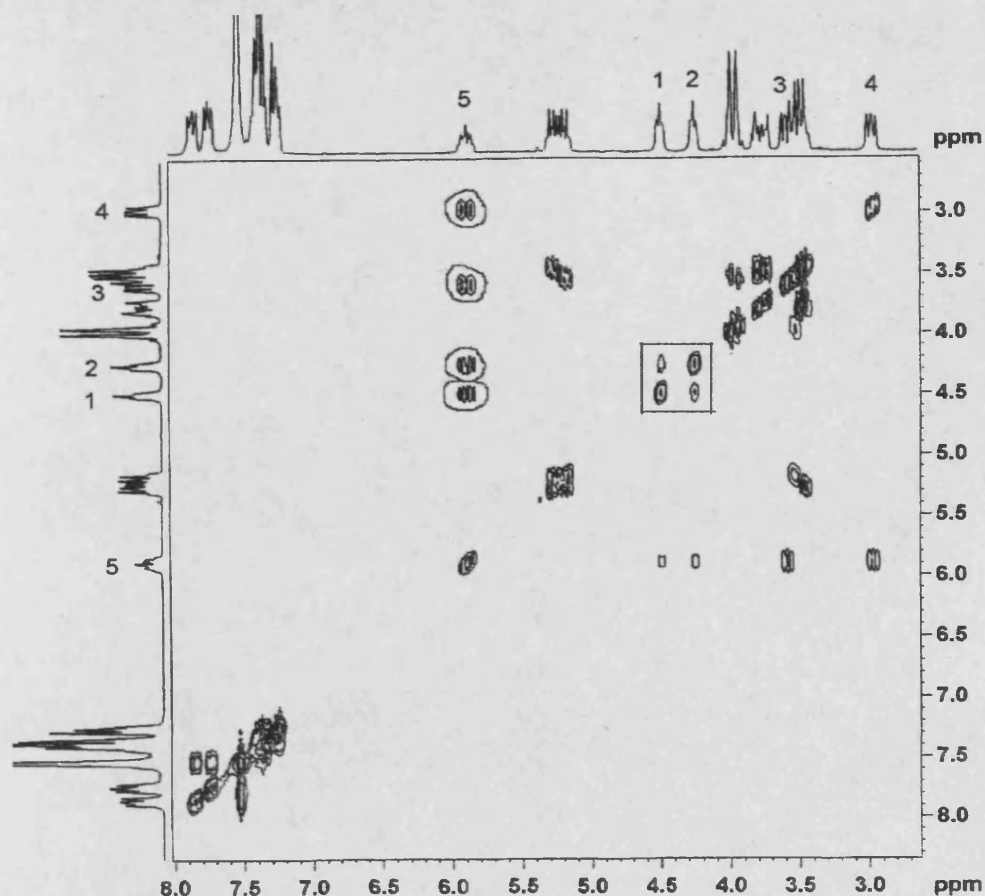


**Figure 3.11:**  $^1\text{H}$  2D-COSY of  $[\text{Pd}(\text{ddppm})(\eta^3\text{-C}_3\text{H}_5)]\text{PF}_6$ , **13** showing the interaction between  $\text{H}^5$  with  $\text{H}^1$ ,  $\text{H}^2$ ,  $\text{H}^3$  and  $\text{H}^4$  (circle peaks).

The NOESY spectrum is shown in Figure 3.12: the central allylic proton,  $\text{H}^5$  exhibits spatial interactions to both allylic *syn*-protons,  $\text{H}^1$  and  $\text{H}^2$  (A). There are also NOE cross-peaks between  $\text{H}^1$  and  $\text{H}^4$  (B) and between  $\text{H}^2$  and  $\text{H}^3$  (C). Figure 3.12 also shows the area of the phenyl protons where there are cross-peaks between *ortho*-phenyl and *para*-phenyl protons with the terminal allylic protons:  $\text{H}^2$  and  $\text{H}^4$  show spatial proximity with the *ortho* protons (E, G respectively) and  $\text{H}^1$  and  $\text{H}^3$  with the *para*-protons (D, F respectively). Each



of them (D, E, F, G) corresponds to the spatial interactions between protons from a different phenyl group.

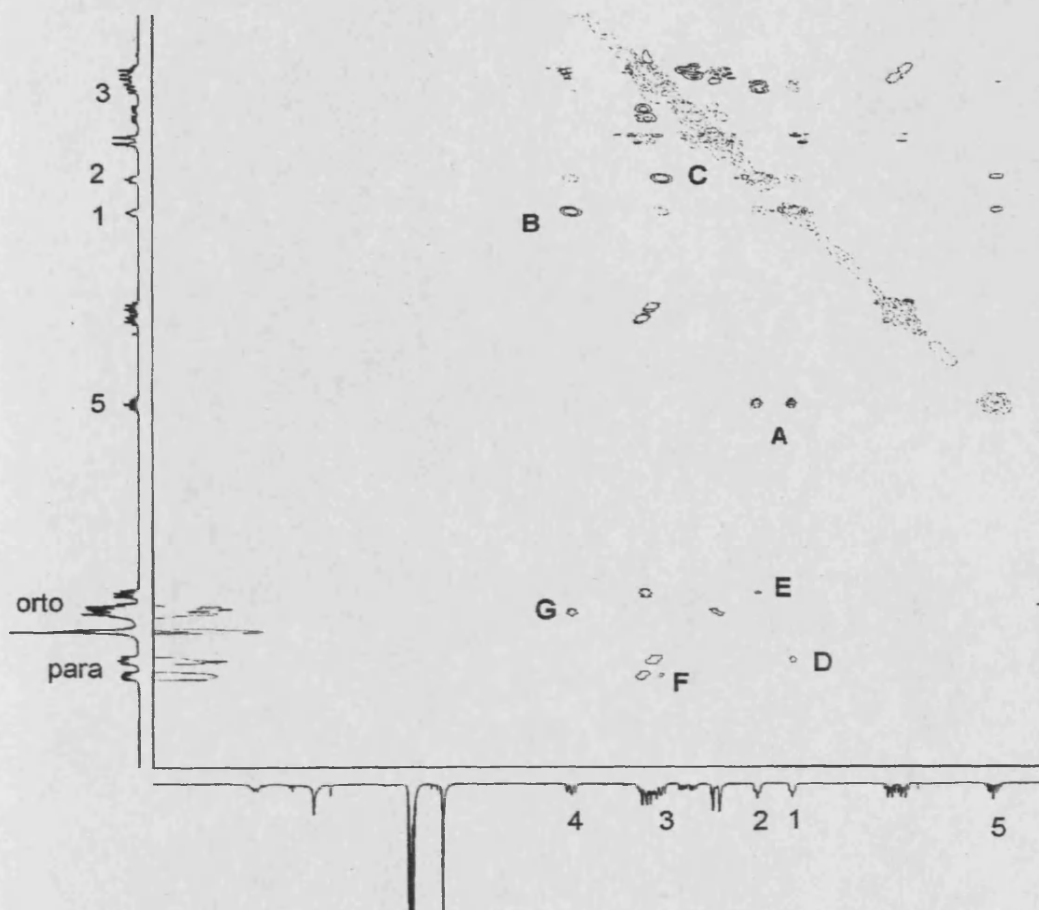


**Figure 3.12:** One possible assignation of the terminal protons with the  $^1\text{H}$  2D-NOESY of  $[\text{Pd}(\text{ddppm})(\eta^3\text{-C}_3\text{H}_5)]\text{PF}_6$ , **13**.

Pale yellow crystals suitable for an X-ray structural analysis were obtained after recrystallisation by diffusion in acetonitrile with ether. Crystallographic and experimental data are given in Table 3.5. A plot of the molecular structure is shown in Figure 3.8 and selected geometric data is presented in Table 3.6.

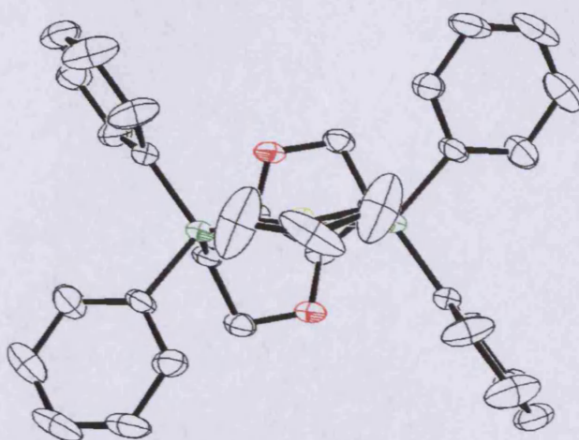


**Figure 3.13:** ORTEP<sup>10</sup> ellipsoid plot at 50% probability of the molecular structure **13**. (Top view with reference to the coordinate plane).

**Table 3.5:** Crystallographic data for [Pd(ddppm)( $\eta^3$ -C<sub>3</sub>H<sub>5</sub>)]PF<sub>6</sub>, **13**

Formula	C <sub>33</sub> H <sub>33</sub> F <sub>6</sub> O <sub>2</sub> P <sub>3</sub> Pd
Mol wt	769.86
Crystal system	Trigonal
Space group	<i>P</i> 3 <sub>1</sub> 2 <sub>1</sub>
<i>a</i> , Å	10.2066(14)
<i>b</i> , Å	10.2066(14)
<i>c</i> , Å	26.143(5)
<i>V</i> , Å <sup>3</sup>	2358.6(6)
Independent reflections	3599 [ <i>R</i> <sub>int</sub> = 0.0565]
Reflections collected	16230
Final <i>R</i> indices [ <i>I</i> > 2σ( <i>I</i> )]	<i>R</i> 1 = 0.0422, <i>wR</i> 2 = 0.0889
<i>R</i> indices (all data)	<i>R</i> 1 = 0.0599, <i>wR</i> 2 = 0.0955
GOF	1.039
Largest diff. peak and hole	0.461 and −0.516 e Å <sup>−3</sup>

**Table 3.6:** Selected bond lengths (Å) and angles (deg) Pd(ddppm)( $\eta^3$ -C<sub>3</sub>H<sub>5</sub>)PF<sub>6</sub>, **13**

P(1)–Pd(1)	2.3134(12)	P(1)–Pd(1)–P(1)i	104.06(6)
Pd(1)–P(1)i	2.3134(12)	C(2)i–C(1)–Pd(1)	70.5(4)
Pd(1)–C(2)i	2.152(8)	C(2)–C(1)–Pd(1)	70.3(4)
Pd(1)–C(1)i	2.205(5)	C(2)i–Pd(1)–C(1)	34.6(2)
C(1)–Pd(1)	2.205(5)	C(2)–Pd(1)–C(1)	34.9(2)
C(1)–C(2)i	1.298(9)	C(1)i–Pd(1)–C(1)	67.4(4)
C1)–C(2)	1.307(9)	C(2)i–Pd(1)–P(1)	128.05(16)
C(2)–C(1)i	1.298(9)	C(2)–Pd(1)–P(1)	126.79(17)
C(3)–C(5)	1.519(6)	C(1)i–Pd(1)–P(1)	94.32(19)
C(3)–C(4)	1.544(5)	C(1)–Pd(1)–P(1)	161.54(18)
C(3)–P(1)	1.845(4)	C(2)i–Pd(1)–P(1)i	126.79(17)
C(4)–O(1)	1.428(5)	C(2)–Pd(1)–P(1)i	128.05(15)
C(5)–O(1)i	1.436(4)	C(1)i–Pd(1)–P(1)i	161.54(18)
C(6)–P(1)	1.825(4)	C(1)–Pd(1)–P(1)i	94.32(19)

As expected for Pd allyl complexes of this type, the coordination geometry of **13** is pseudo-square planar, with the four coordination sites occupied by the two phosphorus atoms and the allylic termini carbons. The bite angle (P<sub>1</sub>–Pd–P<sub>2</sub>) for this complex is 104.06°, it is the largest observed so far within the range of bidentate complexes with ddppm. The two Pd–P distances are both 2.31 Å and the distances between the Pd atom and the two terminal allylic carbon atoms (C<sup>1</sup>) are 2.205 Å. These distances are quite similar to other Pd allyl diphosphine complexes such as [Pd( $\eta^3$ -allyl)(dppn)]BF<sub>4</sub><sup>11</sup> and [Pd ( $\eta^3$ -1,3-diphenylallyl)((S,S)-chiraphos)]BF<sub>4</sub>.<sup>12</sup>

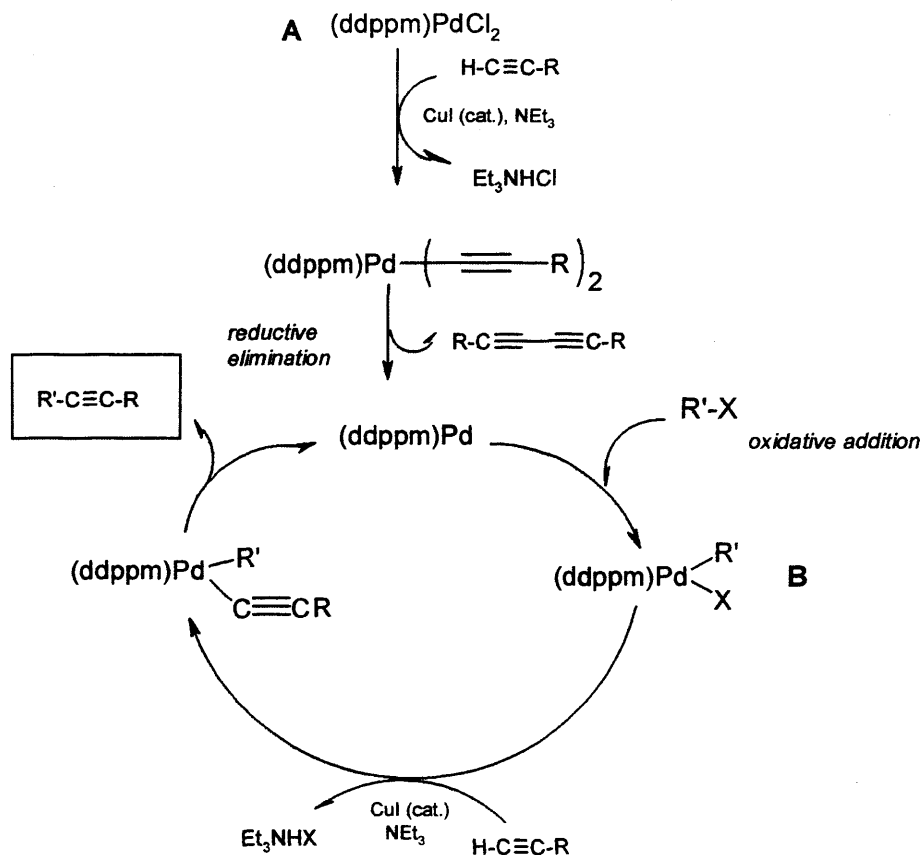
### 3.3 **PALLADIUM CATALYZED REACTIONS.**

Catalytic activity of palladium complex **12** has been tested in the Sonagashira reaction and carbonylation of different substrates. Furthermore, palladium complex **13** was tested in allylic reactions. In the next section, description of these catalytic reactions and their results are described.

#### 3.3.1 **C-C coupling reactions: Sonagashira reaction**

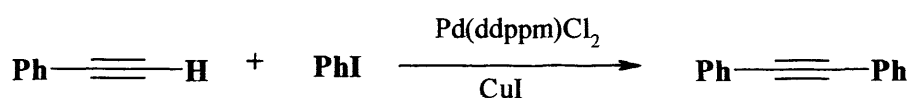
The Sonogashira coupling reaction (a Pd-Cu catalysed cross-coupling reaction) of terminal acetylenes with aryl and vinyl halides provides a powerful method for synthesizing conjugated alkynes, an important class of molecules that have found application in diverse areas ranging from natural product chemistry to materials science.<sup>13</sup> With respect to the organic halide, the following order of reactivity has been observed: vinyl iodide  $\approx$  vinyl bromide > aryl iodide > vinyl chloride  $\gg$  aryl bromide. For aryl bromides, the least reactive of the commonly employed organic halides, efficient Sonogashira coupling typically requires heating to  $\sim 80$  °C.<sup>14</sup>

Although the reaction certainly follows the normal oxidative addition-reductive elimination process common to the Pd-catalyzed C-C bond forming reactions, the exact mechanism for the reaction is not known. In particular, the structure of the catalytically active species and the role of the CuI catalyst remain obscure. The process may be considered to involve Pd<sup>0</sup> species, which is generated from the Pd(II) precatalyst **A** and gives the Pd(II) intermediate **B** by the oxidative addition of the sp<sup>2</sup>-C halide (scheme 3.6).<sup>13</sup>



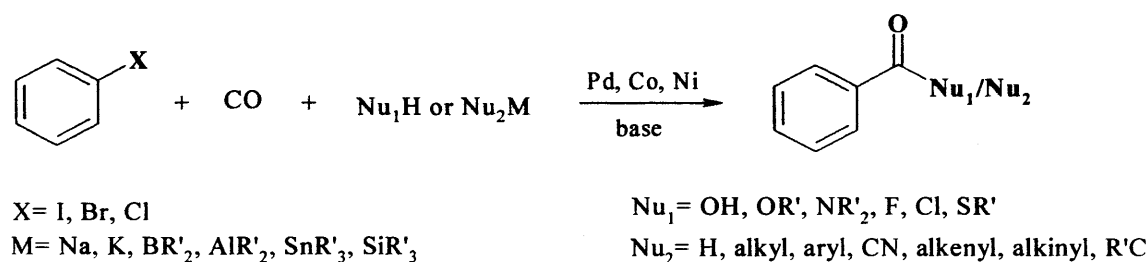
Scheme 3.6: Catalytic cycle of the Sonagashira reaction

The palladium dihalide catalyst,  $\text{Pd}(\text{ddppm})\text{Cl}_2$ , **12** was used in a Sonagashira reaction. Phenylacetylene was reacted with iodobenzene using 1% of Pd catalyst **12**. A catalytic amount of CuI (3% mol) and equimolecular amounts of a base ( $\text{NEt}_3$ ) were necessary to facilitate the substitution reaction.<sup>15</sup> The reaction mixture was stirred for 2h at 60°C obtaining 96% yield of diphenylethyne (Scheme 3.7). For comparison, 3-5% of  $\text{Pd}(\text{PPh}_3)_2\text{Cl}_2$  afford diphenylacetylene at 85 % yield.<sup>16</sup>

Scheme 3.7: Sonagashira reaction of phenylacetylene with  $[\text{Pd}(\text{ddppm})\text{Cl}_2]$  **12**.

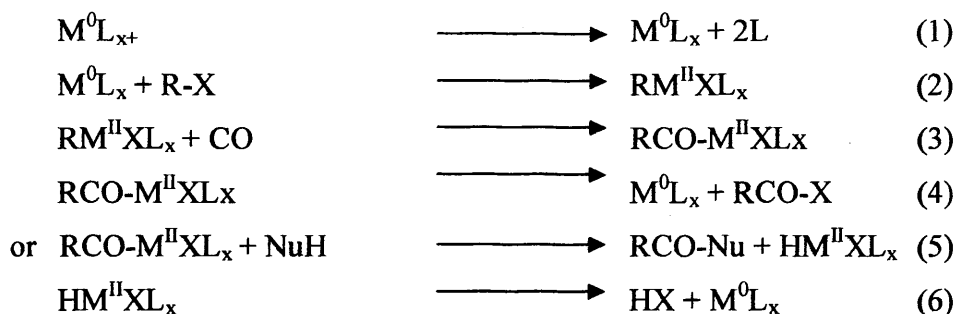
### 3.3.2 Carbonylation of Aryl-halide compounds

Palladium-catalysed C-C bond formation with aryl halides is, at the moment, one of the most important organometallic reactions used in synthetic organic chemistry. However, the palladium-catalysed carbonylation has been investigated far less intensively than the well-known Heck, Suzuki, or Stille reactions, although it offers the practical preparation of a broad spectrum of aromatic carboxylic acid derivatives from simple, commercially available building blocks as shown in Scheme 3.8.<sup>17</sup>



**Scheme 3.8:** Carbonylation of aryl-X compounds.

This reaction is thought to proceed according to the Scheme 3.9. The salient points of the mechanism include: ligand dissociation to the active catalyst (eq. (1)), oxidative addition (eq. (2)) of the organic compound to a metal (0) complex ( $\text{M} = \text{Pd, Co, Ni, Rh, Pt, Fe}$ ;  $\text{L} = \text{PR}_3$ ), CO insertion forming a metal (II) acyl complex (eq. (3)), either reductive elimination (eq. (4)) or reaction of this complex with nucleophiles yielding the carbonylated product and an X(hydrido)metal (II) complex (eq. (5)) and elimination of HX to regenerate the original catalyst (eq. (6)).<sup>18</sup>



**Scheme 3.9:** General mechanism of the carbonylation of C-X.

The palladium dichloride complex **12** has been used as a catalyst in these aryl halide carbonylation reactions. Low carbon monoxide pressures were used (4 bar) however high temperatures are needed for the reaction to be done.

The conversion of iodobenzene to the corresponding carboxylic ester proceeded quantitatively in methanol using  $\text{Na}_2\text{CO}_3$  with 0.5% catalyst at 4 bars of CO and 145 °C (Table 3.7, entry 1). However, when bromobenzene was used, a stronger base was necessary (triethylamine). Using the same amount of Pd catalyst (0.5%) only 30% of the final product was obtained (entry 2).

When chlorobenzene was tested less than 5% yield was obtained (entry 3). This reactivity order was expected because chloroarenes are more inert. This is due to the dissociation energy of the  $\text{C}(\text{sp}^2)\text{-Cl}$  bond being relatively stronger (402, 339 and 272 kJ  $\text{mol}^{-1}$  for PhCl, PhBr, and PhI, respectively, at 298 K). The main problem is the coordination of CO to the metal centre, the  $\pi$ -acceptor character of this ligand reduces the activity of the palladium complex towards oxidative insertion into the C-Cl bond. An additional difficulty is that the agglomeration of Pd atoms and the formation of clusters, which deactivate the catalyst, proceed in the presence of CO.<sup>19</sup>

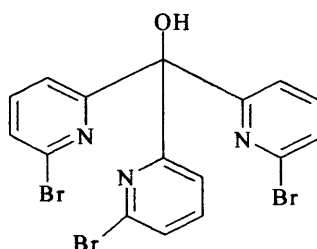
**Table 3.7:** Alkoxycarbonylation of arylhalides in the presence of PdCl<sub>2</sub>(ddppm), 12.<sup>a</sup>

Entry	Substrate	Solvent	Base	p co (bar)	T [°C]	Yield [%] <sup>b</sup>
1 <sup>a</sup>	PhI	MeOH	Na <sub>2</sub> CO <sub>3</sub>	4	145	100
2 <sup>a</sup>	PhBr	EtOH	NEt <sub>3</sub>	4	145	30
3 <sup>a</sup>	PhCl	MeOH	Na <sub>2</sub> CO <sub>3</sub>	4	145	< 5
4 <sup>c</sup>	TBPM <sup>d</sup>	MeOH	NEt <sub>3</sub>	4	100	50%

[a] 2 mmol substrate, 0.5 % Pd catalyst 12, 5 ml of corresponding alcohol, 24 h. [b] Determined by <sup>1</sup>H NMR (400 MHz). [c] 8 mmol substrate, 1% Pd catalyst 12, 79 mmol NEt<sub>3</sub>, 250 mmol MeOH and Toluene. [d] TBPM: tris(2-bromo-6-pyridyl)methanol (see Figure 3.14).

In addition to the carbonylation of these halide benzenes, carbonylation of N-heteroaryl halides have also been of interest. N-heterocyclic carboxylic acid derivatives are useful intermediates for the synthesis of a number of biologically active molecules, with pyridine derivatives being particularly important intermediates for pharmaceuticals and agrochemicals.<sup>20</sup>

Table 3.7 shows the result of the carbonylation of a substrate such as tris(2-bromo-6-pyridyl)methanol (TBPM, Figure 3.14).

**Figure 3.14:** TBPM: tris(2-bromo-6-pyridyl)methanol

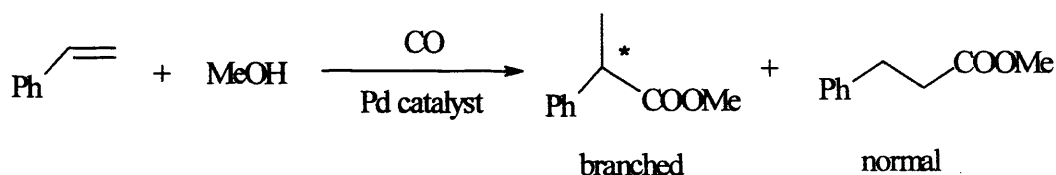


This reaction was carried out at 4 bar of CO in a stainless steel glass autoclave and 100 °C in methanol. Only 1% of palladium complex **12** was employed and the reaction was stirred for 3 days. After that, a chromatographic column was done and 50 % of the product (trisubstituted ester of TBPM) was obtained (entry 4). Any other products have not been characterized. In comparison, the same yield was obtained using Pd(PPh<sub>3</sub>)<sub>4</sub>, though, 5% of the Pd catalyst was necessary.<sup>21</sup>

Beller et al. have done several reactions with a substrate such as 2-chloropyridine with n-butanol. Large chelate ligands such as dppb and dppf were used obtaining conversions up to 95 %. They also observed that decreasing the pressure from 25 to 1 bar decreased the yield from 95 to 9 %.<sup>22</sup>

### 3.3.3 Hydroesterification of styrene

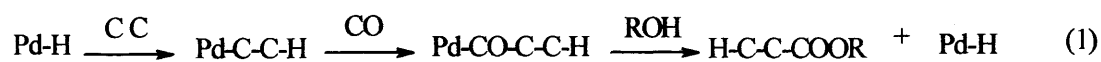
Catalytic hydroesterification of olefins with CO and an alcohol has attracted considerable interest for the synthesis of industrially important carboxylic esters. Transition metal catalysed hydroesterification of olefins usually affords a mixture of normal and branched esters, Scheme 3.10. The branched acid esters derived from arylenes are useful precursors for 2-arylpropionic acids such as ibuprofen and naproxen (non-steroidal anti-inflammatory drugs).<sup>23</sup>



**Scheme 3.10:** Hydroesterification of Styrene

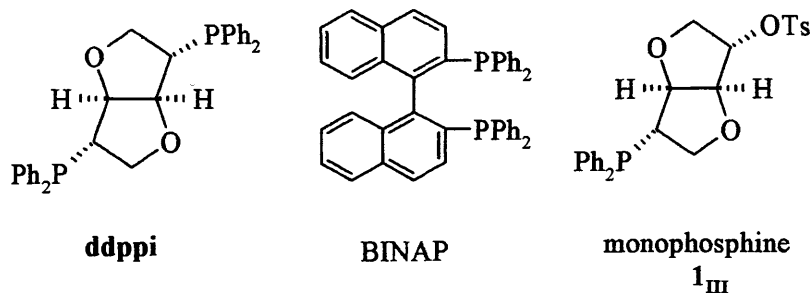
The most investigated catalysts are cobalt and palladium compounds. The synthesis of esters with palladium catalysts requires relatively lower temperatures (50-125°C) as compared to cobalt catalysts (>140°C). However, mixtures of regio isomers are often obtained and a rather high pressure of CO (100 atm or more) is required for the palladium-catalyzed reaction.<sup>24</sup>

Two mechanistic pathways proposed for the hydroesterification of olefins catalysed by palladium complexes are a (a) hydride mechanism, which is initiated by the insertion of an olefin into a palladium-hydride bond and proceeds through the formation of an acyl complex as shown in Eq. 1, and (b) alkoxy mechanism, which is initiated by the insertion of an olefin into a palladium-carboalkoxy bond Eq. 2.<sup>25</sup>



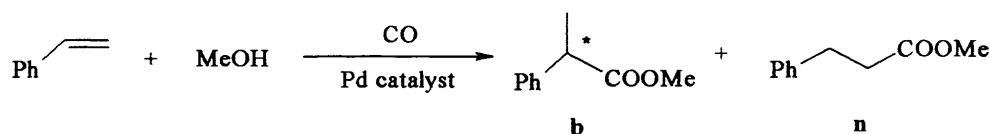
**Scheme 3.11:** Two mechanistic pathways for the hydroesterification of olefins catalysed by palladium complexes.

The first asymmetric hydroesterification of styrene was reported by Zhou et al. using the PdCl<sub>2</sub>-CuCl<sub>2</sub>-chiral phosphine catalyst system.<sup>26</sup> Three different phosphine ligands, **ddppi**, monophosphine **1<sub>III</sub>** and BINAP were used at 50 atm of CO and 100 °C in methanol and methyl ethyl ketone. **ddppi**, is the epimer of **ddppm** and it is a non-chelating ligand (see Chapter 2), BINAP is the well-known bidentate diphosphine and the other phosphine used was a monophosphine derived from D-mannitol.



The nature of chiral phosphine ligands plays an important role in catalytic reactions such as asymmetric hydroesterification. Some results taken from the literature are shown in Table 3.8a. This table shows for example that **ddpfi** was an effective ligand for this reaction affording 93% of the branched product (entry 1). When BINAP was used as a ligand, only 3.6% of the branched product was formed (entry 3). The best enantioselectivity was obtained with **ddpfi** (99%, entry 1) and when monophosphine **1<sub>III</sub>** was used, complete conversion to the branched ester was obtained but the enantioselectivity was poor (38%, entry 2).

**Table 3.8a:** Asymmetric hydroesterification of styrene catalysed by chiral phosphine ligands.



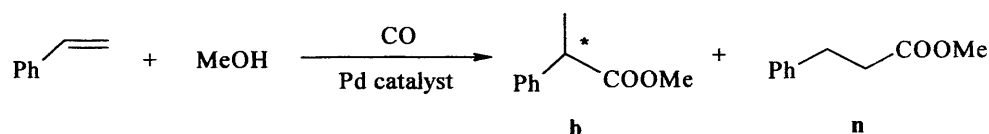
Entry	Ligands	% Pd	p (atm)	Conversion %	Yields of esters		
					(%) <sup>b</sup>		% ee
					b	n	
1 <sup>a</sup>	<b>ddpfi</b>	1.6 %	50	~ 100	92.8	7.2	99
2 <sup>a</sup>	Monophosphine <b>1<sub>III</sub></b>	1.6 %	50	~ 100	~ 100	trace	38
3 <sup>a</sup>	BINAP	1.6 %	50	14.9	3.6	11.3	-

*Reaction conditions:* [a] PdCl<sub>2</sub> 0.08 mmol, CuCl<sub>2</sub> 0.18 mmol, 80°C, 24 h, styrene 0.5 ml, methanol 5 ml, 2-butanone 5 ml. [b] Yields based on the starting olefin, styrene.

Hydroesterification of styrene using palladium dihalide catalyst **12** was carried out under the same conditions and no reaction was observed (entry 1, Table 3.8b). Subsequently, it was decided to employ a cationic palladium complex derived from this palladium dihalide complex (**12**). Cationic complexes are usually preferred for this type of reactions due to the easily displaced coordinating solvent molecules.<sup>24</sup>

The reaction with this cationic complex,  $[\text{Pd}(\text{ddppm})(\text{MeCN})_2](\text{BF}_4)_2$ , was carried out in a stainless steel 300 ml autoclave at 40 atm of carbon monoxide and at 80 °C.  $\text{CuCl}_2$  was not used in this case and the solvent employed was methyl ethyl ketone and methanol as the alcohol. Table 3.8b shows in entry 2 that the branched ester was obtained as the major product (22%) while only 4% of the linear product was obtained. This result is a bit better than when BINAP was used as a ligand (entry 3, Table 3.8a). Enantioselectivities for entry 1 in Table 3.8b was not calculated due to the low yield obtained.

**Table 3.8b:** Asymmetric hydroesterification of styrene catalysed by chiral phosphine ligands.



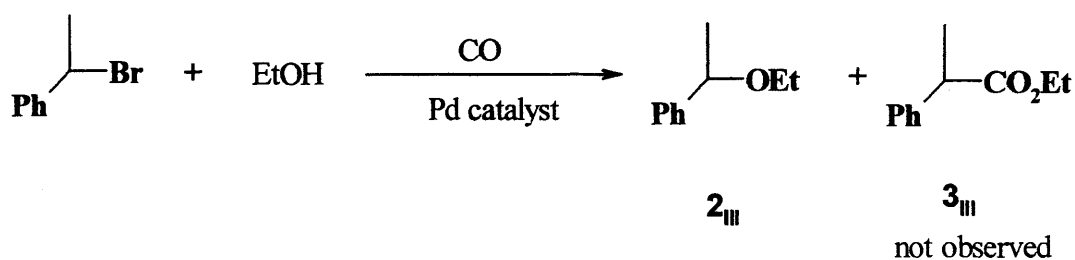
Entry	Ligands	% Pd	p (atm)	Conversion %	Yields of esters		% ee
					(%) <sup>d</sup>		
					b	n	
1 <sup>a</sup>	Pd(ddppm)Cl <sub>2</sub> , <b>12</b>	1 %	50	-	-	-	-
2 <sup>b</sup>	[Pd(ddppm)(MeCN) <sub>2</sub> ](BF <sub>4</sub> ) <sub>2</sub> <sup>c</sup>	1 %	40	26	4	22	-

*Reaction conditions:* [a] Pd(ddppm)Cl, 0.04 mmol, CuCl<sub>2</sub> 0.18 mmol, 48 h, styrene 0.5 ml, methanol 5 ml, DME 45ml [b] Pd precatalyst 0.05 mmol, 80°C, 3 days, styrene 0.5ml, methanol 5 ml, 2-butanone 40 ml. [c] 0.10 mmol of Pd(ddppm)Cl<sub>2</sub> (**12**), 0.20 mmol AgBF<sub>4</sub>, 15 ml MeCN. [d] Yields based on the starting olefin, styrene.

### 3.3.4 Catalytic carbonylation of benzylic substrates.

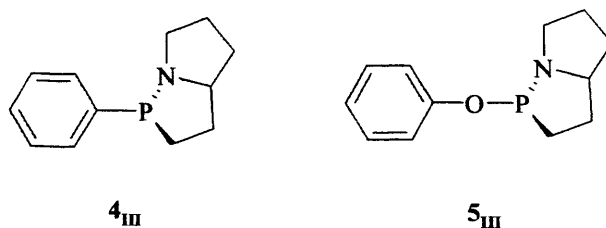
Another possible route for the preparation of arylpropionic esters is carbonylation of benzylic substrates such as 1-bromoethylbenzene, benzyl bromide and benzyl alcohol.

The first one to be described is the carbonylation of 1-bromoethylbenzene. (see Scheme 3.11). This reaction was carried out at 4 bar of CO and 60 °C in ethanol in a 100 ml glass autoclave. 1% of palladium catalyst **12** and Na<sub>2</sub>CO<sub>3</sub> as the base were used (see Table 3.8, entry 1). The result from this reaction was not the desired product ethyl 2-phenylpropionate (**3<sub>III</sub>**) and instead 1-phenylethanol (**2<sub>III</sub>**) was obtained.

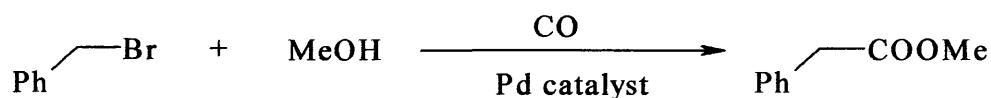


**Scheme 3.11: Carbonylation of 1-bromoethylbenzene**

Carbonylation of  $\alpha$ -bromoethylbenzene is a well established reaction and diphosphines such as DIOP have been tested obtaining low yields. Furthermore, carbonylation with oxazaphospholane-palladium complexes (**4**<sub>III</sub>, **5**<sub>III</sub>) gave better yields (65%). Less than 5% of 1-phenylethanol was also observed.<sup>27</sup>



The second substrate used to synthesize carboxylic esters was benzyl bromide, see following Scheme:

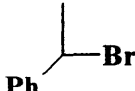
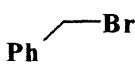
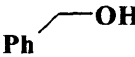


**Scheme 3.12:** Carbonylation of benzyl bromide.

Using benzyl halides to synthesize esters of phenylacetic acid is a less expensive method in comparison to the traditional synthesis based on two-step process – conversion of benzyl chloride to benzyl cyanide and subsequent hydrolysis of cyanide with sulphuric acid.<sup>28</sup>

Unlike aryl halides, benzylic derivatives are susceptible to nucleophilic attack and elimination reactions. Thus, over the past fifteen years, considerable effort has been directed to the development of mild and more selective reaction conditions, e.g. atmospheric pressure carbonylation.<sup>29</sup>

**Table 3.8:** Carbonylation of different organic substrates using PdCl<sub>2</sub>(ddppm), 12.<sup>a</sup>

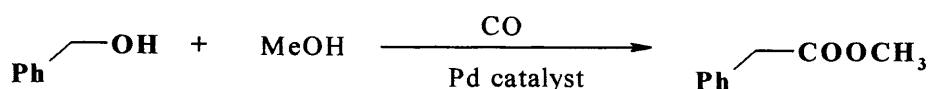
Entry	Substrate	% Pd catalyst	T (°C)	p (bar)	Yield <sup>d</sup>
1 <sup>a</sup>		1	60	4	-
2 <sup>b</sup>		1	60	2	98 %
3 <sup>c</sup>		1	100	40	-

Reaction conditions: [a] 1 mmol substrate, 1% Pd(ddppm)Cl<sub>2</sub> (12), 1.2 mmol Na<sub>2</sub>CO<sub>3</sub>, 4 bar CO, 60°C, EtOH, 16 h. [b] 1 mmol substrate, 0.01 mmol Pd<sub>3</sub>(OAc)<sub>6</sub>, 0.02 mmol **ddppm**, 1.1 mmol NEt<sub>3</sub>, Toluene/MeOH (1:1) 5ml, 2 bar CO, 60° C, 16 h. [c] 5 mmol substrate, 1 mmol p-TsOH, 1% Pd(ddppm)Br<sub>2</sub>, 2% CuCl<sub>2</sub>, 40 bar CO, 100 °C, 5 ml MeOH, 40 ml methyl ethyl ketone. [d] Determined by <sup>1</sup>H NMR analysis.

When **ddppm** was used as a ligand for the carbonylation of benzyl bromide, good conversion of the ester was obtained (98%, entry 2).<sup>30</sup> The reaction was carried out at low pressure of carbon monoxide (4 bar) and only 1 mol % Pd(OAc)<sub>2</sub> and 2 mol % of ligand **ddppm** were used (entry 2). A mixture of toluene and methanol in ratio 1:1 was used as a solvent and an amine such as diisopropylethylamine was also needed to act as a base.

It has been reported that the carbonylation of benzyl chloride to phenylacetic acid is used industrially by Montedison.<sup>31</sup> The carbonylation is conducted in a two-phase medium of an non-polar solvent and 40% aqueous NaOH solution with a cobalt carbonyl complex and a benzyltrialkylammonium surfactant.<sup>28</sup> A major problem for most carbonylations of benzylic halides is the large amount of catalyst (1-20mol %) and phase transfer reagent (5-10 mol %) needed for high conversion and yields. In order to expand industrial use, improvements have to be made in the future. Using water soluble Pd catalysts with TPPTS as ligand offer efficient product separation along with more active catalyst systems reaching TON of more than 1500.<sup>32</sup>

However, using organic halides to prepare carboxylic acids and derivatives has the disadvantage that the halide employed has to be eventually removed as a salt with a base. This is neither environmentally favourable nor preferable from the economic viewpoint.<sup>33</sup> Therefore, the carbonylation of benzyl alcohol to methyl phenyl acetate was attempted. The reaction was tried using the palladium dihalide derived from **ddppm** (**12**), see following Scheme 3.13:



**Scheme 3.13:** Carbonylation of benzyl alcohol

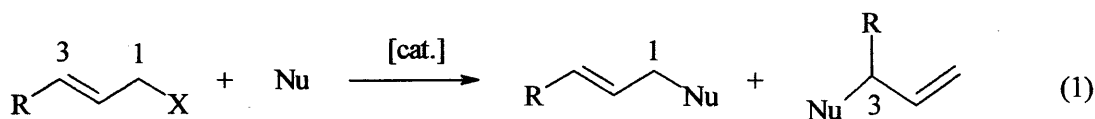
This reaction was carried out in a 300 ml stainless steel autoclave at 40 bar of CO and 100 °C. TsOH and CuCl<sub>2</sub> were used as promoters and only 1% of the palladium complex **12** was employed. Unfortunately, this carbonylation did not proceed under these experimental conditions (Table 3.8, entry 3). The alcohol is not a very good leaving group like a halide and carbonylation with these types of substrates is more difficult and higher pressures might be necessary. The reaction conditions for this process have not been optimised.

The fact that **ddppm** did not work in the carbonylation of benzyl alcohol was unexpected, since **ddppi**, the *exo-exo* diphosphine, had been successful in an asymmetric carbonylation process,<sup>34</sup> in which methyl ester of (s)-naproxen is prepared from 1-(6'-methoxy-2'-naphthyl)ethanol, obtaining high chemical yields and moderate enantioselectivities.

### 3.3.5 Allylic alkylation and allylic amination reactions

Transition metal-catalyzed allylic substitutions or, as these reactions are also called, 'allylic alkylations' or 'allylations', Eq. (1), are highly versatile reactions that have become part of modern organic synthesis. They often proceed under much milder conditions than ordinary S<sub>N</sub>2 or S<sub>N</sub>2' reactions and with different chemo-, regio- and stereoselectivities. Typical leaving groups are acetates or carbonates, rather than the more reactive halides or sulfonates, which may be a considerable advantage in the synthesis of complex multifunctional compounds.

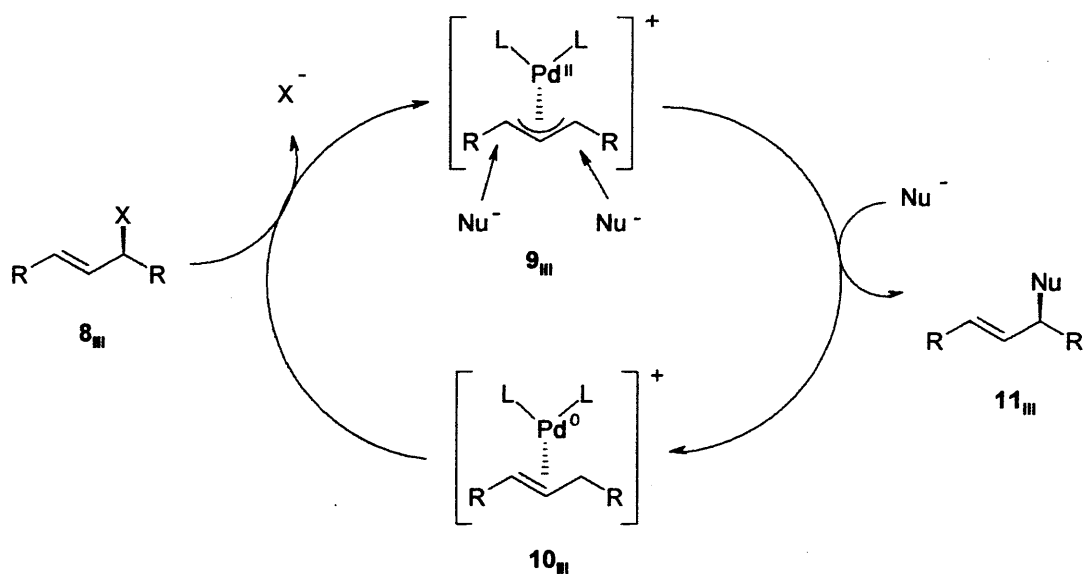




By changing the metal or the ligand, it is often possible to tune the reactivity or selectivity of the catalyst according to the specific requirements of a particular application. A variety of transition metal complexes derived from palladium, nickel, ruthenium, rhodium, iridium, molybdenum, tungsten, and other elements are known to catalyze allylic substitutions. The most widely used catalysts are palladium complexes and their structure and mode of action are well understood. The properties and scope of other transition metal catalysts have not been explored in such depth, although, in certain cases they can offer distinct advantages over Pd complexes, e.g., by reversal of regioselectivity.<sup>35</sup>

Trost and Strege reported the first example of an enantioselective metal-catalyzed allylic substitution in 1977.<sup>36</sup> Since their original results that Pd(PPh<sub>3</sub>)<sub>4</sub> in the presence of the chiral diphosphine DIOP can induce moderate enantioselectivities, strong efforts have been made to develop practically useful catalysts for this important class of reactions. It took many years to reach that target, which is not surprising because the problem of enantiocontrol in allylic substitutions is more complex than in most other metal-catalyzed reactions.

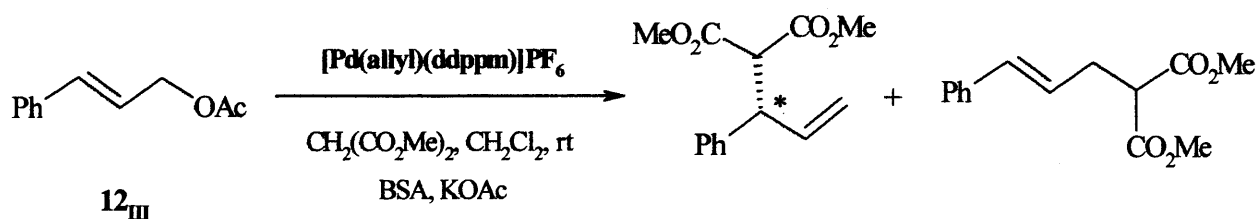
The mechanism of these allylic reactions has been established and a detailed picture of the catalytic cycle can be seen in Scheme 3.14. An allylic substrate **8<sub>III</sub>**, typically acetate or a carbonate, reacts with the catalyst, which enters the catalytic cycle at the Pd(0)



**Scheme 3.14:** Catalytic cycle of allylic alkylations

The palladium allyl complex **13**,  $[\text{Pd}(\text{ddppm})(\eta^2\text{-C}_3\text{H}_5)]\text{PF}_6$  was tested in two allylation-type reactions, allylic alkylation and allylic amination. Two different experimental conditions were used for the allylic alkylation of cinnamyl acetate (**12<sub>III</sub>**). Generally this kind of substrate reacts predominantly at the unsubstituted allyl terminus. Consequently, the achiral linear product is formed rather than the chiral, branched isomer, which is the preferred product for applications in asymmetric synthesis. Although major formation of the branched isomers has been observed with achiral catalysts derived from metals such as W and Ir, the development of enantioselective catalysts for this class of substrate remains a challenge.<sup>38</sup>

The first allylic alkylation with cinnamyl acetate **12<sub>III</sub>** using chiral Pd complex **13** was carried out using dimethyl malonate, N,O-(bistrimethylsilyl)acetamide (BSA), and potassium acetate in dichloromethane at room temperature, Scheme 3.15.



**Scheme 3.15:** Allylic alkylation under the following conditions: 1 mmol of **12<sub>III</sub>**, 0.01 mmol of Pd complex **13**, 2 equiv of  $\text{CH}_2(\text{CO}_2\text{Me})_2$  and N, O, bis(trimethylsilyl)acetamide (BSA), 4 equiv of KOAc, 5 ml of  $\text{CH}_2\text{Cl}_2$ , 17 h at r.t.

The result from this reaction was the achiral linear isomer as the major product with a ratio of 20:80. (Scheme 3.15). Lower results were also obtained by Pétrôt et al. with the chiral diphenylphosphine-oxazoline **13<sub>III</sub>** (see Figure 3.15) under the same reaction conditions. With **13<sub>III</sub>** the ratio achieved was 4:96 for the branched and linear isomers, respectively.<sup>39</sup>

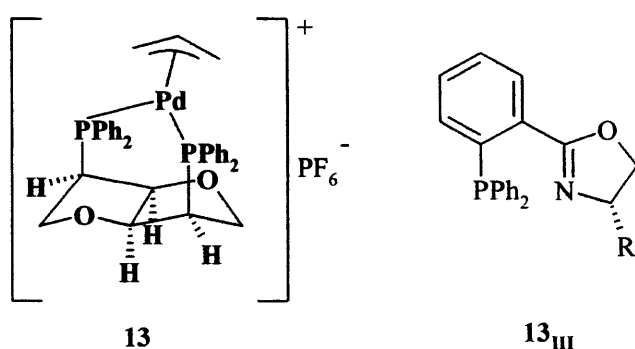
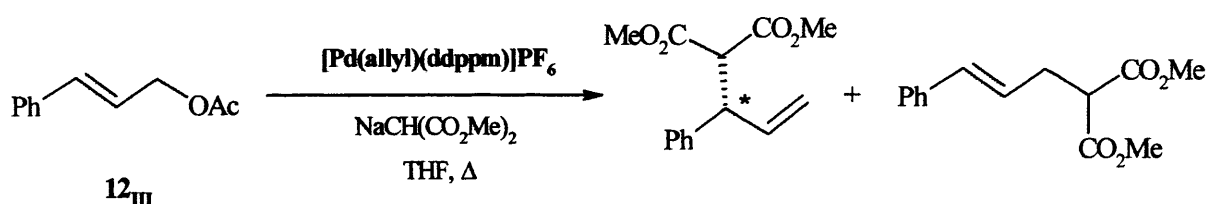


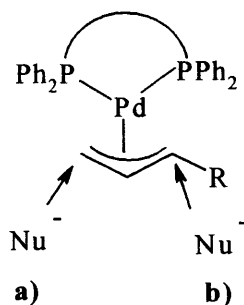
**Figure 3.15:** Palladium allyl complex from ddppm **13** and diphenylphosphine-oxazoline ligand **13<sub>III</sub>**.

The second procedure for the allylic alkylation with cinnamyl acetate **12<sub>III</sub>** using Pd complex **13** was carried out using sodium dimethyl malonate in THF at reflux temperature, Scheme 3.16. In this case stronger conditions were employed and less of the branched product was formed. The ratio in this case was 16:83 for the branched and linear isomers respectively.

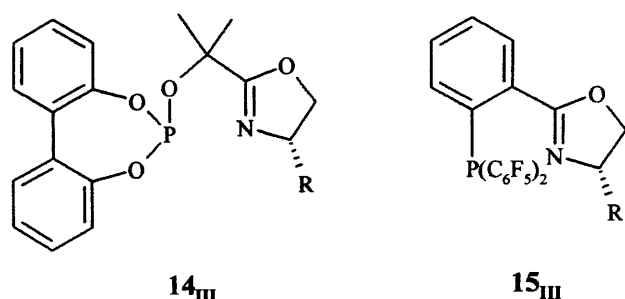


**Scheme 3.15:** Allylic alkylation under the following conditions: 1 mmol of **12<sub>III</sub>**, 0.01 mmol of Pd complex **13**, 2 equiv of  $\text{NaCH}(\text{CO}_2\text{Me})_2$ , 60°C, 5 ml of THF, 24 h.

The formation of the linear product as the major isomer in both cases can be explained because **ddppm** is a symmetrical bidentate ligand with two phenyl groups attached to each phosphorus atom. (Figure 3.15). Having the same environment at both each phosphorus atoms, the nucleophile attacks at the less substituted allyl terminus **a**) and the linear product is formed.

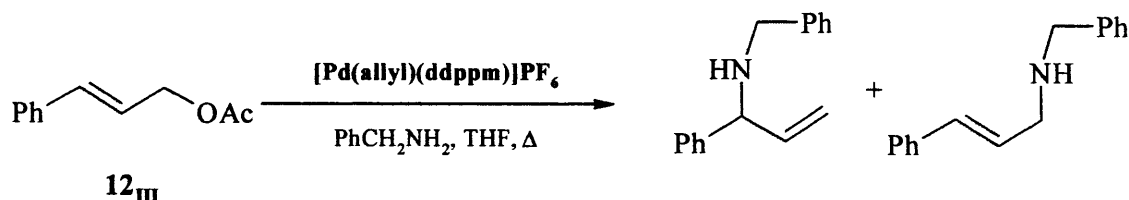


Pétrôt et al. have done studies using chiral phosphine-oxazoline as ligands altering the electronic and steric properties of the ligand and the regioselectivity shifted in the desired direction to the branched isomer. E.g. phenyl groups were replaced by electron-withdrawing groups such as pentafluorophenyl like in **14<sub>III</sub>** or by biphenylphosphite groups like in **15<sub>III</sub>** getting enantioselectivities up to 92% for the branched isomer.<sup>40</sup>



The second allylic reaction attempted with palladium allyl complex **13** was an allylic amination. This reaction is a well-established process in organic synthesis.

The allylic amination was carried out with the same cinnamyl acetate **12<sub>III</sub>** and benzylamine as the nucleophile, Scheme 3.16. The reaction was done in THF and stirred for 48 h at 50°C. The yield obtained was 53% and from this yield, 77% was from the linear product and 22% from the branched product.



**Scheme 3.16:** Allylic amination under the following conditions: 1 mmol of **12<sub>III</sub>**, 0.01 mmol of Pd complex **13**, and 20 mmol of benzyl amine, 5 ml THF, 48 h at 50°C.

To our knowledge, allylic aminations found in the literature use as a substrate a disubstituted allyl such as 1,3-diphenyl-2-propenyl acetate and not allylic aminations with monosubstituted substrate **12<sub>III</sub>** are found. Palladium catalysts using phosphine-oxazoline ligands have been studied with 1,3-diphenyl-2-propenyl acetate and these complexes catalyse allylic amination with very good results, achieving enantioselectivities up to 90% for the branched product.<sup>41</sup>

### 3.4 CONCLUSIONS

**ddppm**-copper complexes,  $[\text{Cu}(\text{ddppm})(\text{CH}_3\text{CN})_2]\text{PF}_6$ , **9** and  $[\text{Cu}(\text{ddppm})_2]\text{PF}_6$ , **10** have been synthesized but they have not been successfully crystallized. A platinum complex,  $\text{Pt}(\text{ddppm})\text{Cl}_2$  (**11**) was formed and it has been characterized crystallographically. The dihalide palladium complexes  $\text{Pd}(\text{ddppm})\text{Cl}_2$  (**12**) and  $\text{Pd}(\text{ddppm})\text{Br}_2$  (**12b**) and the allyl palladium complex,  $[\text{Pd}(\eta^3\text{-allyl})(\text{ddppm})]\text{PF}_6$  (**13**) were also synthesized and characterized crystallographically. These palladium complexes were tested in different catalytic reactions such as in the Sonagashira reaction, in carbonylation of different substrates and in allylic reactions, and the following conclusions inferred from them.

96% yield of diphenylethyne was obtained for the Sonagashira reaction using the palladium dihalide catalyst **12**.

**ddppm** like other bidentate phosphines gave the linear product, rather than the branched one, in the hydroesterification of styrene.

In the carbonylation of 1-bromoethylbenzene, the desired product ethyl 2-phenylpropionate (**3<sub>III</sub>**) was not obtained and 1-phenylethanol (**2<sub>III</sub>**) was formed instead.

In the conversions of aryl halides to carboxylic esters the expected activity is observed, in increasing order: PhCl, PhBr, PhI. This reactivity order was expected because chloroarenes are more inert.

When **ddppm** was used as a ligand for the carbonylation of benzyl bromide, good conversion of the ester was obtained (98%).

Unfortunately, carbonylation of benzyl alcohol did not proceed. The alcohol is not a very good leaving group like a halide and carbonylation with these types of substrates is more difficult and higher pressures might be necessary.

The major products from the allylic alkylations of cinnamyl acetate **12<sub>III</sub>** were the achiral linear isomers with ratios of 20:80 and 16:83. The allylic amination was carried out with the same cinnamyl acetate and 77% yield was obtained for the linear product and 22% for the branched product. The formation of the linear product as the major isomer in all the cases can be explained because **ddppm** is a symmetrical bidentate ligand with two phenyl groups attached to each phosphorus atom. Having the same environment at both each phosphorus atoms, the nucleophile attacks at the less substituted allyl terminus and the linear product is formed.

### 3.5 EXPERIMENTAL

**General considerations:** All manipulations were performed using standard Schlenk techniques under an argon atmosphere, except where otherwise noted. Solvents of analytical grade and deuterated solvents for NMR measurements were distilled from the appropriate drying agents under N<sub>2</sub> immediately prior to use following standard literature methods.<sup>42</sup> Literature methods were employed for the synthesis of [Cu(MeCN)<sub>4</sub>]PF<sub>6</sub>,<sup>43</sup>

$\text{Pd}(\text{PhCN})_2\text{Cl}_2$ <sup>44</sup>,  $[\text{Pd}(\text{allyl})\text{Cl}]_2$ <sup>45</sup> and  $\text{Na}[\text{CH}(\text{CO}_2\text{Me})_2]$ <sup>46</sup>. All other reagents were used as received. A 300 ml stainless steel autoclave and a 100 ml glass autoclave were used for carbonylation reactions. NMR spectra were obtained on Bruker Avance AMX 400 or Jeol Eclipse 300 spectrometers and referenced to external TMS. HPLC analyses were performed on an Agilent 1100 series instrument. Mass spectra were obtained in ES (Electrospray) mode from the EPSRC Mass Spectrometry Service, Swansea University unless otherwise reported.

***[Cu(ddppm)(CH<sub>3</sub>CN)<sub>2</sub>]PF<sub>6</sub>, 9:*** 46 mg (0.131 mmol) of  $[\text{Cu}(\text{CH}_3\text{CN})_4]\text{PF}_6$  were placed in a Schlenk and dissolved in dry and degassed acetonitrile (10 ml). After that, 63 mg (0.131 mmol) of ddppm were added and the mixture was stirred for 2 h at 50°C. Then, the solvent was evaporated affording a white solid. This white solid was recrystallized from acetonitrile and hexane. <sup>1</sup>H NMR (CD<sub>3</sub>CN, 400MHz)  $\delta$  3.53 (m, 2H, CHPh<sub>2</sub>), 3.57 (m, 2H, CH<sub>2</sub>), 3.99 (m, 2H, CH<sub>2</sub>), 5.16 (m, 2H, CCH), 7.35 (m, 12H), 7.54-7.76 (m, 8H); <sup>31</sup>P NMR (CDCl<sub>3</sub>, 121 MHz)  $\delta$  -11.06 (br s). <sup>13</sup>C NMR (CD<sub>3</sub>CN, 75 MHz) 39.93 (t, *J* 9.8 Hz, 2C, CH<sub>2</sub>), 73.91 (s, 2C, CHP), 85.93 (s, 2C, CHP), 128.71 (m, 4C, Ar), 130.01 (m, 4C, Ar), 133.13 (m, 4C, Ar) MS:  $[\text{M}-\text{CH}_3\text{CN}-\text{PF}_6]^+$ , 586;  $[\text{M}-2\text{CH}_3\text{CN}-\text{PF}_6]^+$ , 545.

***[Cu(ddppm)<sub>2</sub>]PF<sub>6</sub>, 10:*** 37 mg of  $[\text{Cu}(\text{CH}_3\text{CN})_4]\text{PF}_6$  (0.1 mmol) were placed in a schlenk and dissolved in dry and degasified acetonitrile (10 ml). Then, 100 mg of ddppm (0.2 mmol) were added into it and the mixture was stirred for 2h at 50°C. After that time the solvent was evaporated affording a white solid. This white solid was recrystallized from acetonitrile and hexane. <sup>1</sup>H NMR (CD<sub>3</sub>CN, 400MHz)  $\delta$  3.19 (m, 4H, CHPh<sub>2</sub>), 3.59 (m, 4H, CH<sub>2</sub>), 3.76 (t, 4H, CH<sub>2</sub>), 4.76 (m, 4H, CCH), 7.21-7.45 (m, 40H); <sup>31</sup>P NMR (CDCl<sub>3</sub>,



121 MHz)  $\delta$  -14.61 (br s).  $^{13}\text{C}$  NMR ( $\text{CD}_3\text{CN}$ , 75 MHz) 42.79 (s, 4C,  $\text{CH}_2$ ), 72.98 (t,  $J$  8.65 Hz, 4C, CHP), 85.98 (s, 4C, CHP), 128.72 (m, 4C, Ar), 129.91 (m, 4C, Ar), 133.27 (m, 4C, Ar).  $[\text{M-ddppm-2CH}_3\text{CN-PF}_6]^+$ : 545.

***Pt(ddppm)Cl<sub>2</sub>*, 11:** 29 mg of  $\text{PtCl}_2$  (0.11mmol) were dissolved in 10 ml of warm acetonitrile and 54 mg of the diphosphine ddppm (0.11mmol) were added. The mixture was stirred at room temperature for 1 day and then the solvent was evaporated and redissolved in chloroform. A white solid was precipitated with dry diethyl ether. Pale yellow crystals were obtained from a mixture of chloroform and diethyl ether. (71 mg, 87% yield).  $^1\text{H}$  NMR ( $\text{CD}_3\text{CN}$ , 400MHz)  $\delta$  3.37 (dd,  $J$  7 Hz, 2H,  $\text{CHPPh}_2$ ), 3.77 (ddd,  $J$  6 Hz, 2H,  $\text{CH}_2$ ), 4.14 (t,  $J$  12 Hz, 2H,  $\text{CH}_2$ ), 5.04 (m, 2H, CCH), 7.31 (m, 7H), 7.47 (m, 5H), 7.53 (m, 4H), 8.44 (m, 4H).  $^{31}\text{P}$  NMR ( $\text{CDCl}_3$ , 121 MHz)  $\delta$  8.47 (s)  $^1J_{\text{Pt-P}} = 3746$  Hz.  $^{13}\text{C}$  NMR ( $\text{CD}_3\text{CN}$ , 75 MHz) 43.5 (t, 2C,  $\text{CH}_2$ ), 72.87 (s, 2C, CHP), 83.43 (s, 2C, CHP), 128.02 (t,  $^2J_{\text{CP}} = 5.7$  Hz, 4C, Ar), 128.36 (t,  $^2J_{\text{CP}} = 5.7$  Hz, 4C, Ar), 130.42 (s, 2C, Ar), 131.41 (s, 2C, Ar), 133.58 (t,  $^2J_{\text{CP}} = 4.9$  Hz, 4C, Ar), 135.16 (t,  $^2J_{\text{CP}} = 4.9$  Hz, 4C, Ar); MS (accurate mass, ES+) calculated mass for [M]: 712.0895, measured: 712.0898.

***Pd(ddppm)Cl<sub>2</sub>*, 12:** A schlenk was charged with 0.177g of ddppm (0.37 mmol) and dissolved in  $\text{CH}_2\text{Cl}_2$  (15 ml). Then, 0.141 g of  $\text{Pd}(\text{PhCN})_2\text{Cl}_2$  (0.37 mmol) were added and the mixture was stirred for 1 h. The solvent was concentrated and ether was added to obtain yellow crystals. (0.207 g, 85% yield).  $^1\text{H}$  NMR ( $\text{CD}_3\text{CN}$ , 400MHz)  $\delta$  3.24 (m, 2H,  $\text{CHPPh}_2$ ), 3.78 (m, 2H,  $\text{CH}_2$ ), 4.05 (t,  $J$  12 Hz, 2H,  $\text{CH}_2$ ), 4.95 (m, 2H, CCH), 7.3-7.55 (m, 12H), 7.75-8.45 (m, 8H)  $^{31}\text{P}$  NMR ( $\text{CDCl}_3$ , 121 MHz)  $\delta$  25.6 (s).  $^{13}\text{C}$  NMR ( $\text{CD}_3\text{CN}$ , 75

MHz) 45.1 (m, 2C, CH<sub>2</sub>), 72.98 (s, 2C, CHP), 83.68 (s, 2C, CHP), 128.09 (m, 4C, Ar), 128.42 (m, 4C, Ar), 130.44 (s, 2C, Ar), 131.44 (s, 2C, Ar), 133.57 (m, 4C, Ar), 135.53 (m, 4C, Ar); MS (accurate mass, ES+) calculated mass for [M]: 657.9971, measured: 657.9986.

***Pd(ddppm)Br<sub>2</sub>, 12b***: A schlenk was charged with 0.224 g of ddppm (0.46 mmol) and dissolved in CH<sub>2</sub>Cl<sub>2</sub> (20 ml). Then, 0.174 g of Pd(COD)Br<sub>2</sub> (0.46 mmol) were added and the mixture was stirred for 1 h. The solvent was concentrated and ether was added to obtain orange crystals. (0.343 g, 87% yield). <sup>1</sup>H NMR (CD<sub>3</sub>CN, 400MHz) δ 3.21 (m, 2H, CHPh<sub>2</sub>), 3.76 (m, 2H, CH<sub>2</sub>), 4.11 (t, *J* 12 Hz, 2H, CH<sub>2</sub>), 5.01 (m, 2H, CCH), 7.3-7.55 (m, 12H), 7.75-8.45 (m, 8H) <sup>31</sup>P NMR (CDCl<sub>3</sub>, 121 MHz) δ 23.4 (s).

***Pd(ddppm)I<sub>2</sub>***: 80 mg of NBu<sub>4</sub>I (3.1 mmol) are dissolved in CH<sub>2</sub>Cl<sub>2</sub> and this solution is mixed with 0.155 mmol of Pd(ddppm)Cl<sub>2</sub>. After this is stirred for 30 min, the solvent is evaporated and the NBu<sub>4</sub>I is extracted with MeOH in which the complex Pd(ddppm)I<sub>2</sub> precipitates. The solid was recrystallized with dichloromethane and hexane. (0.117 g, 90% yield). <sup>1</sup>H NMR (CD<sub>3</sub>CN, 400MHz) δ 3.28 (m, 2H, CHPh<sub>2</sub>), 3.75 (m, 2H, CH<sub>2</sub>), 3.98 (t, *J* 12 Hz, 2H, CH<sub>2</sub>), 4.94 (m, 2H, CCH), 7.3-7.55 (m, 12H), 7.75-8.45 (m, 8H) <sup>31</sup>P NMR (CDCl<sub>3</sub>, 121 MHz) δ 16.4 (s).

***[Pd(ddppm)(η<sup>3</sup>-C<sub>3</sub>H<sub>5</sub>)]PF<sub>6</sub>, 13***: A solution of [Pd(η<sup>3</sup>-C<sub>3</sub>H<sub>5</sub>)Cl]<sub>2</sub> (15 mg, 0.04mmol) and the free ligand ddppm (40 mg, 0.08mmol) in CH<sub>2</sub>Cl<sub>2</sub> (5ml) were stirred at room temperature under nitrogen for 1h. <sup>31</sup>P NMR (D<sub>2</sub>O, 121 MHz) δ 18.37 (br s). To exchange the chloride counterion, the solution was evaporated and the yellow solid obtained

dissolved in acetonitrile. The resulting solution was treated with  $\text{KPF}_6$  (15 mg, 0.08 mmol) and stirred overnight. After one day, the mixture was filtered through a pad of celite and the solution concentrated in vacuum affording a pale yellow solid (51 mg, 86%). Pale yellow crystals were obtained by recrystallization from dichloromethane-diethylether.

$^1\text{H}$  NMR ( $\text{CD}_3\text{CN}$ , 400 MHz)  $\delta$  2.95 (m, 1H, anti-allylic), 3.48 (m, 3H, ddppm), 3.58 (m, 1H, anti-allylic), 3.75 (m, 1H, ddppm), 3.91 (m, 1H,  $\text{CH}_2$ ), 3.95 (m, 1H,  $\text{CH}_2$ ), 4.21 (m, 1H, syn-allylic), 4.48 (m, 1H, syn-allylic), 5.12 (m, 1H, CCH), 5.22 (m, 1H, CCH), 5.86 (septet, 1H, CH, central-allylic), 7.27-7.53 (m, 12H), 7.76-7.85 (m, 8H).  $^{31}\text{P}$  NMR ( $\text{CD}_3\text{CN}$ , 121 MHz)  $\delta$  17.8 (d,  $^2J_{\text{pp}} = 111.19$  Hz) and 18.5 (d,  $^2J_{\text{pp}} = 111.19$  Hz).  $^{13}\text{C}$  NMR ( $\text{CD}_3\text{CN}$ , 75 MHz) 45.1 (d, 2C,  $\text{CH}_2$ ), 72.98 (s, 2C, CHP), 83.68 (s, 2C, CHP), 128.09 (m, 4C, Ar), 128.42 (m, 4C, Ar), 130.44 (s, 2C, Ar), 131.44 (s, 2C, Ar), 133.57 (m, 4C, Ar), 135.53 (m, 4C, Ar); MS (accurate mass, ES+) calculated mass for  $[\text{M-PF}_6]^+$ : 629.0985, measured: 629.0994;  $[\text{M-PF}_6-(\eta^3\text{-C}_3\text{H}_5)]^+$ : 588.1.

**Procedure for the Sonagashira Reaction:** In a Schlenk, 12 mg of  $\text{Pd}(\text{ddppm})\text{Cl}_2$  complex, 12 (0.018 mmol) was dissolved in acetonitrile. Then,  $\text{CuI}$  (10 mg, 0.054 mmol),  $\text{NEt}_3$  (0.4 ml, 3 mmol), phenylacetylene (0.2 ml, 1.8 mmol) and the respective aryl iodide (0.17 ml, 1.5 mmol) were added and the reaction was stirred at  $60^\circ\text{C}$  overnight. Solvents were evaporated and the residue was extracted with ether. Ether washings were subsequently extracted with a solution of  $\text{HCl}$  (0.5 M) and the second time with a saturated solution of  $\text{NaHCO}_3$ . The organic layers were collected and dried with  $\text{MgSO}_4$ . The solvent was evaporated and a brown solid was obtained. (m.p=  $50-60^\circ\text{C}$ ). (314 mg, 98% yield).  $^1\text{H}$  NMR ( $\text{CDCl}_3$ , 300 MHz)  $\delta$  7.22 (m, 6H, Ph), 7.42 (m, 4H, Ph).

**Procedure for the alkoxycarbonylation reaction of iodobenzene:** The corresponding iodobenzene (0.225 ml, 2 mmol), methanol (5ml), Pd(dddppm)Cl<sub>2</sub> complex **12** (7 mg, 0.01 mmol) and sodium carbonate (636 mg, 6 mmol) were added into a 100 ml glass autoclave. This autoclave was closed and evacuation and replacement with argon (three cycles ) was followed. Then, it was filled with 4 bar of CO pressure and heated to 90°C. After 16 h reaction time the autoclave was cooled to room temperature and the mixture diluted with dichloromethane (20 ml). After washing with water (20ml) the aqueous phase was extracted with dichloromethane (2 x 20ml) and the combined organic phases were dried over magnesium sulfate, filtered and concentrated under reduced pressure (100% yield).

With bromobenzene (0.2 ml, 2 mmol), the same procedure was followed but using ethanol (5ml) as a solvent and triethylamine (0.84 ml, 6 mmol) as a base. The reaction temperature was 145°C. (30% yield).

HPLC conditions: Synergi column, 80:20 CH<sub>3</sub>CN/H<sub>2</sub>O, 2 ml/min. 80:20 Acetonitrile:H<sub>2</sub>O,  $\lambda$  = 256nm, 1ml/min. <sup>1</sup>H NMR  $\delta$  (250 MHz, CDCl<sub>3</sub>): *methyl benzoate*: 3.79 (s, 3H, CH<sub>3</sub>), *ethyl benzoate*: 1.11 (t, 3H, CH<sub>3</sub>), 4.25 (q, 2H, CH<sub>2</sub>).

**Procedure for the hydroesterification of styrene:** Into a stainless steel 300 ml autoclave were added 0.05 mmol of the cationic Pd catalyst (33 mg, 0.05mmol), [Pd(dddppm)]BF<sub>4</sub>, 0.5 ml of styrene (5 mmol), 5 ml of MeOH and 40 ml of methyl ethyl ketone under a nitrogen atmosphere. The reaction vessel was then pressurized with 40 bar of CO. The reaction was allowed to proceed with stirring at 80°C for 3 days. After that time, the solvent was evaporated and the yield was determined by NMR. <sup>1</sup>H NMR  $\delta$  (400 MHz, CDCl<sub>3</sub>). 22% of

*methyl 3-phenylpropionate (linear product,):* 2.45 (t, 2H, CH<sub>2</sub>), 2.78 (t, 2H, CH<sub>2</sub>-COO-), 3.46 (s, 3H, -OCH<sub>3</sub>). 4% of *methyl 2-phenylpropionate (branched product):* 1.34 (d, 3H, CH<sub>3</sub>-CH-), 3.43 (s, 3H, -COOCH<sub>3</sub>), 3.55 (q, 1H, CH).

***Procedure for the carbonylation of 1-(bromoethyl)benzene:*** Into a 100 ml glass autoclave were added 7 mg of Pd(ddppm)Cl<sub>2</sub> (0.01 mmol) (**12**), 130 mg of Na<sub>2</sub>CO<sub>3</sub> (1.2 mmol), 5 ml of EtOH and 0.14 ml of 1-(bromoethyl)benzene (1 mmol). Under the conditions of 4 bar and 60°C, the reaction was maintained for 1 day. After that time, a water extraction with ether was done and the organic layers collected and dried over MgSO<sub>4</sub>. The solvent was evaporated and the final product was analysed by NMR. <sup>1</sup>H NMR δ (250 MHz, CDCl<sub>3</sub>): 84% of *(1-ethoxy-ethyl)-benzene*: 1.12 (t, 3H, CH<sub>3</sub>-CH), 1.38 (d, 3H, CH<sub>3</sub>-CH<sub>2</sub>-O-), 3.30 (q, 2H, O-CH<sub>2</sub>-CH<sub>3</sub>), 4.36 (q, 1H, CH-CH<sub>3</sub>). None of *2-phenyl-propionic acid ethyl ester* was obtained.

***Procedure for the carbonylation of benzyl bromide:*** In an autoclave were added 0.12 ml (1 mmol) of benzyl bromide, 10 mg (0.02 mmol) of ddppm, 3 mg (0.01 mmol) of Pd<sub>3</sub>(OAc)<sub>6</sub>, 0.2 ml (1 mmol) of NEt<sub>3</sub> and 5 ml of a mixture 1:1 of toluene and methanol. The reaction mixture was stirred for 2 days at 2 bar of CO and 60°C. After that time, a water extraction with ether was done. The organic layer were collected and dried over MgSO<sub>4</sub>. The solvent was evaporated and the final product was analysed by <sup>1</sup>H NMR and HPLC. <sup>1</sup>H NMR δ (400 MHz, CDCl<sub>3</sub>): *phenyl acetate*: 3.71 (s, 2H, CH<sub>2</sub>), 3.72 (s, 3H, CH<sub>3</sub>). HPLC conditions: Synergi column, 80:20 Acetonitrile:H<sub>2</sub>O, λ = 256nm, 1ml/min.

**Procedure for the carbonylation of benzyl alcohol:** For a typical procedure, 37 mg (0.05 mmol) of Pd(dddppm)Br<sub>2</sub>, 17 mg (0.1 mmol) of CuCl<sub>2</sub>·2H<sub>2</sub>O, 190 mg (1 mmol) of p-TsOH, 5 ml of MeOH, 0.5 ml (5 mmol) of benzyl alcohol and 40 ml of methyl ethyl ketone were added into a stainless steel 300 ml autoclave. Under the conditions of 40 atm CO and 100°C. The reaction mixture was stirred for 40 h and the final product was analysed by <sup>1</sup>H NMR and HPLC. <sup>1</sup>H NMR δ (400 MHz, CDCl<sub>3</sub>): *benzyl alcohol*: 2.51 (br s, 1H, OH), 4.66 (d, 2H, CH<sub>2</sub>), *phenyl acetate*: 3.71 (s, 2H, CH<sub>2</sub>), 3.72 (s, 3H, CH<sub>3</sub>). HPLC conditions: Synergi column, 80:20 Acetonitrile:H<sub>2</sub>O, λ = 256nm, 1ml/min.

**Procedure 1 for the allylic alkylation:** In a 20 ml Schlenk equipped with magnetic stirring bar under N<sub>2</sub>, [Pd(allyl)(dddppm)]PF<sub>6</sub> (8mg, 0.01mmol) was added followed by cinnamic acetate (0.17ml, 1mmol), dimethyl malonate (0.23ml, 2mmol), BSA\* (0.5ml, 2mmol) and potassium acetate (393mg, 4mmol). Then, 5ml of dichloromethane were added and the mixture is stirred for 17h at room temperature. After that time, the mixture was diluted with ether and then extracted with two portions of saturated aqueous ammonium chloride solution. The organic layer is dried over anhydrous magnesium sulphate, concentrated and purified by column chromatography (silica gel, petroleum ether:ethylacetate = 9:1) to give a mixture of dimethyl (1-phenylprop-2-en-1-yl)malonate and dimethyl (3-phenylpro-2-en-1-yl)malonate. <sup>1</sup>H NMRs of these products can be found in the literature.<sup>46</sup>

**Procedure 2 for the allylic alkylation:** In a 20 ml Schlenk equipped with magnetic stirring bar under N<sub>2</sub>, [Pd(allyl)(dddppm)]PF<sub>6</sub> (8mg, 0.01mmol) was added into it followed by

---

\* BSA: N,O-(bistrimethylsilyl)acetamide

cinnamic acetate (0.17ml, 1mmol), sodium dimethyl malonate (0.23ml, 2mmol). Then, 5ml of THF are added and the mixture is stirred at reflux for 24 h. After that time, the mixture was diluted with two portions of saturated aqueous ammonium chloride solution. The organic layer is dried over anhydrous magnesium sulphate, concentrated and purified by column chromatography (silica gel, petroleum ether:ethylacetate = 9:1) to give a mixture of dimethyl (1-phenylprop-2-en-1-yl)malonate and dimethyl (3-phenylpro-2-en-1-yl)malonate. <sup>1</sup>H NMRs of these products can be found in the literature.<sup>46</sup>

**Procedure of allylic amination:** [Pd(allyl)(ddppm)]PF<sub>6</sub> (8mg, 0.01mmol), cinnamic acetate (0.17ml, 1mmol) and benzyl amine (2ml, 20mmol) were added into a small pressure tube and dissolved in 5ml of THF. The reaction mixture was stirred at 50°C for 48h. After that time, the reaction mixture was divided into saturated aqueous ammonium chloride and diethyl ether. Organic layer was dried over anhydrous magnesium sulphate and evaporated to give a mixture of N-(1-phenyl-2-propenyl)benzylamine) and N-[(E)-3-Phenyl-2-propenyl]benzylamine. <sup>1</sup>H NMRs of these products can be found in the literature.<sup>47</sup>

---

<sup>1</sup> S. J. Berners-Price, K. Johnson, C. K. Mirabelli, L. F. Faucette, F. L. McCabe, and P. J. Sadler, *Inorg. Chem.* 1987, 26, 3383-3387.

<sup>2</sup> (a) S. Yao, M. Johannsen, R.G. Hazell, K. S. Jørgensen, *Angew. Chem., Int. Ed.* 1998, 37, 3121. (b) S. Yao, S. Saaby, R.G. Hazell, K. S. Jørgensen, *Chem. Eur. J.*, 2000, 6, 2435. (c) O. Garcia, R. Gómez, and J. C. Carretero. *J. Am. Chem. Soc.*, 2004, 126 (2), 456-457.

<sup>3</sup> J. A. Rahn, L. Balatusis and J. H. Nelson, *Inorg. Chem.*, 1990, 29, 750-755.

- 
- <sup>4</sup> R. D. Jackson, S. James, A. Guy Orpen and Paul G. Pringle, *J. Organomet. Chem.*, 1993, 458, C3-C4.
- <sup>5</sup> X-Seed – A software tool for supramolecular crystallography. *J. Supramol. Chem.*, 2001, 1, 189-191.
- <sup>6</sup> T. Sturm, W. Weissensteiner, K. Mereiter, T. Kegl, *J. Organomet. Chem.*, 2000, 595, 93-101.
- <sup>7</sup> W. Oberhause, C. Bachmann and P. Brüggeller. *Inorganica Chimica Acta*, 1995, 238, 35-43.
- <sup>8</sup> S. Doherty, E. G. Robins, J. G. Knight, C. R. Newman, B. Rhodes, P. A. Champkin, W. Clegg, *J. Organomet. Chem.*, 2001, 640, 182-196.
- <sup>9</sup> C. Amatore, S. Gamez, A. Juttand, *J. Organomet. Chem.*, 2001, 624, 217-222.
- <sup>10</sup> ORTEP III - Thermal Ellipsoid Plot Program for Crystal Structure Illustrations. Dr. Michael, N. Burnett Dr. Carroll K. Johnson. Oak Ridge National Laboratory P.O. Box 2008 Oak Ridge, TN 37831-6197 USA.
- <sup>11</sup> S. L. James, A. Guy Orpen, P. G. Pringle, *J. Organomet. Chem.*, 1996, 525, 299-301.
- <sup>12</sup> M. Yamaguchi, M. Yabuki, T. Yamagishi, M. Kondo and S. Kitagawa, *J. Organomet. Chem.*, 1997, 538, 199-202.
- <sup>13</sup> K. Sonagashira, *J. Organomet. Chem.*, 2002, 653, 46-49.
- <sup>14</sup> T. Hundertmark, A.F. Littke, S.L. Buchwald and G.C. Fu, *Organic Lett.*, 2000, Vol. 2, No. 12, 1729.



- 
- <sup>15</sup> A. Datta, and H. Plenio, *Chem. Commun.*, 2003, 1504-1505.
- <sup>16</sup> K. Sonagashira, Y. Tohda and N. Hagihara, *Tetrahedron Lett.*, 1975, 4467-4470.
- <sup>17</sup> W. Mägelwin, A.F. Indolese, and M. Beller, *Angew. Chem. Int. Ed.* 2001, 40, No. 15, 2856-2859.
- <sup>18</sup> B. Cornil, W.A. Herrmann, *Applied Homogeneous Catalysis with Organometallic Compounds*, Wiley-VCH, New York, 2000, pg 148-149.
- <sup>19</sup> T. A. Strommova, I.I. Moiseev, *Russ. Chem. Rev.* 1998, 67, 485-514. (b) K. Kudo, M. Hidai, Y. Uchida, *J. Organomet. Chem.*, 1971, 33, 393-398 (c) M. Hidai, M. Kokura, Y. Uchida, *J. Organomet. Chem.* 1973, 52, 431-435.
- <sup>20</sup> J. Stetter, F. Lieb, *Angew. Chem., Int. Ed.* 2000, 39, 1724.
- <sup>21</sup> Peng et al., United States Patents, Patent Number 5,861,140, Jan. 19, 1999.
- <sup>22</sup> M. Beller, W. Magerlein, A. F. Indolese, C. Fischer, *Synthesis*, 2001, 7, 1098-1109.
- <sup>23</sup> (a) C. Bottenghi, G. Consiglio and P. Pino, *Chimia*, 1973, 27, 477; (b) G. Consiglio and P. Pino, *Adv. Chem. Ser.* 1982, 196, 371.
- <sup>24</sup> S. Oi, M. Nomura, T. Aiko and Y. Inoue, *J. Mol. Cat. A: Chem.*, 1997, 115, 289-295.
- <sup>25</sup> A. Seayad, S. Jayasree, K. Damodaran, L. Toniolo and R.V. Chaudhari, *J. Organomet. Chem.*, 2000, 601, 100-107.
- <sup>26</sup> H. Zhou, J. Hou, J. Cheng, S. Lu, H. Fu and H. Wang, *J. Organomet. Chem.*, 1997, 543, 227-228.



- 
- <sup>27</sup> H. Arzoumanian, G. Buono, M. Choukrad, and J. F. Petrignani, *Organometallics* 1988, 7, 59-62
- <sup>28</sup> M. Beller, B. Cornils, C.D. Frohning, C. W. Kohlpaintner, *J. Mol. Catal. A: Chem.* 1995, 104, 17-85.
- <sup>29</sup> (a) J. Kiji, T. Okano, W. Nishiumi, H. Konishi, *Chem. Lett.*, 1989, 957; b) J. Kiji, T. Okano, H. Konishi, W. Nishiumi, *Chem. Lett.*, 1989, 1873; c) J. Tsuji, K. Sato, H. Okumoto, *J. Org. Chem.*, 1984, 49, 1341; d) D. Milstein, *Organometallics*, 1982, 1, 888; e) H.R. Gao, Y. Xu, S.J. Liao, D.R. Yu, *Chin. Chem. Lett.*, 1992, 3, 351.
- <sup>30</sup> Result obtained at Johnson Matthey.
- <sup>31</sup> G. Oehme, E. Paetzold, R. Selke, *J. Mol. Catal.*, 1992, 71.
- <sup>32</sup> C.W. Kohlpaintner, M. Beller, *J. Mol. Catal. A: Chem.*, 1997, 116, 259.
- <sup>33</sup> A. Seayad, S. Jayasree, R.V. Chaudhari, *J. Mol. Cat. A: Chem.*, 172, 2001, 151-164.
- <sup>34</sup> B. H. Xie, C.G. Xia, S.J. Lu, K.J. Chen, Y.Kou, Y.Q Yin, *Tetrahedron Lett.*, 1998, 39, 7365-7368.
- <sup>35</sup> (a) R. Takeuchi, M. Kashio, *J. Am. Chem. Soc.*, 1998, 120, 8647. (b) P. A. Evans, J. D. Nelson, *J. Am. Chem. Soc.*, 1998, 120, 5581.
- <sup>36</sup> B. M. Trost, P. E. Strege, *J. Am. Chem. Soc.*, 1977, 99, 1649.
- <sup>37</sup> E.N. Jacobsen, A. Pfaltz, H. Yamamoto, *Comprehensive Asymmetric Catalysis*, Vol. 2, 1999, 834, Ed. Springer.

- <sup>38</sup> (a) W: B. M. Trost, M. H. Hung, *J. Am. Chem. Soc.* 1983, 105, 7757-7759. (b) G.C. Lloyd-Jones, J. Lehmann, *Tetrahedron* 1995, 51, 8863-8874. (c) Ir: R. Takeuchi, M. Kashio, *Angew. Chem.*, 1997, 109, 268-270. (d) Mo: B. M. Trost, M. Lautens, *Tetrahedron* 1987, 43, 4817-4840; (e) Ru: T. Kondo, H. Ono, N. Satake, T. Mitsudo, Y. Watanabe, *Organometallics*, 1995, 14, 1945-1953.
- <sup>39</sup> R. P. Prétôt, G. C. Lloyd-Jones and A. Pfaltz, *Pure & Appl. Chem.*, 1998, 70 (5), 1035-1040.
- <sup>40</sup> R. Prétôt, A. Pfaltz, *Angew. Chem. Int. Ed.* 1998, 27 (3), 323-325.
- <sup>41</sup> a) P. von Matt, O. Loiseleur, G. Koch and A. Pfaltz, *Tetrahedron Asymmetry*, 1994, 5 (4), 573-584. (b) T. Hayashi, T. Suzuka, A. Okada and M. Kawatsura, *Tetrahedron Asymmetry*, 2004, 15, 545-548.
- <sup>42</sup> D. D. Perrin and W. F. A. Amarego, *Purification of Laboratory Chemicals*, Pergamon, Oxford, 1988.
- <sup>43</sup> G.J. Kubas, *Inorg. Synth.*, 1979, 19, 90.
- <sup>44</sup> M.S. Kharasch, R.C. Seyler, F.R. Mayo, *J. Am. Chem. Soc.* 1938, 60, 882. (b) J.R. Doyle, P.E. Slade, H.B. Jonassen, *Inorg. Synth.* 1960, 6, 216.
- <sup>45</sup> Y. Tatsuna, T. Yoshida, S. Otsuka, *Inorg. Synth.* 1990, 28, 342.
- <sup>46</sup> A. V. Malkov, I. R. Baxendale, D. J. Mansfield and P. Kocovsky, *J. Chem. Soc., Perkin Trans. 1*, 2001, 1234-12340.
- <sup>47</sup> R. Takeuchi, N. Ue, K. Tanabe, K. Yamashita, and N. Shiga, *J. Am. Chem. Soc.*, 2001, 123 (39), 9525-9534.

# ***Chapter 4***

## **4 Rh- and Ru-ddppm complexes and their catalytic applications: hydrogenation and hydroformylation.**

### **4.1 INTRODUCTION**

In this chapter the synthesis and properties of the Rh- and Ru- ddppm complexes are discussed. Results from the catalytic reactions in which these complexes are involved such as enantioselective hydrogenation and hydroformylation reactions are also presented.

Organometallic compounds of rhodium have the metal centre in oxidation states ranging from +4 to -3, but the most common oxidation states are +1 and +3. The Rh(I) species have a  $d^8$  electron configuration and both four coordinated square planar and five coordinated trigonal bipyramidal species exist. Oxidative addition reactions to Rh(I) form Rh(III) species with octahedral geometry. The oxidative addition is reversible in many cases and this makes the catalytic transformation of organic compounds possible.

The chemistry of ruthenium complexes has been explored recently. Their chemistry is more complicated than with palladium compounds, and because of that, less applications in organic syntheses have been found so far. In fact, in contrast to palladium (II) compounds, ruthenium complexes generally have 5- or 6-coordinated geometry and their oxidation state can vary between -2 to +6. This complexity, however, leads to many interesting reactions and further developments in this field are expected. Interest for catalytic applications of Ru(II) complexes stems from their much lower cost, when compared to Rh(I) and Pd(II) catalysts.

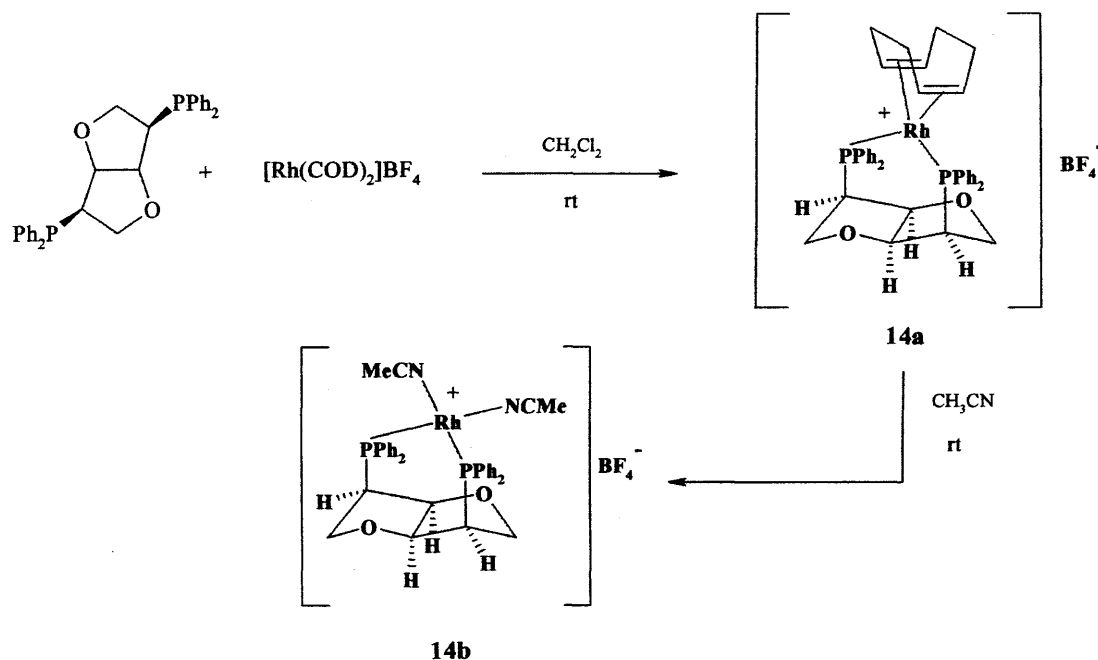
Metal-catalyzed asymmetric hydrogenation and hydroformylations of alkenes are amongst the most efficient methods for building chiral compounds. Rhodium and ruthenium are the most common metals used in this type of reactions. A large number of chiral ligands, mainly P- and N- containing ligands with either  $C_2$ - or  $C_1$ - symmetry have been successfully applied.<sup>1</sup>

## 4.2 RESULTS AND DISCUSSION

### 4.2.1 Synthesis and characterization of rhodium complexes with **ddppm**.

Rhodium catalysts containing chiral phosphine ligands have been proved the most successful catalysts for asymmetric catalytic hydrogenations.<sup>1</sup> Herein, a rhodium complex  $[\text{Rh}(\text{ddppm})(\text{COD})]\text{BF}_4$ , **14a** derived from **ddppm** was synthesized. This chiral diphosphine was reacted with one equivalent of  $[\text{Rh}(\text{COD})_2]\text{BF}_4$  in dichloromethane at room temperature, see Scheme 4.1. The  $^{31}\text{P}$  NMR spectrum of this compound shows a doublet at 24.5 ppm and a Rh-P coupling constant of 143 Hz is observed. This value is in accordance with other  $[\text{Rh}(\text{diene})(\text{diphosphine})]$  complexes which have  $J(\text{P}, \text{Rh})$  values *ca.* 140 Hz.<sup>2</sup>

When compound **14a** was dissolved in acetonitrile, the COD group is displaced with two molecules of acetonitrile affording  $[\text{Rh}(\text{ddppm})(\text{CH}_3\text{CN})_2]\text{BF}_4$ , **14b**, see Scheme 4.1. The  $^{31}\text{P}$  NMR spectrum of this compound shows a doublet at 40.1 ppm with a Rh-P coupling constant of 180 Hz.



**Scheme 4.1:** Synthesis of rhodium complexes **14a** and **14b**.

The  $^1\text{H}$  NMR and  $^{13}\text{C}$  NMR spectra of the compound **14b** were measured in  $\text{CD}_3\text{CN}$  at room temperature and spectral data are presented in Table 4.1.

**Table 4.1:**  $^1\text{H}$  and  $^{13}\text{C}$  chemical shifts of the backbone of **ddppm** from complex **14b**.

H/C group	$^1\text{H}$ NMR, $\delta$ (ppm)	$^{13}\text{C}$ NMR, $\delta$ (ppm)
<b>CH<sub>2</sub></b>	3.91 (2H)	42.03, m
	4.16 (2H)	
<b>CHP</b>	3.16 (2H)	72.13, m
<b>CH</b>	4.83 (2H)	83.26, m

Orange crystals from complex **14b** were obtained after slow diffusion of ether into an acetonitrile solution of the compound. These crystals were suitable for an X-ray structural analysis and crystallographic and experimental data are given in Table 4.2. A plot of the molecular structure of **14b** is shown in Figure 4.1 and selected geometric data are presented in Table 4.3.

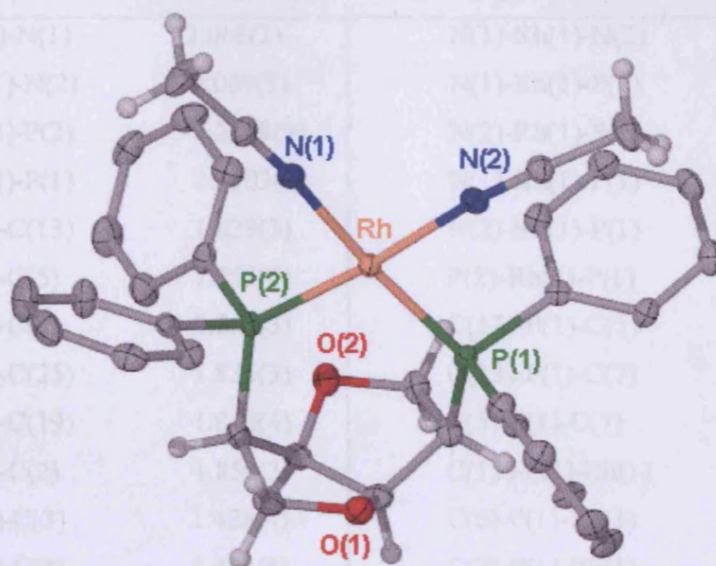


Figure 4.1: X-Seed<sup>3</sup> ellipsoid plot at 50% probability of the molecular structure **14b**. BF<sub>4</sub><sup>-</sup> anion has been omitted for clarity. (Top view with reference to the coordination plane).

Table 4.2: Crystallographic data for rhodium complex **14b**.

Formula	C <sub>36</sub> H <sub>37</sub> B F <sub>4</sub> N <sub>3</sub> O <sub>2</sub> P <sub>2</sub> Rh
Mol wt	795.35
Crystal system	Monoclinic
Space group	P2(1)
a, Å	10.2793(2)
b, Å	15.1367(4)
c, Å	11.5954(4)
V, Å <sup>3</sup>	1772.81(8)
Z	2
Independent reflections	6563 [R(int) = 0.0477]
Reflections collected	16148
Final R indices [I > 2σ(I)]	R1 = 0.0312, wR2 = 0.0698
R indices (all data)	R1 = 0.0345, wR2 = 0.0727
GOF	1.029
Largest diff. peak and hole	0.491 and -0.435 e.Å <sup>-3</sup>



**Table 4.3:** Selected bond lengths (Å) and angles (deg) for rhodium complex **14b**.

Rh(1)-N(1)	2.068(3)	N(1)-Rh(1)-N(2)	88.39(11)
Rh(1)-N(2)	2.069(3)	N(1)-Rh(1)-P(2)	87.21(8)
Rh(1)-P(2)	2.2398(9)	N(2)-Rh(1)-P(2)	174.82(8)
Rh(1)-P(1)	2.2503(9)	N(1)-Rh(1)-P(1)	174.09(8)
P(1)-C(13)	1.829(3)	N(2)-Rh(1)-P(1)	85.84(8)
P(1)-C(5)	1.853(4)	P(2)-Rh(1)-P(1)	98.61(3)
P(1)-C(7)	1.853(3)	C(13)-P(1)-C(5)	103.32(16)
P(2)-C(25)	1.834(3)	C(13)-P(1)-C(7)	103.87(15)
P(2)-C(19)	1.840(4)	C(5)-P(1)-C(7)	99.39(15)
P(2)-C(2)	1.850(3)	C(13)-P(1)-Rh(1)	112.48(11)
O(1)-C(3)	1.428(4)	C(5)-P(1)-Rh(1)	127.01(12)
O(1)-C(4)	1.434(4)	C(7)-P(1)-Rh(1)	107.99(11)
O(2)-C(6)	1.434(4)	C(25)-P(2)-C(19)	102.99(15)
O(2)-C(1)	1.438(4)	C(25)-P(2)-C(2)	104.14(15)
C(1)-C(4)	1.541(5)	C(19)-P(2)-C(2)	98.97(15)
C(1)-C(2)	1.545(5)	C(25)-P(2)-Rh(1)	113.34(12)
C(2)-C(3)	1.523(4)	C(19)-P(2)-Rh(1)	108.32(11)
C(4)-C(5)	1.539(5)	C(2)-P(2)-Rh(1)	126.04(11)
C(5)-C(6)	1.522(5)	C(3)-C(2)-P(2)	112.8(2)
C(7)-C(12)	1.394(5)	C(1)-C(2)-P(2)	113.4(2)
C(7)-C(8)	1.397(5)		

The crystal structure of **14b** confirms again *ddppm* chelation to the metal centre. Figure 4.1 shows the backbone of the ligand adopting an *exo-exo* envelope conformation which places the two phosphine groups at the pseudoaxial positions required for chelation to the metal. A distorted tetrahedral arrangement is observed around the phosphorus atoms imposed from the steric requirements of the isommanide backbone, with tetrahedral angles ranging from 98.97° to 127.01°. *ddppm* has a large bite angle of 98.61° (3) accommodated in the square co-ordination plane by the smaller N-Rh-N angle at 88.39° (11) and P-Rh-N angles at 85.84°(8) and 87.21° (8). For

comparison, the bidentate angle of BINAP (another seven-membered chelate ligand) in an analogous complex is  $91.8^\circ$ .<sup>4</sup> A.S.C. Chan et al. had already reported that P-Rh-P bite angles for seven-membered ring chelates are around  $96^\circ$ .<sup>5</sup>

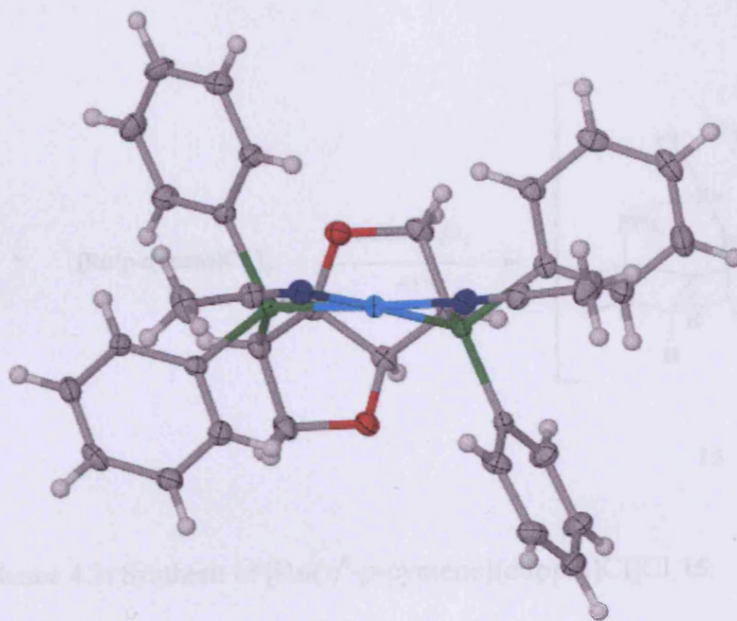
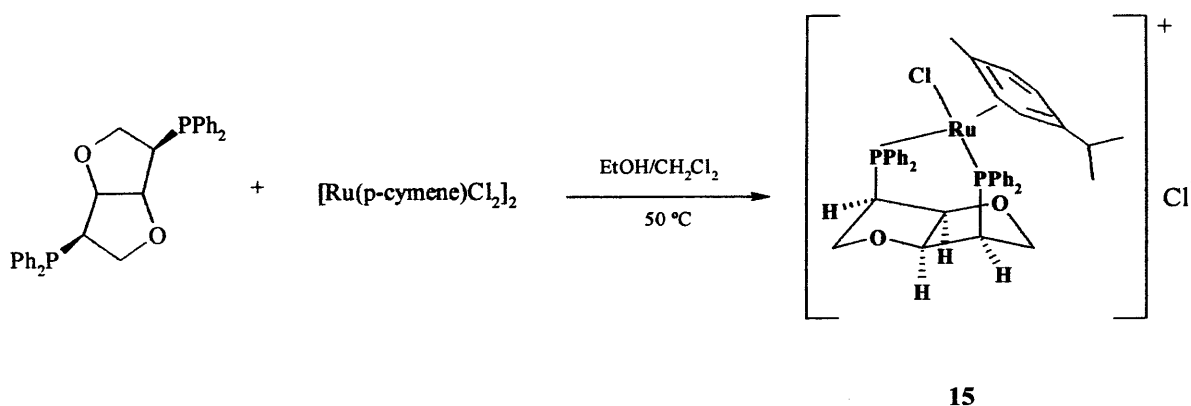


Figure 4.2: X-Seed <sup>3</sup> ellipsoid plot at 50% probability of the molecular structure **14b**. Solvent molecules and the BF<sub>4</sub> anion have been omitted for clarity (side view with reference to the coordination plane).

#### 4.2.2 Synthesis and characterization of Ruthenium complexes with **ddppm**.

Ruthenium chemistry has not been studied extensively despite the wide application of ruthenium catalysts in the asymmetric hydrogenation reactions.<sup>6</sup> Herein, the synthesis of some ruthenium complexes derived from **ddppm** is reported. Unfortunately these complexes did not form crystals suitable for X-Ray characterization however they have been characterized by NMR and mass spectrometry.

The ruthenium complex  $[\text{Ru}(\eta^6\text{-}p\text{-cymene})(\text{ddppm})\text{Cl}]\text{Cl}$ , **15** was synthesized from the reaction of two equivalents of **ddppm** with one equivalent of the dimer  $[\text{Ru}((\eta^6\text{-}p\text{-cymene})\text{X}_2)_2]$  in a mixture of 1:1 dichloromethane and ethanol,<sup>7</sup> see Scheme 4.2.

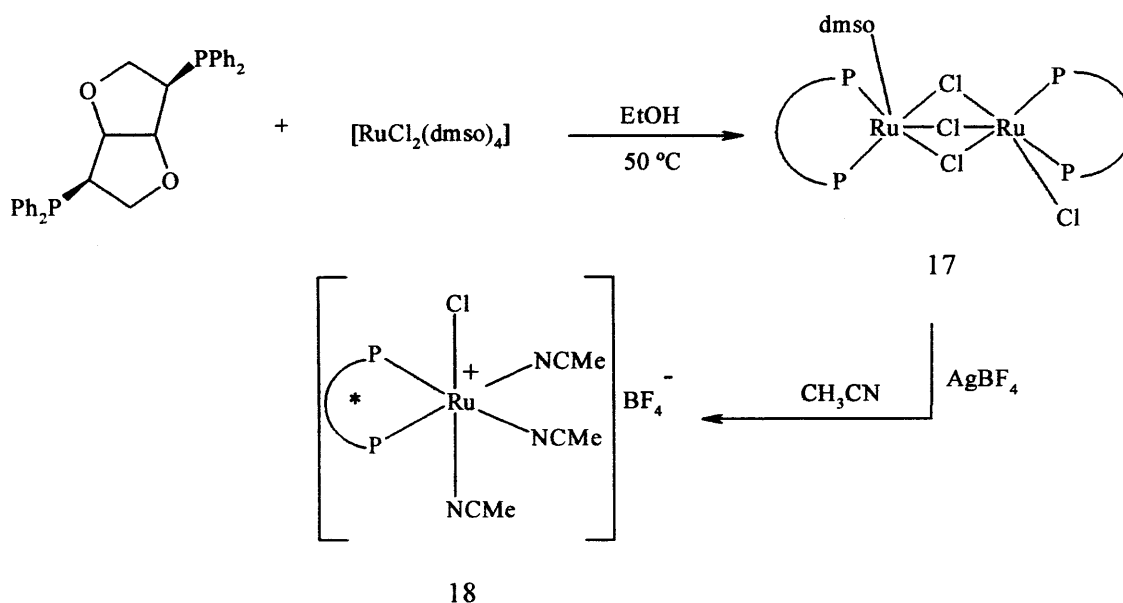


**Scheme 4.2:** Synthesis of  $[\text{Ru}(\eta^6\text{-}p\text{-cymene})(\text{ddppm})\text{Cl}]\text{Cl}$ , **15**.

The  $^{31}\text{P}$  NMR spectrum of **15** shows two unresolved coupling signals at 66 and 23 ppm. However, when the  $\text{Cl}^-$  counter-ion of complex **15** is replaced with  $\text{PF}_6^-$  the  $^{31}\text{P}$  NMR spectrum shows two doublets at 34.4 ppm and 40.1 ppm with a coupling constant of 25 Hz. There is also a septet at 143 ppm due to the free  $\text{PF}_6^-$  ion. This new complex,  $[\eta^6\text{-}p\text{-cymene})\text{Ru}(\text{ddppm})\text{Cl}]\text{PF}_6$ , **16** was formed from the reaction of one equivalent of **ddppm** with  $[\eta^6\text{-}p\text{-cymene})\text{Ru}(\text{NCMe})_2\text{Cl}]\text{PF}_6$ <sup>8</sup> in acetonitrile at room temperature, Scheme 4.4.

The  $^1\text{H}$  NMR spectrum of **16** was measured in  $\text{CD}_3\text{CN}$  and it displays features indicative of a  $\eta^6$ -coordinated arene with resonances of the **ddppm** backbone hydrogens at 5.44 (m, 2H), 3.95 (ddd, 2H), 3.58 (t, 2H) and 3.42 (m, 2H). The methyl group of the coordinate *p*-cymene appears as a singlet at 1.11 ppm while the isopropyl group appears as a septet at 2.29 ppm and a doublet at 0.80 ppm.

characterized by  $^{31}\text{P}$  NMR and an unresolved signal at 66.4 ppm was observed. Treatment of complex **17** with two equivalents of silver tetrafluoroborate in an acetonitrile solution to yield complex **18**, gave inconclusive results. A structure based on literature has been proposed.<sup>7</sup> (See, Scheme 4.5).



**Scheme 4.5:** Possible structures of complexes **17** and **18** from ddpmm with  $\text{RuCl}_2(\text{dmsO})_4$

### 4.2.3 Enantioselective hydrogenation reactions of olefins

**Background:** The development of homogeneous asymmetric hydrogenation was initiated by Knowles and Horner in the late 1960s, after the discovery of Wilkinson's homogeneous hydrogenation catalyst  $[\text{RhCl}(\text{PPh}_3)_3]$ . By replacing triphenylphosphine of the Wilkinson's catalyst with resolved chiral monophosphines, Knowles and Horner reported the earliest examples of enantioselective hydrogenation, although with poor enantioselectivity. Further exploration by Knowles with an improved monophosphine

CAMP provided 88% *ee* and Kagan reported the first bisphosphine ligand, DIOP, for Rh catalysed asymmetric hydrogenation. The successful application of DIOP resulted in several significant directions for ligand design in asymmetric hydrogenation. Chelating bisphosphorus ligands could lead to superior enantioselectivity compared to monodentate phosphines. Additionally, P-chiral phosphorus ligands were not necessary for achieving high enantioselectivity, and ligands with backbone chirality could also provide excellent *ee*'s in asymmetric hydrogenation. Furthermore,  $C_2$  symmetry was an important structural feature for developing new efficient chiral ligands. Kagan's seminal work immediately led to the rapid development of chiral bisphosphorus ligands. Knowles made his significant discovery of a  $C_2$ -symmetric chelating diphosphine ligand, DIPAMP. Due to its high catalytic efficiency in Rh-catalyzed asymmetric hydrogenation of dehydroamino acids, DIPAMP was quickly employed in the industrial production of L-Dopa via asymmetric hydrogenation constituted a milestone work and for this work Knowles was awarded the Nobel Prize in 2001. This work has enlightened chemists to realize the power of asymmetric hydrogenation for the synthesis of chiral compounds.<sup>11</sup>

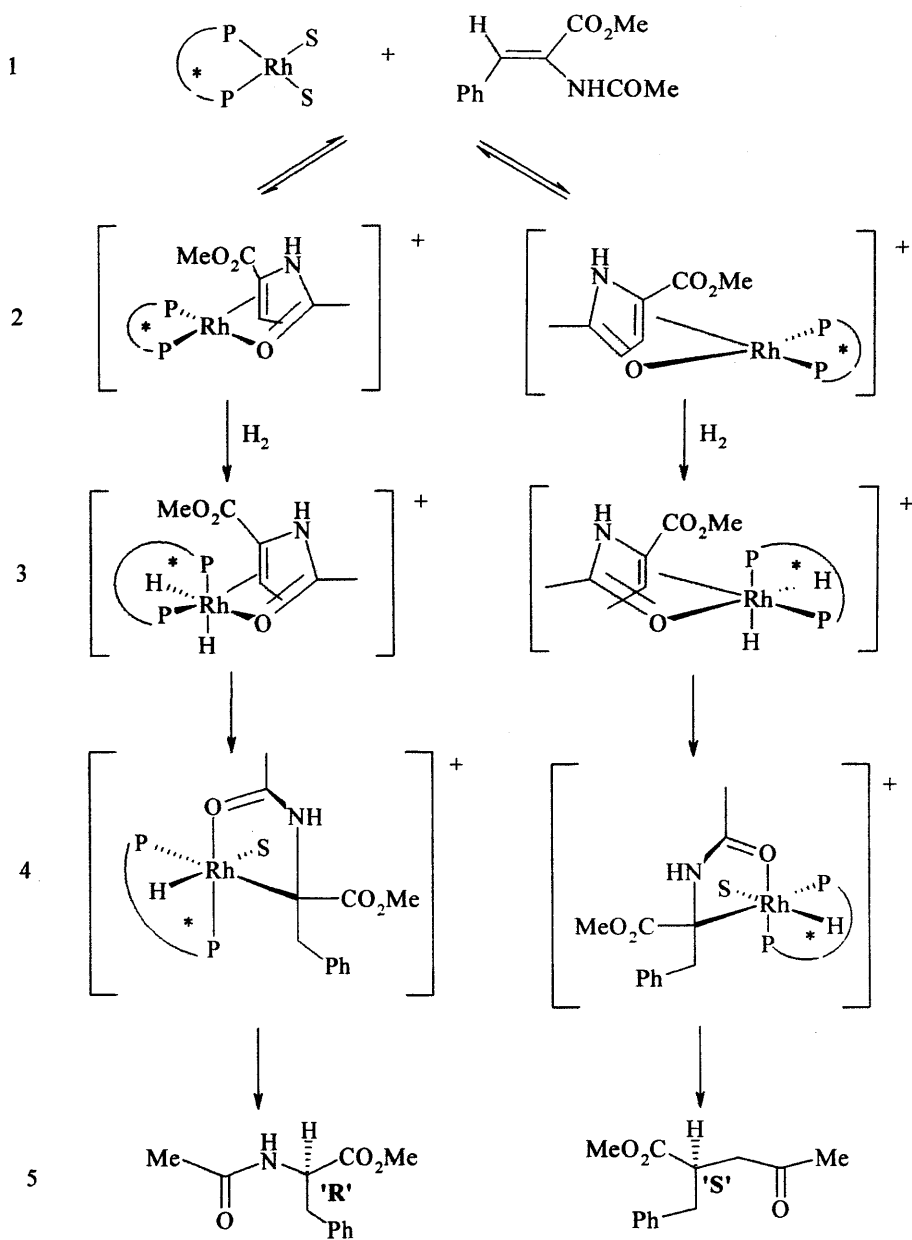
Many of the mechanisms in homogeneous catalysis are only partly known or are still unknown. This is different for the hydrogenation reactions, particularly as far as Wilkinson-type catalysts are concerned which have been intensely studied since the 1970s.<sup>12</sup> Therefore, many of the mechanisms operating in hydrogenation reactions are well understood. The famous mechanism of the enantioselective hydrogenation of dehydroamino acids and their esters is an important example, see Scheme 4.6.

The species starting the catalytic cycle of the hydrogenation of dehydroamino acid derivatives is a square planar  $Rh^I$  complex containing a chelating phosphine,  $P^*P$ , such as

chiraphos, and two solvent molecules S, e.g., methanol, ethanol, or acetone. This species reacts with substrate, methyl (Z)- $\alpha$ -acetamidocinnamate (Scheme 4.6, line 1). The substrate displaces the solvent molecules, giving the square planar species in line 2 of Scheme 4.6. The substrate acts as a bidentate ligand bonded via the olefinic double bond and the oxygen atom of the acetyl group.

The square planar species of line 2 are diastereomers. They contain the same optically active chelating phosphine CHIRAPHOS, but the rhodium atom is coordinated to different sides of the prochiral olefin (*re/si* sides). The two diastereomers of line 2 are rapidly interconverting. In this equilibrium the isomer shown on the left-hand side (*si*-coordination of the olefin) is the minor isomer and the isomer shown on the right-hand side (*re*-coordination of the olefin) is the major isomer.<sup>13</sup>

The next step is the oxidative addition of hydrogen, converting the square planar diastereomers of line 2 into the octahedral dihydrides of line 3.<sup>14</sup> In the present system this reaction is the rate-determining step. The fast step following is the insertion of the coordinated olefin into one of the Rh-H bonds, giving rise to the two diastereomeric  $\sigma$ -alkyl complexes of line 4. By reductive elimination they generate the enantiomeric forms of the product, regenerating the catalytically active square planar species, which re-enters the catalytic cycle.



**Scheme 4.6:** Mechanism of the hydrogenation of methyl (Z)- $\alpha$ -acetamidocinnamate with Wilkinson-type catalysts.

**Results:** The catalytic performance of ddppm- rhodium and ruthenium complexes in olefin hydrogenation reactions was tested and results are discussed in this section.

Standard substrates such as (Z)-N-acetamido cinnamic acid and its methyl ester were used.

**Table 4.4:** Results from hydrogenation reactions of N-acetamido cinnamic derivatives.

R: H (Z)-2-acetamidocinnamic acid  
 R: Me methyl (Z)-2-acetamidocinnamate

(R,S)-2-acetamido-3-phenyl-propionic acid  
 (R,S)-2-acetamido-3-phenyl-propionic ac. dimethyl ester

Entry	R	Catalyst	Pressure (H <sub>2</sub> )	Solvent	T (°C)	Ee <sup>b</sup> (%)	Conv. (%)	Config.
1	H	[Rh]	1 atm	MeOH	r.t.	30	100	R
2	H	[Rh]	3.5 atm	MeOH	r.t.	36	85	R
3	H	[Ru]	3.5 atm	MeOH	40 °C	73	50	R
4	H	[Ru]	3.5 atm	THF/CH <sub>2</sub> Cl <sub>2</sub>	40 °C	<5	-	-
5	CH <sub>3</sub>	[Rh]	1 atm	MeOH	r.t.	17	30	R
6	CH <sub>3</sub>	[Ru]	3.5 atm	EtOH	40 °C	<5	-	-

a) Reaction conditions: [Rh] = [Rh(COD)<sub>2</sub>]BF<sub>4</sub>/ddppm (1:1), [Ru] = [Ru(*p*-cymene)Cl<sub>2</sub>]<sub>2</sub>/ddppm (1:2). 0.01 mmol of precatalyst and 1.0 mmol of prochiral olefin in 15 ml of solvent, 24 h. b) *ee* values were determined by HPLC with Chiralcel OD column, Hexane/IPA, 8:2, 1ml/min, 254 nm. The acids were converted to the corresponding methyl esters with methyl iodide/KHCO<sub>3</sub> before HPLC analysis.

Table 4.4 summarizes the results at 1 and 3.5 atmospheres of hydrogen pressure. The best enantioselectivity achieved (73%) was when (Z)-N-acetamido cinnamic acid was hydrogenated with the ruthenium catalyst under a pressure of 3.5 atm (entry 3). Reactions with the Ru catalyst were heated to 40° C in order to form a homogeneous solution. With the rhodium system, better enantioselectivities were achieved when the (Z)-N-acetamido cinnamic acid was hydrogenated rather than the (Z)-N-acetamido cinnamic ester which gave quantitative yields but moderate enantioselectivities (entries 1, 2 and 5 ). All the reactions gave the 'R' configuration of the product.

With the Ru precatalyst **15** reduction of the (Z)-N-acetamido cinnamic ester was ineffective. When hydrogenating the (Z)-N-acetamido cinnamic acid with the Ru system



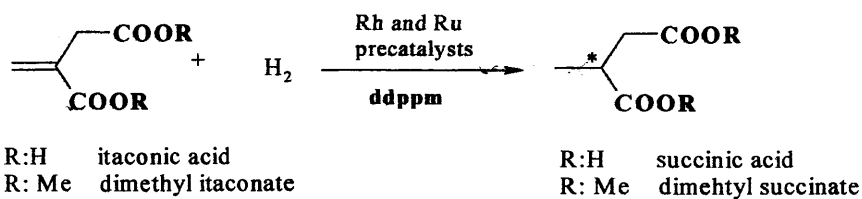
the solvent played an important role. In a mixture of aprotic solvents such as THF and dichloromethane (entry 5) the substrate was hardly reduced, on the other hand, in methanol a 50% yield was obtained (entry 3).

When **ddppi**, the non-chelating diastereoisomer studied by Bakos<sup>15</sup>, was tested in the homogeneous catalytic reactions of (*Z*)-*N*-acetamide cinnamic acid derivatives, moderate results were also achieved (38% *ee*), but in contrast with **ddppm** the (*S*)-enantiomer was formed.

Itaconic acid and its methyl ester, our second test olefins, gave the (*S*)-configured product after hydrogenation with the Rh catalyst **14** and Ru catalyst **15**, see Scheme 4.8 and Table 4.5.

From Table 4.5 it can be seen better enantioselectivities were observed for the acid than for its methyl ester derivative (entries 7-10) even though half the amount of the catalyst was used (0.5%). This is in accordance with results obtained with the acetamide acid (Table 4.4). A similar performance was observed with the diphosphine DIOP, which is also a seven-membered ring. The DIOP/Rh system hydrogenates itaconic acid with good enantioselectivities (70-68%) and its methyl ester, however with lower *ee*'s (53-36%).<sup>16</sup> In all reactions, the (*S*)-enantiomer was also formed as with the **ddppm**/Rh or **ddppm**/Ru systems.

The data in Table 4.5 also show the influence of different solvents and hydrogen pressure on conversion (entries 1-3). The higher the pressure used (20 bar) the less yield and *ee* were obtained (entry 3). Using ruthenium complex **15** does not give a good enantioselectivity as it happened with acetamide derivatives, however good conversions to the final product were obtained (entry 5 and 6).

**Table 4.5:** Results from hydrogenation reactions of itaconic derivatives.

Entry	R	Catalyst	Pressure (H <sub>2</sub> )	Solvent	ee (%) <sup>c</sup>	Conv. (%)	Config.
1	CH <sub>3</sub>	[Rh]	1 atm	CH <sub>2</sub> Cl <sub>2</sub>	41	100	S
2	CH <sub>3</sub>	[Rh]	3.5 atm	EtOH	12	100	S
3	CH <sub>3</sub>	[Rh]	20.3 atm	CH <sub>2</sub> Cl <sub>2</sub>	31	20	S
4	CH <sub>3</sub>	[Ru]	3.5 atm	EtOH	9	75	S
5	CH <sub>3</sub>	[Ru]	3.5 atm	CH <sub>2</sub> Cl <sub>2</sub>	7	100	S
6 <sup>b</sup>	H	[Rh]	1 atm	THF	3	100	S
7 <sup>b</sup>	H	[Rh]	1 atm	EtOH	64	72	S
8 <sup>b</sup>	H	[Rh]	3.5 atm	EtOH	59	72	S
9 <sup>b</sup>	H	[Ru]	1 atm	MeOH	18	60	S
10 <sup>b</sup>	H	[Ru]	3.5 atm	EtOH	20	65	S

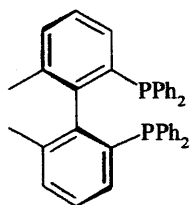
*Reaction conditions:* [Rh] ≡ [Rh(COD)<sub>2</sub>]BF<sub>4</sub>/ddppm (1:1), [Ru] ≡ [Ru(*p*-cymene)Cl<sub>2</sub>]<sub>2</sub>/ddppm (1:2). 0.01 mmol of precatalyst and 1.0 mmol of prochiral olefin in 15 ml of solvent, 24 h. Reactions with Ru precatalyst were heated up to 40 °C, the rest were done at room temperature. *c*) ee values were determined by HPLC with Chiralcel OD column, Hexane/IPA, 98:2, 0.75ml/min, 220 nm. The acids were converted to the corresponding methyl esters with SOCl<sub>2</sub> before HPLC analysis.

The solvent plays also a crucial role in the hydrogenation of these substrates since using other solvents than dichloromethane such as ethanol or THF decreases the enantioselectivity (entries 2, 4 and 6).

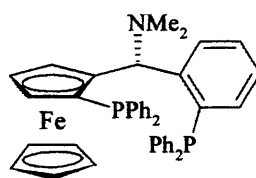
In the literature, excellent enantioselectivities, up to 99%, have been reported with phosphite ligands derived from D-isomannide,<sup>17</sup> and with BINAP.<sup>18</sup>

#### 4.2.4 Enantioselective hydrogenation reactions of ketones.<sup>19</sup>

Asymmetric hydrogenations of  $\alpha$ - and  $\beta$ -ketoesters have been very successful using chiral ruthenium catalysts; a detailed review has been presented by Ager et al..<sup>20</sup> A BINAP-Ru system catalysed the hydrogenation of a variety of  $\beta$ -keto esters to chiral  $\beta$ -hydroxyl esters with high enantioselectivities.<sup>21</sup> In addition to BINAP, many other chiral atropoisomeric biaryl ligands such as (S)-Biphemp and Taniaphos have demonstrated to be very efficient for this transformation, reaching enantioselectivities *ca.* 99%.<sup>22</sup>



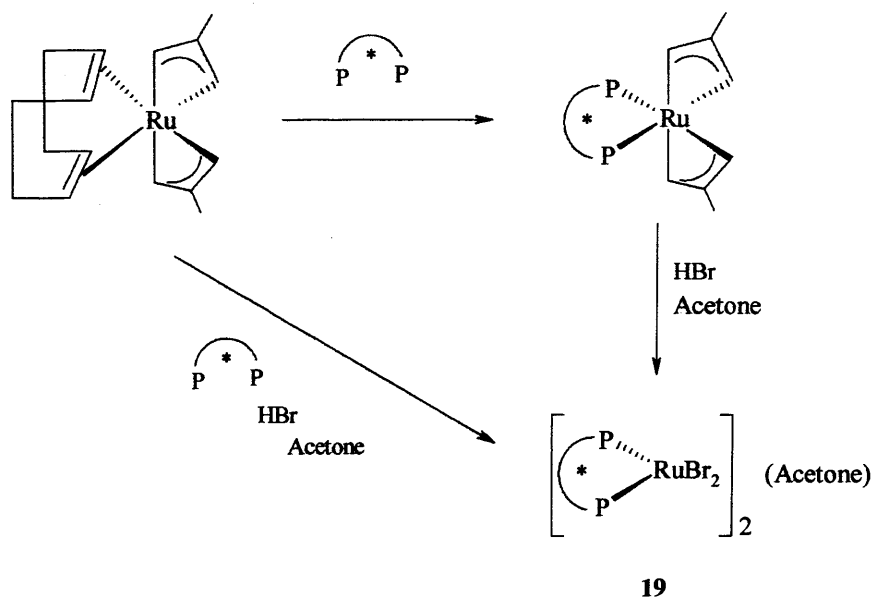
(S)-Biphemp



Taniaphos

Furthermore, Junge et al., have recently developed monodentate phosphine ligands which are efficient for the ruthenium-catalysed hydrogenation of  $\beta$ -ketoesters obtaining *ee*'s up to 95% at 100 °C.<sup>23</sup>

The diphosphine **ddppm** was tested in this type of reactions. The ruthenium precursor, [Ru(COD)(methylallyl)<sub>2</sub>], was mixed with the **ddppm** ligand in acetone in a ratio of 1:2 followed by 2 equivalents of methanolic HBr to form the catalytic species Ru(**ddppm**)Br<sub>2</sub>, **19** (Scheme 4.10).<sup>24</sup> The catalyst concentration used was 1 mol % and all the reactions were carried out in methanol or ethanol depending on the ester group.

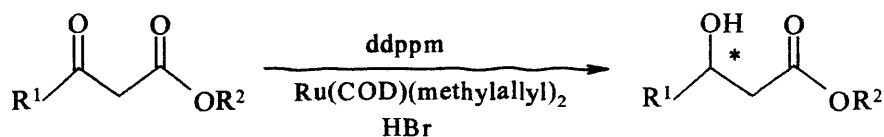


**Scheme 4.10:** Preformed Ru catalyst for hydrogenation of  $\beta$ -ketoesters.

A series of  $\beta$ -ketoesters were reduced with the *in situ* formed ruthenium complex 19 and the results are presented in Table 4.6.

All reactions were carried out under 60 bar of hydrogen pressure at three different temperatures (60, 80 and 100° C) and they were run for 16 h. In the case of 60° C, reactions were repeated and left stirring for 48 h to see whether an increase in conversion was observed (entries 4,8,12 and 16). All reactions have been carried out twice at each temperature, as a test of reproducibility, and Table 4.6 presents the average of the two.

Hydrogenation of methyl acetoacetate (**20a**) was studied first (entries 1-4). The best conversion (41%) was obtained when the reaction was heated at 100 °C (entry 3). With increasing the temperature from 60 to 100 °C (entries 1-3) an increase in the yield is observed from 8.9 to 41.1 % with a concomitant change in the enantioselectivity from the '*R*' to the '*S*' isomer.

**Table 4.6:** Results from hydrogenation reactions of  $\beta$ -ketoesters using Ru(II) catalyst **19**.

20a-d				21a-d			
Entry	$\beta$ -ketoester <sup>a,b</sup>	R <sup>1</sup>	R <sup>2</sup>	ee (%) <sup>c</sup>	Yield (%)	t (h) <sup>d</sup>	T (°C)
1	20a	Me	Me	17.5 (R)	8.9	16	60
2	20a	Me	Me	7.6 (S)	17.8	16	80
3	20a	Me	Me	5.2 (S)	41.1	16	100
4	20a	Me	Me	16.2 (S)	26.5	48	60
5	20b	Et	Me	26.7 (R)	9.5	16	60
6	20b	Et	Me	14.1 (S)	18.2	16	80
7	20b	Et	Me	5.2 (S)	38.9	16	100
8	20b	Et	Me	9.5 (R)	17.0	48	60
9	20c	CH <sub>2</sub> Cl	Et	23.9 (R)	16.1	16	60
10	20c	CH <sub>2</sub> Cl	Et	22.0 (R)	61.4	16	80
11	20c	CH <sub>2</sub> Cl	Et	20.8 (R)	67.1	16	100
12	20c	CH <sub>2</sub> Cl	Et	<i>rac</i>	32.5	48	60
13	20d	Ph	Et	5.5 (S)	5.1	16	60
14	20d	Ph	Et	7.9 (S)	8.5	16	80
15	20d	Ph	Et	3.4 (R)	36.2	16	100
16	20d	Ph	Et	21.5 (R)	9.0	48	60

Reaction conditions: a) Ru(II) precatalyst **19** (1% mol) was formed *in situ*: Ru(COD)(methylallyl)<sub>2</sub>/ddppm/HBr (1:1:2). b) Solvent: the corresponding alcohol of the  $\beta$ -ketoester (methanol or ethanol). c) % ee's were determined by GC (25 m Lipodex E, 95°C isothermal or HPLC (OD-H, hexane/ethanol 95:5, 0.5 ml/min). d) Reaction times are not optimised.

When the reaction is left to run to 48 hrs at 60 °C again the opposite stereochemistry is observed (entries 1 and 4). A likely explanation might be due to the following equilibrium, where the ruthenium species catalyses the dehydrogenation of the ROH.

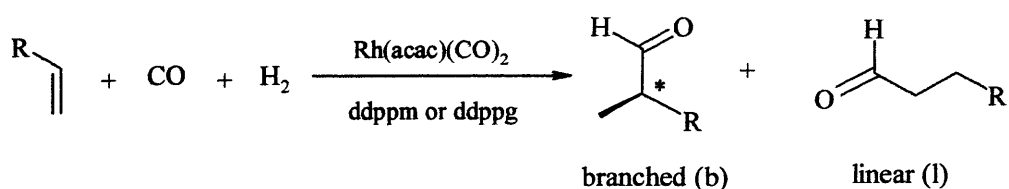


Such equilibrium is taking place in the transfer hydrogenations of ketones.<sup>25</sup> The same behaviour was observed when methyl 3-oxo-pentanoate (**20b**) was reduced (entries 5-8). In all the cases the '*S*' enantiomer seems to be the final product. The third  $\beta$ -ketoester to be reduced was ethyl 4-chloro-3-oxobutyrate (**20c**) and in this case no change in the configuration was observed. Furthermore, increasing the temperature gives better conversions (67%, entry 11) and the '*R*' enantiomer was obtained for this ketoester. When the reaction is left for 48 h at 60 °C (entry 12) the racemic enantiomer was achieved. The last  $\beta$ -ketoester studied was ethyl 3-oxo-3-phenylpropionate (**20d**) and low conversion (6-8%) was gained (entry 13-14). The '*R*' configuration was obtained upon increasing the temperature and the time (entry 15-16).

#### 4.2.5 Asymmetric hydroformylation.<sup>26</sup>

The metal-catalysed asymmetric hydroformylation of alkenes has attracted much attention as a potential tool for preparing enantiomerically pure aldehydes, which are important precursors for synthesizing biologically active compounds, biodegradable polymers, and liquid crystals.<sup>1c,27</sup> (Scheme 4.11) Since 1970, transition metal complexes based on rhodium, platinum and palladium have been employed as catalysts in asymmetric hydroformylation.<sup>27</sup> Using Pd/diphosphine catalysts, high enantioselectivities have been

obtained but these suffer from low chemo- and regio-selectivity.<sup>28</sup> Rh/diphosphine catalysts give high catalytic activities and regioselectivities in branched aldehydes, but the *ee*'s do not exceed 60%.<sup>29</sup>

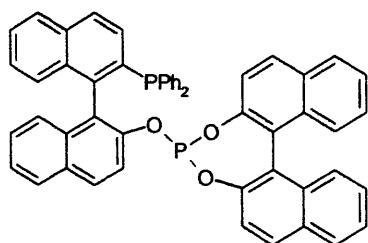


22: R = OAc (Vinyl Acetate)

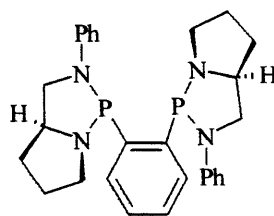
23: R = Ph (Styrene)

**Scheme 4.11:** Hydroformylation reaction of alkenes 22 and 23.

Despite the scientific and commercial attractiveness of this process, few efficient catalysts are available for this reaction. Hydroformylation of vinyl acetate and styrene with rhodium(I) complex of (R,S)-BINAPHOS has given excellent results. The branched products were found in up to 92% *ee*. Hydroformylation of vinyl acetate with a bis(diazaphospholidine) ligand ESPHOS gave good results even at low pressures (e.g. 8 bar, 90% *ee*). Racemic products were obtained when ESPHOS was used in hydroformylation of styrene.<sup>30</sup> Other derivatives of ESPHOS have been proved to be poor in this catalytic reaction, in both terms of conversion and *ee*.<sup>31</sup>



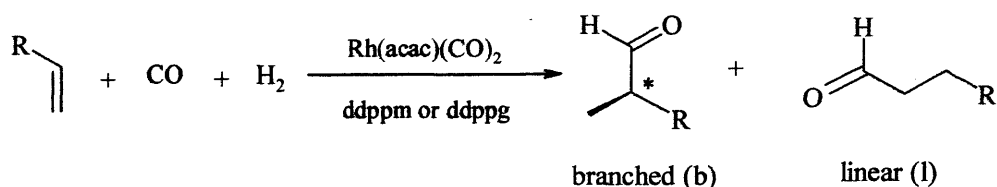
(R,S)-BINAPHOS



ESPHOS

This catalytic reaction has been tested with the two phosphines synthesised in Chapter 2 (**ddppm** and **ddppg**). Two different substrates, vinyl Acetate (**22**) and styrene (**23**), were reduced and  $\text{Rh}(\text{acac})(\text{CO})_2$  was used as the rhodium precursor. The results are presented in table 4.7:

**Table 4.7:** Results from hydroformylation reactions of alkenes **22** and **23**.



**22:** R = OAc (Vinyl Acetate)

**23:** R = Ph (Styrene)

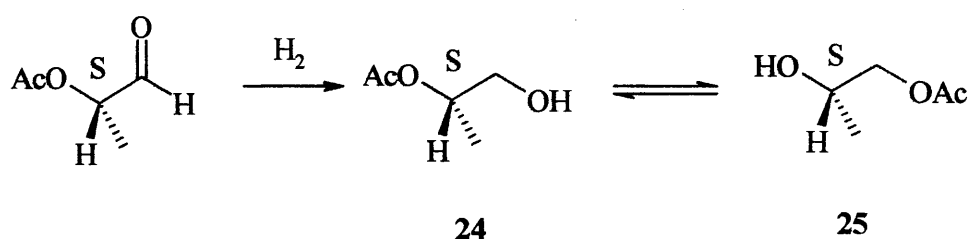
Entry	Ligand	Substrate	t (h)	Conversion (%)	Branched selectivity (%)	Aldehyde (%)	Aldehyde ee (%) <sup>a</sup>	Alcohol (%)	Alcohol ee (%) <sup>a</sup>
1	ddppm	22	21	75.3	80.5	97.3	-32.1	0.9	-34.3
2	ddppg	22	21	81.9	86.6	97.6	-31.3	1.1	-
3	ddppm	23	12	95.1	74.7	100	-4.7	-	-
4	ddppg	23	3	98.8	84.3	100	2.3	-	-

*Conditions and reagents:* 8 bar, 60°C. Vinyl acetate 10.8 mmol, styrene 8.72 mmol,  $\text{Rh}(\text{acac})(\text{CO})_2$  51.2 mmol, ddppm or ddppg 76.8 mmol. The products were identified using chiral GCMS and comparison with authentic samples of each enantiomer. [a] +ve ee indicates *S* configuration is favoured, -ve indicates *R* is favoured.

When the two phosphines (**ddppm** and **ddppg**) are compared, for vinyl acetate, both gave similar enantioselectivities. However for styrene, **ddppm** gave higher enantioselectivity than **ddppg**. This could be because **ddppm** is a chelating diphosphine and better results were expected than for **ddppg**, which is a non-chelating ligand. Surprisingly ee's with **ddppm** and **ddppg** are pretty close.



Hydroformylation of vinyl acetate gave small amounts of the corresponding 2-acetoxypropan-1-ol, **24** (Scheme 4.12). This alcohol tautomerises to give 1-acetoxypropan-2-ol, **25**. These reactions and the amounts of the individual products are shown in Table 4.7 (entries 1 and 2). These alcohols have also been found by Breeden et al., when reducing vinyl acetate with Rh/ ESPHOS system.<sup>30</sup>



**Scheme 4.12:** Further hydrogenation of aldehydes.

In the case of styrene, only aldehydes were obtained. Both linear and branched aldehydes were obtained with the selectivity to the branched isomer being 74-84 % and very low ee, *ca.* 2-5% (entries 3 and 4). For vinyl acetate, the main products were aldehydes. In this case, the linear products were not detected and acetic acid was detected as a by-product. It was determined that the linear product decomposes with loss of acetic acid, whilst the branched product is stable. It is, therefore, assumed that all the acetic acid produced comes from the linear aldehydes and have used this assumption in calculating the branched selectivity.

In all the reactions the conversions are quite good, *ca.* 99 % for styrene and 75-82 % for vinyl acetate but both phosphines proved to be poor in this application in terms of

enantioselectivities. However, higher enantioselectivities were found for vinyl acetate (31-32%, entries 1 and 2) than for styrene (4.7-2.3%, entries 3 and 4).

### 4.3 CONCLUSIONS

Rhodium complex,  $[\text{Rh}(\text{ddppm})(\text{COD})]\text{BF}_4$  (**14a**) was synthesized. In acetonitrile the COD group was displaced by the solvent to afford the complex  $[\text{Rh}(\text{dddppm})(\text{CH}_3\text{CN})_2]\text{BF}_4$  (**14b**) which was characterized crystallographically.

Several attempts to isolate ruthenium complexes with **ddppm** did not meet with success. However, we were able to characterize the ruthenium *p*-cymene complex  $[\text{Ru}(\text{ddppm})(p\text{-cymene})\text{Cl}]\text{PF}_6$  (**16**).

It was shown that the cationic rhodium-**ddppm** complex **14b** is an efficient catalyst for the hydrogenation of itaconic derivatives exhibiting moderate enantioselectivities, up to 64% at low hydrogen pressures. The ruthenium-**ddppm** system was used for the hydrogenation of acetamidocinnamic derivatives at low pressures and good to high enantioselectivities (73%) were obtained. Aprotic solvents such as THF were not suitable solvents for the reduction of these substrates and an alcohol such as methanol or ethanol were used instead.

Hydrogenation of ketones with the Ru-**ddppm** system and hydroformylation with the Rh-**ddppm** and Rh-**ddppg** systems were also studied and the results indicate that these ligands do not form efficient catalysts for this type of reactions.

#### 4.4 EXPERIMENTAL

**General considerations:** All manipulations were performed using standard Schlenk techniques under an argon atmosphere, except where otherwise noted. Solvents of analytical grade and deuterated solvents for NMR measurements were distilled from the appropriate drying agents under N<sub>2</sub> immediately prior to use following standard literature methods.<sup>32</sup> Literature methods were employed for the synthesis of [Rh(COD)Cl]<sub>2</sub><sup>33</sup>, [Ru(*p*-cymene)Cl<sub>2</sub>]<sub>2</sub><sup>34</sup>, [Ru(*p*-cymene)I<sub>2</sub>]<sub>2</sub><sup>35</sup>, RuCl<sub>2</sub>(dmsO)<sub>4</sub><sup>36</sup>. All other reagents were used as received. A 300 ml stainless steel autoclave and a 100 ml glass autoclave were used for the hydrogenation reactions of olefins (Section 4.3). NMR spectra were obtained on Bruker Avance AMX 400 or Jeol Eclipse 300 spectrometers and referenced to external TMS. HPLC analyses were performed on an Agilent 1100 series instrument. Mass spectra were obtained in ES (Electrospray) mode unless otherwise reported from the EPSRC Mass Spectrometry Service, Swansea University.

**[Rh(COD)<sub>2</sub>]BF<sub>4</sub>:** To a dichloromethane solution (15 ml) of [Rh(COD)Cl]<sub>2</sub> (1g, 2.03 mmol) 1,5-cyclooctadiene (0.5 ml, 4.06 mmol), previously purified by passing through a plug of silica gel, and 0.79 g mg (4.06 mmol) of AgBF<sub>4</sub> were added. The colour changed from orange to dark red. The dark red slurry formed was stirred in the dark for 1 hour. After that time the white precipitate formed was filtered through celite and washed with CH<sub>2</sub>Cl<sub>2</sub> (2 ml). The solvent was concentrated and anhydrous Et<sub>2</sub>O (15 ml) was added to precipitate the complex. The red solid formed was filtered, washed with anhydrous Et<sub>2</sub>O (3 x 10mL) and dried (1.49 g, 90% yield). <sup>1</sup>H NMR (CDCl<sub>3</sub>, 250MHz): δ = 2.49 (s, 16H;

$\text{CH}_2$ ); 5.30 (s, 8H; CH);  $^{13}\text{C}$  NMR (100 MHz,  $\text{CDCl}_3$ ):  $\delta$  = 29.63 ( $\text{CH}_2$ ), 107.44 (d,  $J_{\text{Rh-C}}$  7.61 Hz, CH).

**Synthesis of  $[\text{Rh}(\text{COD})(\text{ddppm})]\text{BF}_4$ , 14a:** To a solution of the phosphine ddppm (147mg, 0.3 mmol) in dichloromethane, some  $[\text{Rh}(\text{COD})_2]\text{BF}_4$  (123mg, 0.3 mmol) were added. After 1 day of stirring at room temperature a yellow solid was obtained in quantitative yield.  $^{31}\text{P}$  NMR ( $\text{CDCl}_3$ , 121MHz)  $\delta$  24.5 ( $^1J_{\text{PRh}}$  = 143 Hz). **Synthesis of  $[\text{Rh}(\text{ddppm}(\text{CH}_3\text{CN})_2)\text{BF}_4$ , 14b:** If complex 14a is dissolved in acetonitrile, the COD group is displaced for two molecules of  $\text{CH}_3\text{CN}$ . The solvent is concentrated and then, ether is added to precipitate a solid. This orange-yellow solid obtained is filtered and crystallized in a mixture of acetonitrile and diethyl ether.  $[\text{Rh}(\text{ddppm}(\text{CH}_3\text{CN})_2)\text{BF}_4$ , 14b.  $^1\text{H}$  NMR ( $\text{CD}_3\text{CN}$ , 400MHz)  $\delta$  3.16 (m, 2H,  $\text{CHPh}_2$ ), 3.91 (m, 2H,  $\text{CH}_2$ ), 4.16 (m, 2H,  $\text{CH}_2$ ), 4.83 (m, 2H, CCH), 7.2-7.4 (m, 20H);  $^{31}\text{P}$  NMR ( $\text{CD}_3\text{CN}$ , 121MHz)  $\delta$  40.1 ( $^1J_{\text{PRh}}$  = 180 Hz);  $^{13}\text{C}$  NMR ( $\text{CD}_3\text{CN}$ , 100 MHz) 42.03 (m, 2C,  $\text{CH}_2$ ), 72.13 (s, 2C, CHP), 83.26 (s, 2C, CHP), 127.62 (m, 4C, Ar), 127.80 (m, 4C, Ar), 129.45 (s, 2C, Ar), 129.87 (s, 2C, Ar), 133.42 (m, 4C, Ar), 133.93 (m, 4C, Ar); MS (accurate mass, ES+) calculated mass for  $[\text{M-BF}_4]^+$ : 667.1145, measured: 667.1147;  $[\text{M-BF}_4\text{-CH}_3\text{CN}]^+$ : 626.2,  $[\text{M-BF}_4\text{-2CH}_3\text{CN}]^+$ : 585.2.

**Synthesis of  $[\text{Ru}(\text{ddppm})(p\text{-cymene})\text{Cl}]\text{Cl}$ , 15a:** To a mixture of ddppm (134 mg, 0.28 mmol) and red brown  $[\text{RuCl}_2(p\text{-cymene})]_2$  (95 mg, 0.15 mmol) placed in a schlenk tube were added ethanol (20 ml) and dichloromethane (20 ml). The mixture was stirred at 50°C

for 1 h. Then, the solvent was evaporated. A pink solid was obtained.  $^{31}\text{P}$  NMR ( $\text{D}_2\text{O}$ , 300 MHz) 66.4 (m), 23 (m)).

**Synthesis of  $[\eta^6\text{-}(p\text{-cymene})\text{Ru}(\text{ddppm})\text{Cl}]\text{PF}_6$ , 16:** 41 mg (0.083 mmol) of  $[\text{Ru}(p\text{-cymene})(\text{CH}_3\text{CN})_2\text{Cl}]\text{PF}_6$  were placed in a schlenk and dissolved in 10 ml of acetonitrile. Then, 40 mg (0.083 mmol) of the diphosphine ddppm was added into it. The solution changes rapidly to red-orange colour. After stirring it at room temperature for 1 day, the solvent was evaporated and diethyl ether was added to break the oil in an orange solid. The solid was washed several times with more portions of diethyl ether.  $^{31}\text{P}$  NMR ( $\text{CD}_3\text{CN}$ , 121 MHz),  $\delta$  ppm: 34.4 (d), 40.1 (d)  $^2J_{\text{PP}} = 25$  Hz).  $^1\text{H}$  NMR ( $\text{CD}_3\text{CN}$ , 400 MHz),  $\delta$  ppm: 0.80 (d, 6H,  $\text{CH}(\text{CH}_3)_2$ ), 1.11 (s, 3H,  $\text{C}_6\text{H}_4\text{CH}_3$ ), 2.29 (sept, 1H,  $\text{CH}(\text{CH}_3)_2$ ), 3.42 (m, 2H,  $\text{CHPh}_2$ ), 3.58 (t, 2H,  $\text{CH}_2$ ), 3.95 (ddd, 2H,  $\text{CH}_2$ ), 3.95 (ddd, 2H,  $\text{CH}_2$ ), 5.44 (m, 2H,  $\text{CCH}$ ) and 7.21-8.29 (m, 24H). MS ( $\text{ES}^+$ ) calculated mass for  $[\text{M}-(p\text{-cymene})\text{-PF}_6]^+$ : 619.

**Synthesis of  $\text{Ru}(\text{ddppm})_2(\eta^3\text{-Cl})(\text{Cl})\text{dmsO}$ , 17:** A mixture of ddppm (100 mg, 0.21 mmol) and orange crystals of  $\text{RuCl}_2(\text{dmsO})_4$  (100 mg, 0.21 mmol) in ethanol was refluxed (80-90°C) for 1.5 h. The solvent was evaporated and an orange solid was obtained.  $^{31}\text{P}$  NMR ( $\text{CDCl}_3$ , 300 MHz)  $\delta$  66.4 (br. s).

**Synthesis of  $[\text{Ru}(\text{ddppm})(\text{CH}_3\text{CN})_3\text{Cl}]\text{BF}_4$ , 18:** To a solution of  $\text{AgBF}_4$  (81mg, 0.42 mmol), a solution in acetonitrile of complex 17 was added. The mixture was stirred for 30 min and then, the white solid ( $\text{AgCl}$ ) was filtered through celite. After filtration the solvent was evaporated and an orange-yellow crystalline solid was obtained.  $^{31}\text{P}$  NMR ( $\text{CDCl}_3$ , 300 MHz)  $\delta$  38.2 (s).

After the end of the reaction the obtained solution was filtered through a short pad of silica gel to remove the catalyst. Conversion and enantiomeric excesses were determined by chiral HPLC.

***Procedures of hydrogenation reactions of olefins:***

***Rh/acetamide acid:*** A 20 ml schlenk was charged with a solution of ddppm (5.3 mg, 0.011 mmol),  $[\text{Rh}(\text{COD})_2]\text{BF}_4$  (4mg, 0.01 mmol) and (Z)-2-acetamidocinnamic acid (205 mg, 1 mmol) in methanol. A stream of  $\text{H}_2$  was bubbled at ambient temperature for 24 h. After the end of the reaction the obtained solution was filtered through a short pad of silica gel to remove the catalyst. ***Ru/acetamide acid:*** A 20ml schlenk was charged with a solution of ddppm (5.3 mg, 0.011mmol),  $[\text{Ru}(p\text{-cymene})\text{Cl}_2]_2$  (3.3 mg, 0.005 mmol) and (Z)-2-acetamidocinnamic acid (205 mg, 1 mmol) in methanol. A stream of  $\text{H}_2$  was bubbled at 40°C for 24 h. After the end of the reaction the obtained solution was filtered through a short pad of silica gel to remove the catalyst. The acids were converted to their methyl ester (methyl (Z)-2-acetamidocinnamate) before HPLC analysis following a literature procedure,<sup>37</sup> the acid (1 mmol) and anhydrous potassium carbonate (2mmol) were refluxed in acetone (6 ml) with mechanical stirring, while MeI (1 mmol) was added slowly. The resulting solutions were then submitted to analysis to determine the enantiomeric excess by HPLC with Chiralcel OD column, Hexane/IPA, 8:2, 1ml/min, 254 nm.

***Rh/itaconic acid:*** A 20 ml schlenk was charged with a solution of ddppm (5.3 mg, 0.011mmol),  $[\text{Rh}(\text{COD})_2]\text{BF}_4$  (4 mg, 0.01 mmol) and itaconic acid (250 mg, 1.92 mmol) in

dichloromethane. A stream of H<sub>2</sub> was bubbled at ambient temperature for 24 h. After the end of the reaction the obtained solution was filtered through a short pad of silica gel to remove the catalyst. ***Ru/itaconic acid:*** A 20 ml schlenk was charged with a solution of ddppm (5.3 mg, 0.011 mmol), [Rh(COD)<sub>2</sub>]BF<sub>4</sub> (3.3 mg, 0.01 mmol) and itaconic acid (250 mg, 1.92 mmol) in dichloromethane. A stream of H<sub>2</sub> was bubbled at 40°C for 24 h. After the end of the reaction the obtained solution was filtered through a short pad of silica gel to remove the catalyst. The acids were converted to their methyl ester (dimethyl itaconate) following a literature procedure<sup>38</sup>, the acid (1.92 mmol) dissolved in MeOH was reacted with SOCl<sub>2</sub> (0.2 ml) and it was refluxed for 2h. The resulting solutions were then submitted to analysis to determine the enantiomeric excess by HPLC with Chiralcel OD column, Hexane/IPA, 98:2, 0.75 ml/min and 220 nm.

***Rh/dimethyl itaconate:*** A 20 ml schlenk was charged with a solution of ddppm (5 mg, 0.011 mmol), [Rh(COD)<sub>2</sub>]BF<sub>4</sub> (4 mg, 0.01 mmol) and dimethyl itaconate (158 mg, 1 mmol) in dichloromethane. A stream of H<sub>2</sub> was bubbled at ambient temperature for 24 h. After the end of the reaction the obtained solution was filtered through a short pad of silica gel to remove the catalyst. ***Ru/dimethyl itaconate:*** A 20 ml schlenk was charged with a solution of ddppm (5.3 mg, 0.011 mmol), [Ru(*p*-cymene)Cl<sub>2</sub>]<sub>2</sub> (3.3 mg, 0.01 mmol) and dimethyl itaconate (158 mg, 1 mmol) in dichloromethane. A stream of H<sub>2</sub> was bubbled at ambient temperature for 24 h. After the end of the reaction the obtained solution was filtered through a short pad of silica gel to remove the catalyst. The resulting solutions were then submitted to analysis to determine the enantiomeric excess by HPLC with Chiralcel OD column, Hexane/IPA, 98:2, 0.75 ml/min and 220 nm.

**Procedures for hydrogenation reaction of ketones: preparation *in situ* of the ruthenium catalyst<sup>19</sup>:** [Ru(COD)(methallyl)<sub>2</sub>] (0.038 mmol) and ligand ddppm (0.076 mmol) were placed in a dried 25-ml Schlenk tube under an argon atmosphere, and anhydrous and degassed acetone (5 ml) was added. After the dropwise addition of solution of HBr in methanol (0.33 ml, 0.29 M) a brown precipitate was formed. Stirring was then continued over 30 min, the solvent was removed *in vacuum*, and methanol (20 ml) or ethanol (for substrates 20c and 20d) was added.

Catalytic hydrogenation experiments were carried out in a Parr stainless-steel autoclave (100 ml). In a typical experiment, the autoclave was charged with a mixture of the catalyst [L<sub>2</sub>RuBr<sub>2</sub>] prepared *in situ* and 20a (3.80 mmol) in methanol (20 ml) under a stream of argon. The autoclave was stirred under 60 bar pressure of hydrogen at 60-100 °C for 16-48 h. the autoclave was cooled to room temperature, and the hydrogen was released. The reaction mixture was filtered over silica gel, and the enantiomeric excess was determined by GC (25 m, Lipodex E, 95 °C isothermal) or HPLC (Chiralcel OD-H, hexane/ethanol 95:5, 0.5 ml/min).

**Procedures for hydroformylation reactions<sup>26</sup>:** An autoclave, fitted with a substrate injector containing the substrate (1 ml, vinyl acetate 10.8mmol; styrene 8.72 mmol), a mechanical stirrer, a gas delivery system, an injection port and a thermocouple was flushed with CO/H<sub>2</sub> (1:1) to remove air. Degassed toluene (4 ml) containing dicarbonyl(2,4-pentanedionato)rhodium(I), [Rh(acac)(CO)<sub>2</sub>], (0.0132 g, 0.051 mmol) and ddppm or ddppg (0.037 g, 0.076 mmol) was added through the injection port against a stream of CO/H<sub>2</sub> using a syringe. The autoclave was pressurised with CO/H<sub>2</sub> (1:1) to 8 bar and the pressure



released. This flushing procedure was repeated twice more. The autoclave was repressurised to 4 bar, the stirrer was started (600 rpm) and the autoclave was heated to 60° C for 45-85 min. The substrate was then added to the autoclave by forcing it in through the substrate injector using a CO/H<sub>2</sub> pressure of 8 bar. The data recorder was started and the temperature, pressure in the autoclave and pressure in a ballast vessel, from which gas was fed into the autoclave through a mass flow controller to keep the pressure within the autoclave constant at 8 bar, were monitored and recorded every 5s.

After the time stated in the table, the stirrer was stopped and the autoclave was allowed to cool. The gases were vented and the mixture was syringed into a sample vial. The products were analysed by chiral GC using an FID detector. The compounds were identified using chiral GC-MS and by comparison with authentic samples of each enantiomer.

---

<sup>1</sup> (a) R. Noyori, *Asymmetric Catalysis in Organic Synthesis*; Wiley: New York, 1994. (b) I. Ojima, *Catalytic Asymmetric Synthesis*; Wiley: New York, 2000. (c) E. N. Jacobsen, A. Pfaltz and H. Yamamoto, *Comprehensive Asymmetric Catalysis*; Springer: Berlin, 1999.

<sup>2</sup> J. M. Ernsting, C.J. Elsevier and W.G.J. De Lange, *Magnetic Resonance in Chemistry*, 1991, Vol. 29, S118-124

<sup>3</sup> X-Seed – A software tool for supramolecular crystallography. *J. Supramol. Chem.*, 2001, 1, 189-191.

<sup>4</sup> K. Toriumi, T. Ito, H. Takay, T. Souchi and R. Noyori, *Acta Crystallogr., Sect. B: Struct. Crystallogr. Cryst. Chem.*, 1982, B38, 807.

<sup>5</sup> A. S. C. Chan, J. J. Pluth, and J. Halper, *Inorg. Chim. Acta*, 1979, 37, L477-L479..

<sup>6</sup> (a) T. Ikariya, Y. Ishii, H. Kawano, T. Arai, M. Saburi, S. Yoshikawa, S. Akutagawa, *J. Chem. Soc., Chem Commun.* 1985, 922; (b) H. Kawano, T. Ikariya, Y. Ishii, M. Saburi, S. Yoshikawa, Y. Uchida, H. Kumobayashi, *J. Chem. Soc., Perkin Trans. 1* 1989, 1571. (c) B.R. James, A. Pacheco, S.J. Rettig, J. S. Thorburn, R.G. Ball, J.A. Ibers, *J. Mol. Catal.* 1987, 41, 147.

<sup>7</sup> C. Bianchini, P. Barbaro, G. Scapacci, F. Zanobini, *Organometallics*, 2000, 19 (13), 2450-2461.

<sup>8</sup> F. B McCormick, D.D. Cox, W. B. Gleason, *Organometallics*, 1993, 12, 610.

<sup>9</sup> (a) S. B. Jensen, S.J. Rodger, M.D. Spicer, *J. Organomet. Chem.*, 1998, 556, 151-158. (b) M. Kitamura, T. Tokunaga, T. Ohkuma, R. Noyori, *Org. Syn.* 1993, 71, 1.

<sup>10</sup> K. Mashima, K. Kusano, T. Ohta, R. Noyori and H. Takaya, *J. Chem. Soc., Chem. Commun.*, 1989, 128-1210.

<sup>11</sup> Wenjun Tang and Xumu Zhang, *Chem. Rev.* 2003, 103, 3029-3069 and references therein.

<sup>12</sup> J. Halpern in *Asymmetric Synthesis*, Vol. 5 (Ed.: J.D. Morrison), Academic press, Orlando, FL, 1985, p.41.

<sup>13</sup> (a) A.S.C. Chan, J.J. Pluth, J. Halpern, *J. Am. Chem. Soc.* 1980, 102, 5952. (b) P. S. Chua, N.K. Robert, B. Bosnich, S.J. Okrasinski, J. Halpern, *J. Chem. Soc, Chem. Commun.* 1980, 344.

<sup>14</sup> A. S. C. Chan, J. Halpern, *J. Am. Chem. Soc.* 1980, 102, 838.

<sup>15</sup> J. Bakos, B. Heil and L. Markó, *J. Organomet. Chem.*, 1983, 253, 249-252.

- 
- <sup>16</sup> T. Morimoto, M. Chiba, and K. Achiwa, *Tetrahedron Letters*, 1988, Vol. 29, No. 37, 4755-4758.
- <sup>17</sup> M. T. Reetz, T. Neugebauer, *Angew. Chem. Int. Ed.*, 1999, 38, o1/2, 179-181.
- <sup>18</sup> A. Miyashita, A. Yasuda, H. Takaya, K. Toriumi, T. Ito, T. Souchi and R. Noyori, *J. Am. Chem. Soc.*, 1980, 102, 7932.
- <sup>19</sup> Results obtained in the University of Rostock: Catalysis. Prof. Mathias Beller laboratory.
- <sup>20</sup> D. J. Ager, S. A. Laneman, *Tetrahedron: Asymmetry* 1997, 8, 3327.
- <sup>21</sup> R. Noyori, T. Okhuma, M. Kitamura, H. Takaya, N. Sayo, H. Kumobayashi, S. Akutagawa, *J. Am. Chem. Soc.*, 1987, 109, 5856.
- <sup>22</sup> W. Tang and X. Zhang, *Chem. Rev.*, 2003, 103, pg 3052.
- <sup>23</sup> K. Junge, B. Hagemann, S. Enthaler, G. Oehme, M. Michalik, A. Monsee, T. Riermerier, U. Dingerdissen, M. Beller, *Angew. Chem.*, 2004, 116, 5176-5179.
- <sup>24</sup> J. P. Genet, C. Pinel, R. Vidal, S. Mallert, X. Pfister, L. Bischoff, M.C. Caño De Andrade, S. Dorses, C. Galopin, J.A. Lafitte, *Tetrahedron Asymmetry*, 1994, Vol 5, No 4, 675-690.
- <sup>25</sup> a) G. Zassinovich, G. Mestroni, S. Gladiali, *Chem. Rev.* 1992, 92, 1051-1069; b) C. F. de Graauw, J. A. Peters, H. van Bekkum, J. Huskens, *Synthesis* 1994, 1007-1017; c) R. Noyori, S. Hashiguchi, *Acc. Chem. Res.* 1997, 30, 97-102.
- <sup>26</sup> Results obtained in St. Andrews University.

- 
- <sup>27</sup> (a) M. Beller, B. Comils, C.D. Frohning, C.W. Kohlpainter, *J. Mol. Catal.* 1995, 104, 17. (b) F. Agboussou, J. F. Carpentier, A. Mortreux, *Chem. Rev.* 1995, 95, 2485, (c) S. Gladiali, J. Bayón, C. Claver, *Tetrahedron: Asymmetry* 1995, 7, 1453. (d) P.W.N.M. van Leeuwen, C. Claver. *Rhodium Catalyzed Hydroformylation*; Kluwer Academic Press: Dordrecht, 2000.
- <sup>28</sup> (a) J.K. Stille, H. Su, P. Brechot, G. Parrinello, L. S. Hegedus, *Organometallics*, 1991, 10, 1183. (b) G. Consiglio, S.C.A. Nefkens, A. Borer, *Organometallics*, 1991, 10, 2046.
- <sup>29</sup> M. Dieguez, M.M. Pereira, A. M. Masdeu Bultó, C. Claver, J.C. Bayón, *J. Mol. Catal. A: Chem.* 1999, 143, 111 and references therein.
- <sup>30</sup> S. Breeden, D. J.Cole-Hamilton, D.F. Foster, G.J. Schwarz and M. Wills. *Angew. Chem. Int. Ed.*, 2000, 39, No 22, 4106-4108.
- <sup>31</sup> G. Clarkson, J. Ansell, D. J.Cole-Hamilton, J. Whittel and M. Wills, *Tetrahedron: Asymmetry*, 2004, 1-6.
- <sup>32</sup> D. D. Perrin and W. F. A. Amarego, *Purification of Laboratory Chemicals*, Pergamon, Oxford, 1988.
- <sup>33</sup> G. Giordano, R.H. Crabtree, *Inorg. Synth.*, 28, 1989, 88.
- <sup>34</sup> M.A. Bennett, T.N. Huang, T.W. Matheson, A.K. Smith, *Inorg. Synth.* 21, 1982, 74.
- <sup>35</sup> K. Mashima, K. Kusano, T. Ohta, R. Noyori, H. Takaya, *J. Chem. Soc., Chem. Commun.*, 1989, 1208.
- <sup>36</sup> I.P. Evans, A. Spencer, G. Wilkinson, *J. Chem. Soc., Dalton*, 1973, 204.
- <sup>37</sup> R.E. Ireland, D. A. Evan, D. Glover, G. M. Rubottom and H. Young, *J. Org. Chem.*, 1969, 34, 3717.

<sup>38</sup> R. ter Halle, E. Schulz, M. Spagnol and M. Lemaire, *Tetrahedron Letters*, 2000, 4,1, 3323-3326.

# *Chapter 5*

## 5. Ir-ddppm complexes and their catalytic applications: enantioselective hydrogenation of imines.

### 5.1 INTRODUCTION

In this chapter the synthesis of Ir- **ddppm** complexes and their catalytic activity towards the metal-catalysed hydrogenation of imines are described.

In the last few decades, several types of Ir-based catalysts were developed and applied successfully in hydrogenation reactions. The most efficient type, prepared from  $[\text{Ir}(\text{COD})\text{Cl}]_2$ , is a chiral diphosphine and a halide (iodide), proved to be much more active for the enantioselective hydrogenation of N-arylketimines than the rhodium analogs.<sup>1</sup> Regardless of a tendency for deactivation (dependent on temperature, ligand structure, solvent and the basicity of the formed aniline derivative) several Ir catalysts are of practical use for the production of enantiomerically enriched N-arylamines. Additives play a dominant but unpredictable role, acting either as promoters (acid, iodide, amines) or as deactivators (amines, iodide). Enantioselectivities up to 90% were achieved for several types of imines with the newly developed ferrocenyldiphosphines and DIOP.<sup>2</sup>

A particular sub-class, that of aryl-amines, has attracted much interest due to their applications in the pharmaceutical and agrochemical industries. However such acyclic imines have *syn* and *anti* isomers which combined with their configurational instability, causing *syn-anti* isomerisation, tend to lower enantioselectivity. Most research so far in this area and promising results have been obtained from iridium-catalysed imine hydrogenations.<sup>3</sup>

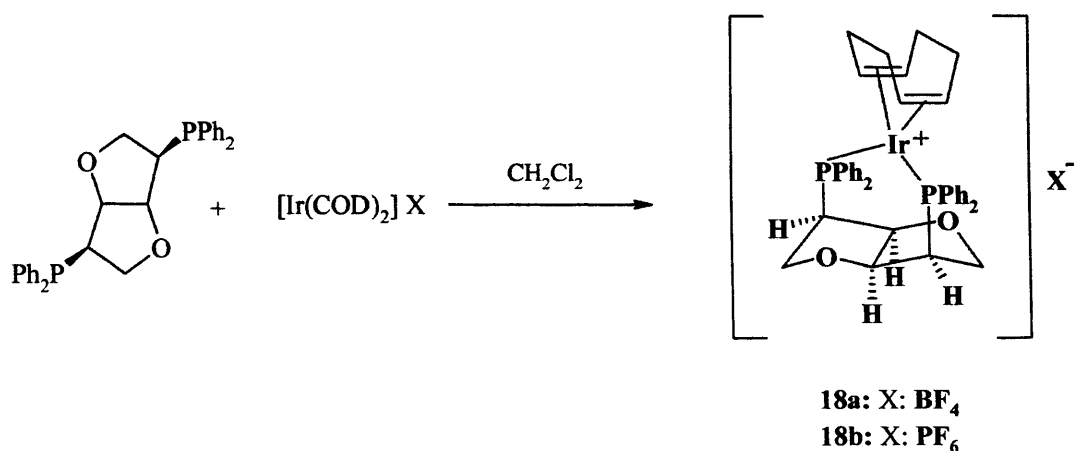
Despite recent advances in iridium imine hydrogenations this area is still limited and further research is necessary. The main obstacles that need to be overcome are: i) the normally high operating hydrogen pressures, (ii) the moderate enantioselectivities usually obtained, (iii) the limited range of imines hydrogenated and (iv) the often rapid catalyst deactivation to iridium-hydride clusters.

In the next sections, an account of the synthesis of the iridium complexes and results from hydrogenations of prochiral imines with them is discussed.

## 5.2 RESULTS AND DISCUSSION

### 5.2.1 Synthesis and characterization of Iridium complexes with ddppm.

Both the  $\text{BF}_4$  and  $\text{PF}_6$  salts of the cationic complex  $[\text{Ir}(\text{ddppm})(\text{COD})]\text{X}$  were prepared as shown in Scheme 5.1. Attempts in isolating an Ir-ddppm chloride complex from reaction of  $[\text{Ir}(\text{COD})\text{Cl}]_2$  with **ddppm** did not afford a distinct complex.



**Scheme 5.1:** Synthesis of the iridium complexes **18a** and **18b**.



Reaction of  $[\text{Ir}(\text{COD})_2]\text{BF}_4$  with one equivalent of **ddppm** formed the cationic complex  $[\text{Ir}(\text{ddppm})(\text{COD})]\text{BF}_4$  (**18a**) in quantitative yield. In the  $^{31}\text{P}$  NMR spectrum of **18a** reveals a singlet at  $\delta$  15.2. In the  $^1\text{H}$  NMR complex **18a** shows four unresolved multiplets for the **ddppm** protons at  $\delta$  3.98, 4.12, 4.24, and 5.38. The most characteristic  $^1\text{H}$  NMR shifts for **ddppm** upon coordination are those of the CH protons. The resonance for the bridging CH protons shifts from  $\delta$  2.94 ppm in the free ligand to  $\delta$  3.98 in the iridium complex. Similarly, the methane CHP protons shift from  $\delta$  4.52 to 5.38. Two signals were observed for the olefinic protons of the 1,5-COD ligand, consistent with the  $C_2$ -symmetric environment, at  $\delta$  3.53 and 4.32.

The hexafluorophosphate derivative  $[\text{Ir}(\text{ddppm})(\text{COD})]\text{PF}_6$  (**18b**) was prepared from the reaction of **ddppm** with  $[\text{Ir}(\text{COD})\text{Cl}]_2$  and  $\text{KPF}_6$  following a previously reported protocol.<sup>3k</sup> NMR spectroscopic data were identical with the ones for the  $\text{BF}_4$  complex. These Ir(I) complexes are air-stable and consequently easier to handle than their rhodium analogue,  $[\text{Rh}(\text{ddppm})(\text{COD})]\text{BF}_4$  (**14**), which has a moderate stability under aerobic conditions.

The crystal structure of the iridium complex  $[\text{Ir}(\text{ddppm})(\text{COD})]\text{BF}_4$  (**18a**) was determined. Needle-shaped red crystals suitable for X-ray crystallographic analysis were obtained after slow diffusion of ether into a chloroform solution. Structural representation of **18a** is given in Figure 5.1, showing the **ddppm** ligand chelating to the metal centre. Of note is the nearly eclipsed conformation of the two  $\text{PPh}_2$  phenyl groups, shown more clearly in the second drawing (Figure 5.2). This orientation of the aromatic rings in **18a** lifts the pseudo- $C_2$  symmetry, of the M-**ddppm** fragment observed in the other **ddppm**-complexes synthesized so far. Such an arrangement although sterically more demanding is

not unusual in the solid state for Ir<sup>I</sup>(diphosphine)-COD complexes, and it is attributed to crystal packing effects.<sup>4</sup> The ligand bite angle at 94.50° is the smallest observed so far within the range of bidentate complexes with dppm<sup>5</sup>. The Ir–P bonds at 2.335(3) and 2.337(2) Å are close to those reported for other Ir(cod) complexes. The Ir–C distances from 2.179(12) to 2.251(12) Å for the Ir–C(4) and Ir–C(5) bonds respectively lie within the expected range.

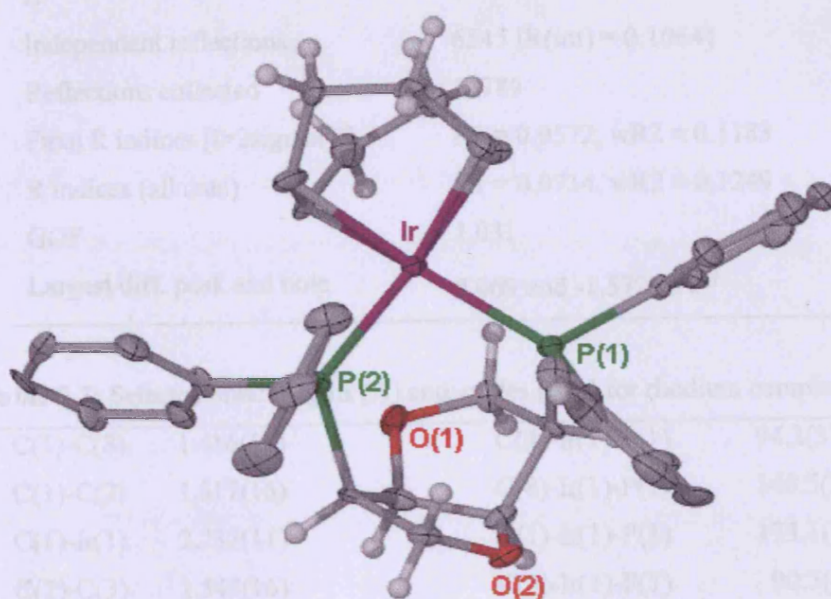


**Figure 5.1:** X-Seed<sup>6</sup> elipsoid plot at 50% probability of the molecular structure **18a**. (Top view with reference to the coordination plane). Solvent molecules and the anion BF<sub>4</sub> have been omitted for clarity.

**Table 5.1:** Crystallographic data for rhodium complex 18.

Formula	C <sub>39</sub> H <sub>37</sub> B Cl <sub>3</sub> F <sub>4</sub> Ir O <sub>2</sub> P <sub>2</sub>
Mol wt	984.99
Crystal system	Orthorhombic
Space group	P2(1)
a, Å	10.4744(4)
b, Å	18.1714(7)
c, Å	19.9436(7)
V, Å <sup>3</sup>	3796.0(2)
Z	4
Independent reflections	6545 [R(int) = 0.1064]
Reflections collected	16789
Final R indices [I > 2σ(I)]	R1 = 0.0572, wR2 = 0.1183
R indices (all data)	R1 = 0.0714, wR2 = 0.1249
GOF	1.031
Largest diff. peak and hole	2.069 and -1.572 e.Å <sup>-3</sup>

**Table 5.2:** Selected bond lengths (Å) and angles (deg) for rhodium complex 14.

C(1)-C(8)	1.416(16)	C(4)-Ir(1)-P(1)	94.2(3)
C(1)-C(2)	1.517(16)	C(8)-Ir(1)-P(1)	148.5(3)
C(1)-Ir(1)	2.237(11)	C(1)-Ir(1)-P(1)	173.1(3)
C(2)-C(3)	1.545(16)	C(5)-Ir(1)-P(1)	90.5(4)
C(3)-C(4)	1.547(16)	C(4)-Ir(1)-P(2)	150.6(3)
C(4)-C(5)	1.396(17)	C(8)-Ir(1)-P(2)	91.4(3)
C(4)-Ir(1)	2.179(12)	C(1)-Ir(1)-P(2)	88.5(3)
C(5)-C(6)	1.514(16)	C(5)-Ir(1)-P(2)	170.2(3)
C(5)-Ir(1)	2.251(12)	P(1)-Ir(1)-P(2)	94.50(10)
C(6)-C(7)	1.523(16)	C(21)-P(1)-C(15)	97.2(5)
C(7)-C(8)	1.499(16)	C(21)-P(1)-C(10)	108.1(5)
C(8)-Ir(1)	2.192(9)	C(15)-P(1)-C(10)	100.7(5)
C(9)-O(1)	1.454(13)	C(21)-P(1)-Ir(1)	121.7(4)
P(1)-Ir(1)	2.335(3)	C(15)-P(1)-Ir(1)	116.5(4)
P(2)-Ir(1)	2.337(2)	C(10)-P(1)-Ir(1)	110.1(4)

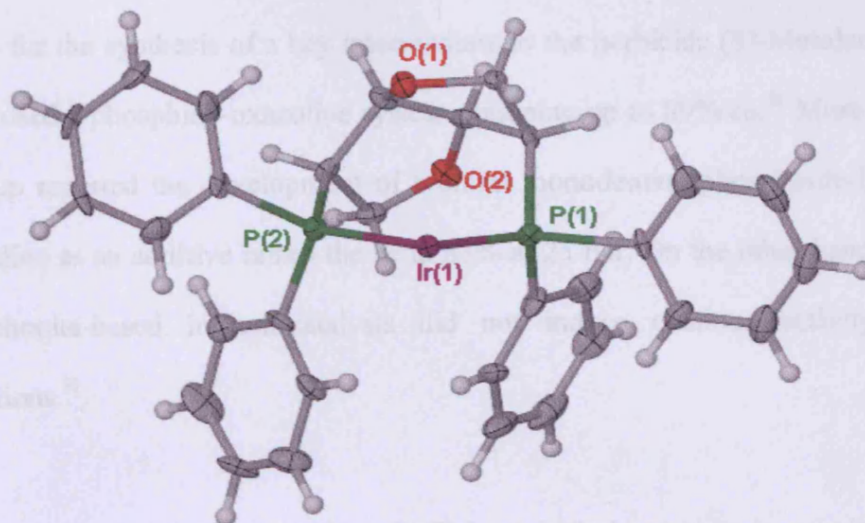


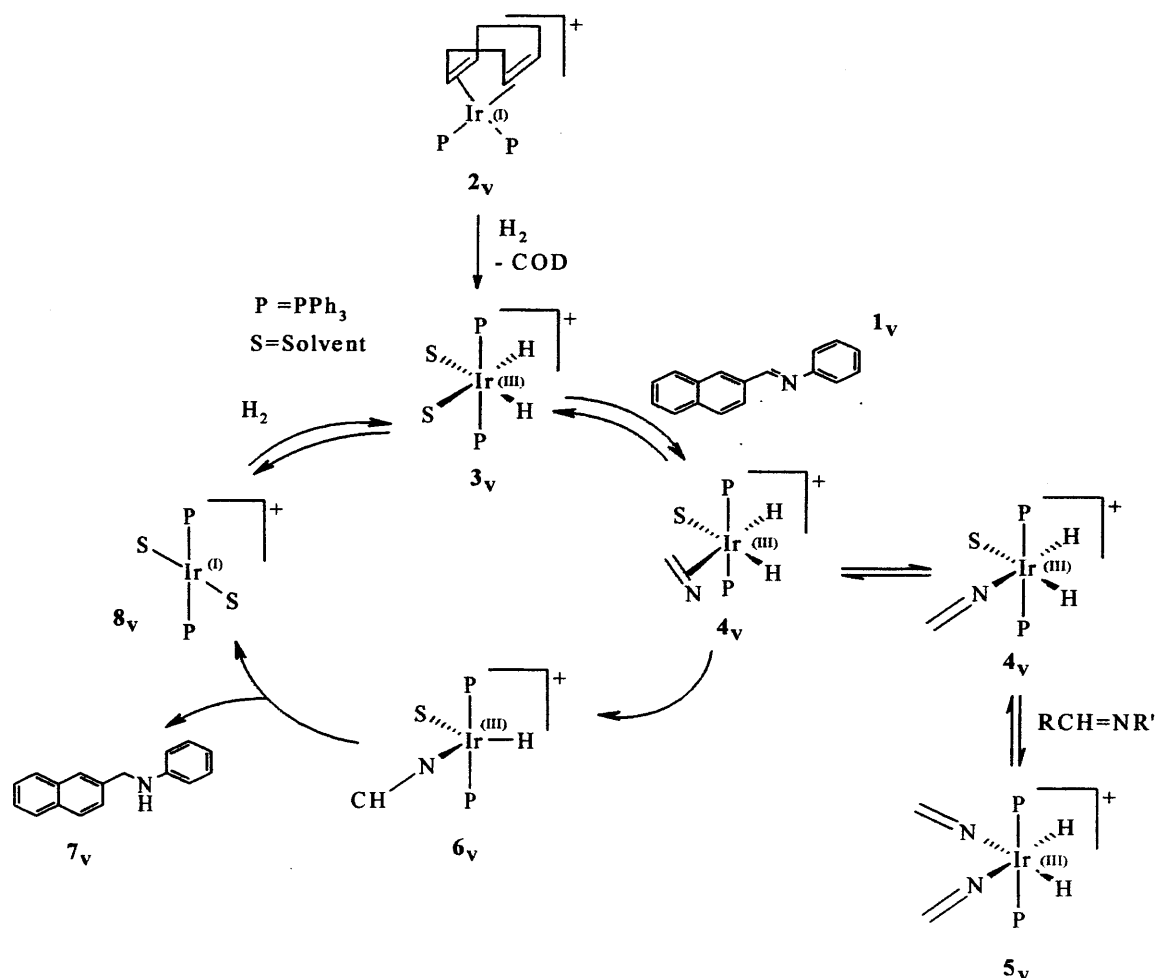
**Figure 5.2:** X-Seed<sup>6</sup> elipsoid plot at 50% probability of **18b**. Side view with reference to the coordination plane. Only the Ir(ddppm) fragment is shown for clarity.

### 5.2.2 Enantioselective hydrogenation of imines

Iridium systems are known to catalyse otherwise difficult to hydrogenate substrates including imines and sterically crowded, non-functionalized olefins.<sup>7</sup> Transfer hydrogenations of imines have received some success with a ruthenium catalyst developed by Noyori *et al.*<sup>8</sup> but otherwise Ru and Rh systems usually show inferior activities and selectivities to those based on Ir.<sup>3f, 9</sup> Enantioselective imine hydrogenations have attracted much research interest in the last decade. However, compared to the state of the art in alkene hydrogenation chemistry, they are still underdeveloped. There are a few catalysts known that give rise to good enantioselectivities, but in order to achieve reasonable hydrogenation rates high pressures of H<sub>2</sub> are required, typically 25-100 bar. An Ir-ferrocenyl-diphosphine system, developed by Blaser *et al.*, achieved high reaction rates (tof

$\approx 2800 \text{ h}^{-1}$ ) albeit with some lack in enantioselectivity (79% ee).<sup>10,11</sup> This catalyst is used industrially for the synthesis of a key intermediate to the herbicide (S)-Metolachlor. Pfaltz *et al.* have used a phosphine-oxazoline system obtaining up to 89% ee.<sup>3k</sup> More recently de Vries' group reported the development of a chiral monodentate phosphinite-Ir catalyst.<sup>3g</sup> Using pyridine as an additive raised the ee to 83% at 25 bar. On the other hand phosphite- and phosphonite-based iridium-catalysts did not induce enantioselectivity in imine hydrogenations.<sup>3i</sup>

Despite the fact that the number of efficient catalytic systems is growing very fast, there are very few studies on the mechanistic details of this reaction, and the catalytic cycle is not yet well established. One of the few mechanistic and kinetic studies that has been made determines the experimental rate equation and the corresponding activation parameter of enthalpy and entropy for the non-asymmetric hydrogenation of N-( $\beta$ -naphthylmethylene)aniline (**1v**) using  $[\text{Ir}(\text{COD})(\text{PPh}_3)_2]\text{PF}_6$  (**2v**) as catalyst precursor.<sup>9</sup> A catalytic cycle is proposed on the basis of the kinetic experiments and some NMR data (Scheme 5.2).



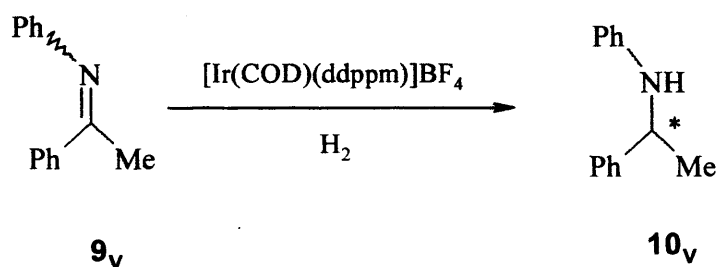
**Scheme 5.2:** Schematic catalytic cycle postulated for the non-asymmetric hydrogenation of N-(β-naphthylmethylene)aniline (**1<sub>v</sub>**) using  $[\text{Ir}(\text{COD})(\text{PPh}_3)_2]\text{PF}_6$  (**2<sub>v</sub>**)

Under the conditions of the catalytic reaction and in the presence of a solvent, complex **2<sub>v</sub>** reacts with hydrogen to give **3<sub>v</sub>**, which is proposed as the initial species entering the catalytic cycle. Then, **3<sub>v</sub>** coordinates one imine molecule (**1<sub>v</sub>**) to form **4<sub>v</sub>**. The next step is the first transfer of the hydride to the imine to yield the iridium-alkylaminium intermediate **6<sub>v</sub>**, which evolves to release the product amine **7<sub>v</sub>** by reductive elimination, the rate determining step, and produce the species  $[\text{Ir}(\text{S})_2(\text{PPh}_3)_2]\text{PF}_6$  (**8<sub>v</sub>**). This species



makes it possible for the cycle to begin again. It is important to note that imines can coordinate in two different modes to the metal centre, by the nitrogen atom ( $\eta^1\text{-N}$ ) or by the double C=N bond ( $\eta^2\text{-N,C}$ ), where the  $\eta^2$ -bonding mode is more likely to occur in the hydrogenation reaction. Although there is no experimental evidence for the existence of these species, it is assumed that while the  $\eta^1\text{-N}$  mode is out of the cycle, the  $\eta^2$ -bonding mode is the olefin-like intermediate that undergoes selective hydrogenation of the C=N bond.

The new iridium complexes **18a** and **18b** were tested in the asymmetric hydrogenation of imines, using N-(1-phenylethylidene)aniline (**9v**) as a representative N-aryl imine (Scheme 5.3). Under the reaction conditions, the cationic iridium complexes afford quantitative amounts of the product, N-(1-phenylethyl)aniline (**10v**), with enantioselectivities at the top of the range for this class of compounds.

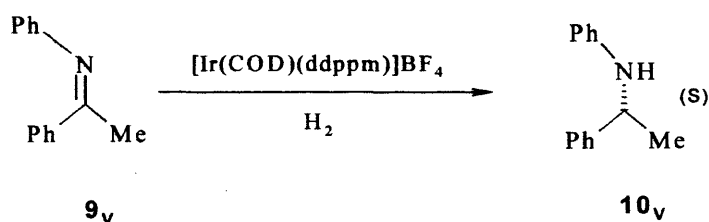


**Scheme 5.3:** Asymmetric hydrogenation of phenylimine with iridium complex **18a**.

The effect of the solvent, hydrogen pressure and other variables in the yield and selectivity of the reaction have been studied and discussed in the following paragraphs.

**Hydrogen pressure effect:** Table 5.3 shows the effect of hydrogen pressure in the hydrogenation of imine **9<sub>v</sub>**, using  $[\text{Ir}(\text{COD})(\text{ddppm})]\text{BF}_4$  as the catalyst precursor (**18a**). Changes in the hydrogen pressure had an unexpected effect in imine hydrogenations with the Ir-ddppm system. Contrary to previous observations<sup>3</sup> the iridium-ddppm catalyst becomes inactive at hydrogen pressures of 10 bar or greater, with best results obtained under 1 bar of hydrogen gas, as shown in table 5.3. Increasing the hydrogen pressure from 1 to 4 bar resulted in a small increase in imine formation from 68 to 72%, however this was followed by an appreciable drop in enantioselectivity from 80 to 73% ee (entries 1 and 2).

**Table 5.3:** Effect of the H<sub>2</sub> pressure in the asymmetric hydrogenation of N-phenyl imine **1<sub>v</sub>**.



Entry	p(bar)	Yield %	Hydrolysis % <sup>c</sup>	e.e. %
1	1	68	6	80 ( <i>S</i> )
2	4	72	11	73 ( <i>S</i> )
3	10	<5	26	n.d. <sup>[b]</sup>
4	45	14	22	n.d.
5	4	5 <sup>[a]</sup>	20	n.d.

*Reaction conditions:* 0.01 mmol  $[\text{Ir}(\text{COD})(\text{ddppm})]\text{BF}_4$  (2mM), 1mmol substrate (0.2M) in 5mL of  $\text{CH}_2\text{Cl}_2$ , at room temperature, 24h. [a] Catalyst solution saturated with hydrogen before addition of imine **9<sub>v</sub>**. [b] n.d.= not determined. [c] The degree of hydrolysis was depending on the purity of the imine.

A negative hydrogen pressure effect on product enantioselectivity has been observed previously, although within a greater range of hydrogen pressures (20–50 bar).<sup>7a</sup> Further increase of the hydrogen pressure to 10 bar resulted in almost complete



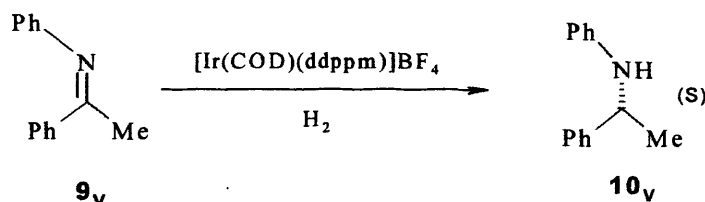
deactivation of the catalyst with significant imine hydrolysis to acetophenone and aniline (26%). Although solvents and reagents were dried and distilled prior to use the presence of adventitious water in the reaction mixture cannot be excluded leading to hydrolysis of the imine substrate. This process is most likely accelerated by the iridium species present in solution. At 45 bar of H<sub>2</sub> pressure there was only a small yield increase, at 14%. Contrary to the above observations catalytic iridium systems known to date usually hydrogenate imine substrates much slower or are inactive at ambient hydrogen pressures.<sup>3g, 12, 15</sup> Indeed, kinetic studies for the related [Ir(COD)(PPh<sub>3</sub>)<sub>2</sub>][PF<sub>6</sub>] precatalyst show a linear increase in the reaction rate with increasing hydrogen pressure.<sup>9</sup> The observed decrease in catalyst activity with increasing hydrogen pressure for the Ir-ddppm catalysts may be attributed to the formation of inactive iridium-polyhydride clusters at such pressures. Formation of inactive Ir(III)-H species is further supported by the results of entry 5 (table 5.4) where saturation of the catalyst solution with hydrogen gas before addition of the substrate produced a nearly inactive catalyst affording the corresponding amine in only 5% yield. The Ir(III)-H species have been characterised and their properties discussed in a later section.

**Solvent effects:** After establishing that hydrogenation reactions are preferably carried out under an atmospheric hydrogen pressure, the effect of different reaction media was studied. Table 5.4 shows that effect of different solvents in the hydrogenation of imine **9<sub>v</sub>** with [Ir(COD)(ddppm)][BF<sub>4</sub>] as the precatalyst. In 1,2-dichloroethane (entry 1) the catalyst affords amine **10<sub>v</sub>** in good yield (62%) and enantioselectivity (82% ee of the S isomer). However, when the catalyst loading was reduced to 0.1% the secondary amine

was formed in only 23% yield and significant hydrolysis (37%) to acetophenone and aniline was observed (entry 2). In  $\text{CH}_2\text{Cl}_2$  comparable yields and enantioselectivities were obtained (entry 3). Other weakly co-ordinating solvents such as toluene were much less effective affording both very low yields and selectivities. In co-ordinating solvents such as methanol a low yield was obtained (20%) but this reaction gave the best enantioselectivity observed at 89% ee. Finally in THF the catalyst is almost inactive with less than 5% of conversion to the secondary amine.

A similar solvent dependence has been reported for the cationic Ir(I)-COD systems with triphenylphosphine<sup>9</sup> and phosphinodihydrooxazole ligands.<sup>3f</sup> On the other hand neutral precursors based on  $[\text{Ir}(\text{COD})\text{Cl}]_2$ /diphosphine systems, such as Blaser's et al. ferrocenyl-based phosphines, perform better in toluene.<sup>10,11, 13</sup> A catalytic run with the  $[\text{Ir}(\text{COD})\text{Cl}]_2$  / ddppm system in dichloromethane (entry 7) showed negligible activity in imine reduction. In order to gain some more insight about the nature of the catalytic species we also tested the  $-\text{PF}_6$  complex **18b** which outperformed the  $-\text{BF}_4$  analogue affording the reduced amine in quantitative yields and 84% ee, with no hydrolysis observed. Pfaltz et al. have reported a similar counterion dependence with iridium catalysts, with the more bulky and weakly coordinating anions forming better catalysts.<sup>7a</sup> The above results show that a cationic catalyst is formed with the Ir-ddppm system that its activity is enhanced in non-coordinating solvents and counterions (in increasing order  $\text{Cl}$ ,  $\text{BF}_4$ ,  $\text{PF}_6$ ).

**Table 5.4:** Effect of the solvent in the asymmetric hydrogenation of imine **1v**.



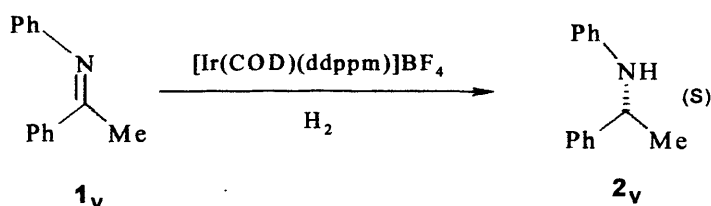
Entry	Solvent	Yield % <sup>[a]</sup>	Hydrolysis %	<i>e.e.</i> %
1	(CH <sub>2</sub> Cl) <sub>2</sub>	62	8	82 ( <i>S</i> )
2	(CH <sub>2</sub> Cl) <sub>2</sub>	23 <sup>[b]</sup>	37	n.d. <sup>[c]</sup>
3	CH <sub>2</sub> Cl <sub>2</sub>	68	6	80 ( <i>S</i> )
4	PhCH <sub>3</sub>	7	10	n.d. <sup>[c]</sup>
5	CH <sub>3</sub> OH	20	12	89 ( <i>S</i> )
6	THF	<5	12	n.d. <sup>[c]</sup>
7	CH <sub>2</sub> Cl <sub>2</sub>	<5 <sup>[c]</sup>	10	n.d. <sup>[c]</sup>
8	(CH <sub>2</sub> Cl) <sub>2</sub>	100 <sup>[d]</sup>	-	84 ( <i>S</i> )

**Reaction conditions:** 0.01 mmol [Ir(COD)(ddppm)]BF<sub>4</sub> (2mM), 1 mmol substrate (0.2M) in 5mL of solvent, P(H<sub>2</sub>) = 1 bar, at room temperature, 24h. % *ee* values were measured by chiral HPLC using a Chiralcel OD column and hexane/IPA as the eluent. [a] Determined by NMR. [b] 0.01 mmol of **18a**, 5mL of solvent, 4 days. [c] [Ir(COD)Cl]<sub>2</sub>/ddppm. [d] **18b** used as catalysts. [e] n.d. = not determined.

**Effect of additives:** Table 5.5 summarises the effect that additives and changes in the reaction conditions have in the hydrogenation of N-(1-phenylethylidene)aniline (**9v**). Normally reactions were run for 24 hours without monitoring the end of the reaction; entry 2 shows that after 1 hour the reaction hasn't reached completion yet. The isolated yield was 11% instead of 68% after 24 hours. However, an increase in the enantioselectivity was observed from 80 to 86% ee. Contrary to literature reports, acid additives such as molecular sieves and trifluoroacetic acid gave low yields and considerable amounts of hydrolysis products (up to 60%, entries 3 and 4).<sup>11</sup> Reactions were normally run at 0.2M substrate concentrations, more dilute solutions (at 0.07M) afforded, as expected, slightly lower yields but with an increase in enantioselectivity from 73 to 77% ee (entries 5 and 6).<sup>3k</sup> Addition of

methanol to the reaction reduced drastically the imine conversion however the %ee was increased from 73% to 80% (entry 7).

**Table 5.5:** Effect of additives in the asymmetric hydrogenation of imine **1<sub>v</sub>**.



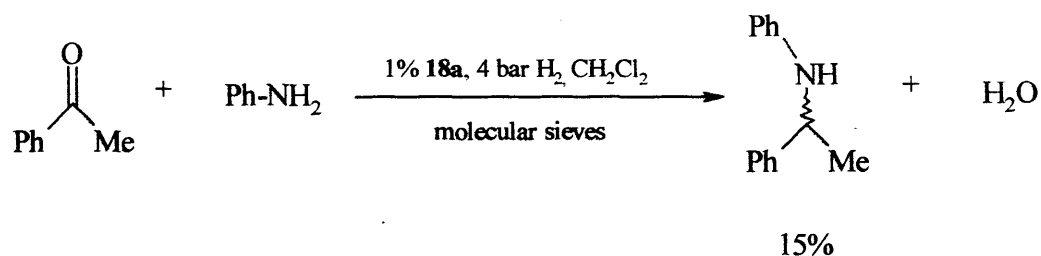
Entry	P (H <sub>2</sub> ) bar	Conditions/ Additives	Yield % <sup>[a]</sup>	Hydrolysis %	<i>e.e.</i> %
1	1	-	68	6	80
2	1	Reaction time: 1 h	11	6	86
3	1	CF <sub>3</sub> CO <sub>2</sub> H <sup>[a]</sup>	7	60	n.d. <sup>[d]</sup>
4	1	Molecular sieves	32	24	64
5	4	-	72	11	73
6	4	CH <sub>2</sub> Cl <sub>2</sub> (15ml)	65	4	77
7	4	CH <sub>3</sub> OH (1 ml)	15	31	80
8	1	PhCH <sub>3</sub> , CF <sub>3</sub> CO <sub>2</sub> H <sup>[b]</sup> (N <sup>t</sup> Bu <sub>4</sub> )I <sup>[c]</sup>	48	36	40

*Reaction conditions:* 0.01 mmol [Ir(COD)(ddppm)]BF<sub>4</sub> (2mM), 1 mmol substrate (0.2M) in 5mL of solvent, at room temperature, 24h. [a] 0.35 mmol. [b] 0.2 mmol. [c] 0.01 mmol. [d] n.d. = not determined.

The effect of iodide additives was also investigated. A number of reports in the literature show that additives such as iodide,<sup>11</sup> phthalimide<sup>14</sup> and pyridine<sup>3c</sup> can have a dramatic effect on the rate of hydrogenation and selectivity of the reaction. Addition of tetrabutylammonium iodide salt (TBAI) has been shown to be particularly advantageous for Ir(I)-chloride systems, where most likely an anion exchange is taking place. The role of iodide additives is believed to prevent formation of inactive Ir-H clusters. Indeed, Ir(III)-iodide dimers were shown to be highly active catalysts in imine hydrogenations.<sup>15</sup> Addition

of TBAI in the Ir-ddppm system however had a negative effect in both yield and enantioselectivity (entry 8). This behaviour is in agreement with other cationic systems. For example, in the phosphino-dihydrooxazole iridium-based system addition of TBAI had a dramatically negative effect on enantioselectivity.<sup>3k</sup>

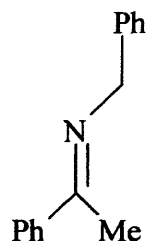
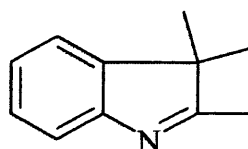
Since iridium hydrogenation catalysts do not appear to hydrogenate ketonic substrates a mixture of acetophenone and aniline was hydrogenated (Scheme 5.4).<sup>10a</sup> NMR analysis after termination of the reaction showed formation of the secondary amine at 15% yield together with equimolar amounts of acetophenone and the corresponding imine. The low reaction yields observed in this case may be attributed to the competition of acetophenone and aniline with imine substrate for coordination to the active site of the metal.



**Scheme 5.4:** Hydrogenation reaction using acetophenone and aniline as reactants.

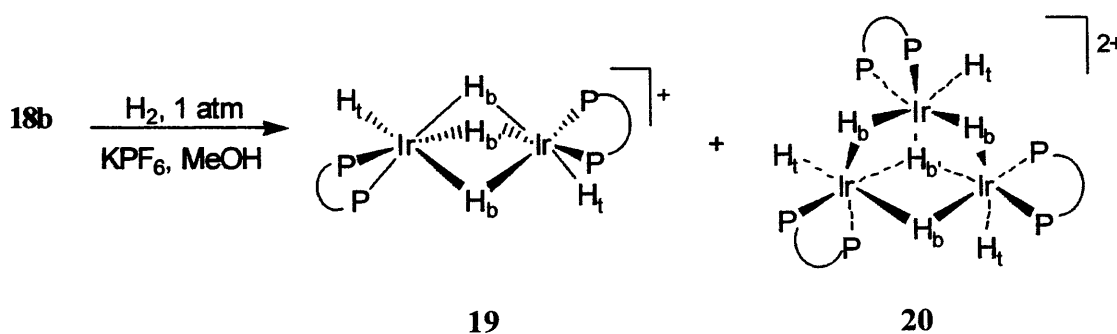
The benzyl imine **11v** and cyclic imine **12v** were also tested as hydrogenation substrates using **18a** under the same hydrogenation conditions as in entry 2 (Table 5.3). Under these conditions imine **11v** gave the corresponding amine in low yield (20%) with no hydrolysis observed. Imine **12v** however remained unreacted possibly due to the greater

steric hindrance of the substrate. No further tests were carried out with these substrates to optimise reaction conditions.

**11<sub>v</sub>****12<sub>v</sub>**

### 5.2.3 Iridium-ddppm hydride complexes

Iridium complexes of the type  $[\text{Ir}(\text{COD})\text{L}_2]\text{X}$ , where L is a P or N donor ligand, react with hydrogen to form dimeric and trimeric Ir-H clusters analogous to structures **19** and **20**, respectively (scheme 3).<sup>16</sup> In the case of phosphino-oxazoline based catalytic systems such hydride species were inactive in hydrogenation reactions.<sup>16a</sup>



**Scheme 5.5:** Hydride complexes obtained from the reaction of  $[\text{Ir}(\text{COD})(\text{ddppm})]\text{PF}_6$  with  $\text{H}_2$

(**19/20** = 3:2).

During hydrogenation experiments with the Ir-ddppm catalyst an immediate colour change was observed when H<sub>2</sub> gas was introduced from bright red to pale yellow attributed to the formation of Ir-ddppm hydride species. In addition, catalytic activity was inhibited when the catalyst solution was treated with hydrogen gas prior to addition of the imine substrate (Table 1, entry 5). These observations prompted us to study further the reactivity of the Ir-ddppm system with molecular hydrogen. In a typical experiment, a methanol solution of complex **18b** containing a twenty-fold excess of KPF<sub>6</sub> was stirred for one day under an atmosphere of hydrogen. During that period a microcrystalline solid precipitated. NMR analysis of the isolated solid showed the formation of the iridium clusters: [Ir<sub>2</sub>(ddppm)<sub>2</sub>(μ<sup>2</sup>-H)<sub>3</sub>(H)<sub>2</sub>](PF<sub>6</sub>) (19) and [Ir<sub>3</sub>(ddppm)<sub>3</sub>(μ<sup>3</sup>-H)(μ<sup>2</sup>-H)<sub>3</sub>(H)<sub>3</sub>](PF<sub>6</sub>)<sub>2</sub> (20), in a 3/2 ratio (Scheme 5.5). Although attempts to separate the two complexes did not meet with success, by using a variety of one- and two-dimensional NMR techniques, including <sup>1</sup>H-<sup>31</sup>P correlation measurements, their identities were confirmed (Table 5.6).

The <sup>31</sup>P NMR signals of 19 at 17.6 and 9.9 ppm are part of an AX system showing a small but unresolved *cis* P-P coupling. Figure 5.3 shows the <sup>31</sup>P, <sup>1</sup>H correlation spectrum for complexes 19 and 20. Dimer 19 displays four cross-peaks in the hydride region arising from <sup>2</sup>J<sub>PH</sub> interactions. The doublet at δ-6.54 (<sup>2</sup>J<sub>PH</sub> = 83.6 Hz) arises from the two equivalent bridging hydrides (H<sub>b</sub>) *trans* to a single phosphorous atom. The remaining bridging hydride (H<sub>b</sub>) resonates as a triplet, due to two *trans* phosphorous atoms, at δ-8.48 (<sup>2</sup>J<sub>PH</sub> = 67.1 Hz). The observed coupling constants for the bridging iridium hydrides are smaller than the ones reported for terminal hydrides *trans* to phosphorus (120 – 160 Hz) due to their reduced bond order.<sup>17,18</sup> The two equivalent terminal hydrides resonate at a significantly lower frequency at δ-24.42 showing a multiplet with a small coupling

constant,  $^2J_{\text{PH}} \approx 25$  Hz, as a result of coupling to two *cis* phosphorous atoms. The  $^1\text{H}$  NMR data for dimer **19**, including coupling constants, are in good agreement with those reported for the analogous  $\text{PPh}_3$  and  $\text{dppp}$  complexes.<sup>16d,f</sup>

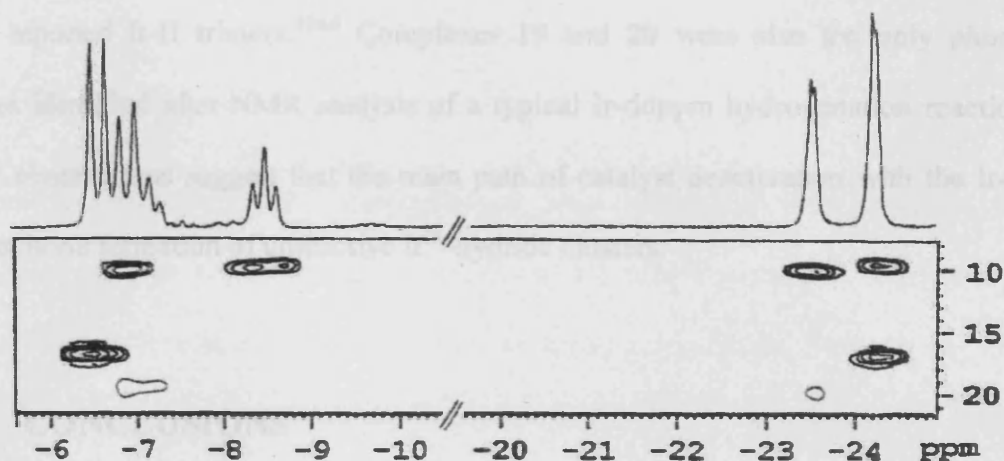


**Figure 5.3:** Section of the  $^1\text{H}$ ,  $^{31}\text{P}$  correlation for **19** and **20** showing the three hydride resonances associated with the signals at 17.6 and 9.9 ( $\delta_{\text{P}}$ ) for **19** and the hydride cross peaks owing to complex **20** (correlating with the signals at  $\delta_{\text{P}}$  9.9 and 20.3 ppm).

**Table 5.6:** NMR data for the iridium-hydride complexes **19** and **20**.<sup>[a]</sup>

Complex	$\delta(^{31}\text{P})$ <sup>[b]</sup>	Bridging H ( $^2J_{\text{PH}}$ , Hz)	Terminal H ( $^2J_{\text{PH}}$ , Hz)
<b>19</b>	17.6	-6.54 (d, 83.6, 2 $\text{H}_b$ )	-24.42 (m, $\approx 25$ , 2 $\text{H}_t$ )
	9.9	-8.48 (t, 67.1, 1 $\text{H}_b$ )	
<b>20</b>	20.3	-6.88 (d, 92.4, 3 $\text{H}_b$ )	-23.71 (m, $\approx 20$ , 3 $\text{H}_t$ )
	9.9	-7.12 (qt, 34.7, 1 $\text{H}_b$ )	

[a] in  $\text{d}^2$ -dichloromethane. [b] unresolved multiplets.



The  $^{31}\text{P}$  NMR spectrum of trimer **20** reveals two signals at 20.3 and 9.9 ppm showing unresolved *cis* P-P coupling. The correlated hydride resonances appear at -6.88 (d,  $^2J_{\text{PH}} = 92.4$ ), -7.12 (qt,  $^2J_{\text{PH}} = 34.7$ ) and -23.71 (m,  $^2J_{\text{PH}} \approx 20$ ) ppm, in 3/1/3 ratio; the two bridging hydride signals at  $\delta_{\text{H}}$  6.88 and 7.12 overlap with each other as shown in fig. 2. The magnitudes of the  $^2J_{\text{PH}}$  coupling constants are consistent with their assignment and close to other reported Ir-H trimers.<sup>16a,d</sup> Complexes **19** and **20** were also the only phosphorus species identified after NMR analysis of a typical Ir-ddppm hydrogenation reaction. The above observations suggest that the main path of catalyst deactivation with the Ir-ddppm system is *via* formation of unreactive  $\text{Ir}^{\text{III}}$ -hydride clusters.

### 5.3 CONCLUSIONS

Iridium complexes,  $[\text{Ir}(\text{ddppm})(\text{COD})]\text{BF}_4$  (**18a**) ,  $[\text{Ir}(\text{ddppm})(\text{COD})]\text{PF}_6$  (**18b**) were effectively synthesized and one of them characterized crystallographically. These complexes have shown to form efficient imine hydrogenation catalysts displaying good to high enantioselectivities without the need to operate at high hydrogen pressures for effective hydrogenation. The complexes are readily prepared, easily handled and air-stable. In contrast to the cationic complexes **18a-b**, the neutral  $[\text{Ir}(\text{COD})\text{Cl}]_2 - \text{ddppm}$  system was inactive in the hydrogenation of imines suggesting that cationic, unsaturated intermediates are preferred with the Ir-ddppm catalyst. This was further supported from the pronounced effect that different solvents had on the catalyst's activity. Coordinating solvents such as THF and methanol virtually deactivated the catalyst, whereas in 1,2-dichloroethane quantitative yields of the secondary amine were obtained. Our results indicate a

considerable potential for this class of catalysts especially for hydrogenations under atmospheric pressure, which merits further investigation. Based on our current understanding of the system, the negative effect of hydrogen pressure on the activity and selectivity of the catalyst has been attributed to the formation of inactive iridium-polyhydride species.

## 5.4 EXPERIMENTAL

**General considerations:** All manipulations were performed using standard Schlenk techniques under an argon atmosphere, except where otherwise noted. Complexes **18a** and **18b** after their formation were treated under aerobic conditions. Solvents of analytical grade and deuterated solvents for NMR measurements were distilled from the appropriate drying agents under N<sub>2</sub> immediately prior to use following standard literature methods.<sup>19</sup> Literature methods were employed for the synthesis of **ddppm**<sup>5</sup>, [Ir(COD)Cl]<sub>2</sub><sup>20</sup> All other reagents were used as received. Microanalyses were obtained from Warwick analytical service Ltd. Where reproducible microanalyses could not be obtained the NMR spectra of the samples suggested their purity was greater than 95%. NMR spectra were obtained on Bruker Avance AMX 400 or Jeol Eclipse 300 spectrometers and referenced to external TMS. HPLC analyses were performed on an Agilent 1100 series instrument. Mass spectra were obtained in ES (Electrospray) mode unless otherwise reported from the EPSRC Mass Spectrometry Service, Swansea University.

**[Ir(COD)<sub>2</sub>BF<sub>4</sub>]:** To a dichloromethane solution (2 ml) of [Ir(COD)Cl]<sub>2</sub> (0.135 g, 0.2 mmol) 1,5-cyclooctadiene (0.5 ml, 4.07 mmol), previously purified by passing through a

plug of silicagel, and 92.5 mg (0.475 mmol) of  $\text{AgBF}_4$  were added. The dark red slurry formed was stirred in the dark for 1.5 hours. After that time the white precipitate formed was filtered through celite and washed with  $\text{CH}_2\text{Cl}_2$  (2 ml). The solvent was concentrated and anhydrous  $\text{Et}_2\text{O}$  (15 ml) was added to precipitate the complex. The red solid formed was filtered, washed with anhydrous  $\text{Et}_2\text{O}$  (3 x 10ml) and dried (0.18 g, 91% yield).  $^1\text{H}$  NMR ( $\text{CDCl}_3$ , 250MHz):  $\delta$  2.43 (s, 8H;  $\text{CH}_2$ ); 5.18 (s, 4H; CH);  $^{13}\text{C}$  NMR (100 MHz,  $\text{CDCl}_3$ ):  $\delta$  30.55 ( $\text{CH}_2$ ), 100.09 (CH).

**Synthesis of  $[\text{Ir}(\text{COD})(\text{ddppm})]\text{BF}_4$ , 18a:** To a solution of  $[\text{Ir}(\text{COD})_2]\text{BF}_4$  (103 mg, 0.207 mmol) in  $\text{CH}_2\text{Cl}_2$  ddppm (100 mg, 0.207 mmol) was added. The resulted bright red solution was left stirring for 1 h and then the solvent was evaporated under vacuum. The resulting bright red slurry was washed twice with ether (20 ml) and dried (154 mg, 86%). The pure compound was obtained after slow diffusion of ether into a chloroform solution. The crystal structure of **18a** is in agreement with the spectroscopic data and confirms ddppm chelation to the metal centre.

$^1\text{H}$  NMR ( $\text{CDCl}_3$ , 400MHz) 1.67 (m, 2H,  $\text{H}_2\text{C}$  of cod), 2.07 (m, 4H,  $\text{H}_2\text{C}$  of cod), 2.32 (m, 2H,  $\text{H}_2\text{C}$  of cod) 3.53 (m, 2H, HC for cod), 3.98 (m, 2H,  $\text{CHPh}_2$ ), 4.12 (m, 2H,  $\text{CH}_2$ ), 4.24 (m, 2H,  $\text{CH}_2$ ) 4.32 (m, 2H, HC for cod), 5.38 (m, 2H, CCH), 7.2-7.5 (m, 20H);  $^{13}\text{C}$  NMR ( $\text{CDCl}_3$ , 100 MHz)  $\delta$  28.48 ( $\text{H}_2\text{C}$  for cod) 34.70 ( $\text{H}_2\text{C}$  for cod) 45.15 (m, 2C,  $\text{CH}_2$ ), 74.99 (m, 2C, CHP), 83.71 (m, 2C, CHP), 84.33 (HC for cod), 88.18 ( $\text{H}_2\text{C}$  for cod), 128.77 (m, 4C, Ar), 129.53 (m, 4C, Ar), 131.66 (s, 2C, Ar), 132.03 (s, 2C, Ar), 133.94 (m, 4C, Ar), 134.17 (m, 4C, Ar);  $^{31}\text{P}$  NMR ( $\text{CDCl}_3$ , 121MHz)  $\delta$  15.25 ; MS (accurate mass, ES+) calculated mass for  $[\text{M}-\text{BF}_4]^+$ : 783.2127, measured: 783.2130;  $[\text{M}-\text{BF}_4-\text{cod}]^+$ : 675.2.

**Synthesis of [Ir(COD)(ddppm)]PF<sub>6</sub>, 18b:** ddppm (88mg, 0.182mmol) and [Ir(COD)Cl]<sub>2</sub> (61 mg, 0.0912 mmol) were stirred for two hours in CH<sub>2</sub>Cl<sub>2</sub> (5 ml). <sup>31</sup>P NMR (121 MHz, D<sub>2</sub>O) -21.0 (br. s), 18.0 (m)]. The resulting orange solution was washed twice with an aqueous solution of NH<sub>4</sub>PF<sub>6</sub> (0.4 M, 5ml). Subsequently the bright red dichloromethane layer was collected, washed with water and dried over MgSO<sub>4</sub>. Filtration of the MgSO<sub>4</sub> and evaporation of the volatiles afforded **18b** in 88% yield (163 mg) after column chromatography using CH<sub>2</sub>Cl<sub>2</sub>/MeOH 99:1 as the eluent (R<sub>f</sub> = 0.2). <sup>31</sup>P NMR (121 MHz, CDCl<sub>3</sub>): δ = 15.3 (s, ddppm), -143.8 (septet, PF<sub>6</sub>). All other NMR data were identical to complex **18a**.

**General procedure for the preparation of imines:** 3 Å molecular sieves were activated in a schlenk by flaming them under vacuum and then a solution of acetophenone (3.5 ml, 30 mmol) and freshly distilled aniline (3.3g, 36 mmol) in dry benzene (20 ml) were added. After being stirred at room temperature for 1 day, the reaction mixture was filtered. Evaporation of the solvent *in vacuum* and distillation afforded N-(1-phenylethylidene)aniline (**9v**) (4.8 g, 82% as a pale orange solid). R<sub>f</sub>: 0.38 (90:10 PE:IPA). b.p.: 125°C/0.04mbar; m.p. 38-39°C. <sup>1</sup>H NMR (300 MHz, CDCl<sub>3</sub>): δ 2.22 (s, 3H, CH<sub>3</sub>), 6.77-6.81 (m, 2H, arom. CH), 7.05-7.10 (m, 1H arom. CH), 7.31-7.36 (m, 2H, arom. CH), 7.40-7.45 (m, 3H, arom. CH), 7.89-7.93 (m, 2H, arom. CH); <sup>13</sup>C NMR (75 MHz, CDCl<sub>3</sub>): δ 17.3 (CH<sub>3</sub>), 119.3, 123.2, 127.1, 128.3, 128.9, 130.4 (arom. CH), 139.4, 151.7 (arom. C), 165.4 (C=N); MS (70 eV, EI): m/z (%): 195 (55) [M<sup>+</sup>], 180 (100) [(M-CH<sub>3</sub>)<sup>+</sup>], 118 (11) [(M-C<sub>6</sub>H<sub>5</sub>)<sup>+</sup>], 77 (61) [C<sub>6</sub>H<sub>5</sub><sup>+</sup>]; C<sub>14</sub>H<sub>13</sub>N (195.26). IR (CHCl<sub>3</sub>): 1639 cm<sup>-1</sup> (C=N).

3 Å molecular sieves were activated in a schlenk by flaming them under vacuum and then a solution of acetophenone (11.5 ml, 100 mmol) and benzylamine (13.5 ml, 120 mmol) in dry toluene (40 ml) were added into it. After being stirred at room temperature for 3 days, the reaction mixture was filtered. Evaporation of the solvent *in vacuum* and distillation afforded **N-(1-phenylethylidene)benzylamine (11<sub>v</sub>)**: (12.4 g, 60% as a pale yellow solid). Rf: 0.46 (90:10 PE:IPA) C<sub>15</sub>H<sub>15</sub>N (209.9); m.p. 39-41°C; <sup>1</sup>H NMR (300 MHz, CDCl<sub>3</sub>): δ 2.31 (s, 3H, CH<sub>3</sub> (major isomer)), 2.37 (t, 3H, CH<sub>3</sub> (minor isomer)), 4.42 (s, 2H, H<sub>2</sub>CPh (minor isomer)), 4.73 (s, 2H, H<sub>2</sub>CPh (major isomer)), 7.20-7.45(m, 8H, arom. CH), 7.82-7.91 (m, 2H, arom. CH): (E)/(Z) isomer ratio 28:1; <sup>13</sup>C NMR (75 MHz, CDCl<sub>3</sub>): δ 15.9 (CH<sub>3</sub>), 55.7 (CH<sub>2</sub>), 126.6, 126.8, 127.7, 128.2, 128.4, 129.6 (arom. CH), 140.6, 141.7 (arom. C), 166 (C=N); MS (70 eV, EI): m/z (%): 209 (14) [M<sup>+</sup>], 194 (2) [(M- CH<sub>3</sub>)<sup>+</sup>], 91 (100) [C<sub>7</sub>H<sub>7</sub><sup>+</sup>]; IR (CHCl<sub>3</sub>): 1631 cm<sup>-1</sup> (C=N).

**General procedure for the Ir-catalyzed enantioselective hydrogenation for imines:** A glass vessel (100 ml) with a magnetic stirring bar was charged in air with **N-(1-phenylethylidene)aniline (9<sub>v</sub>)** (195 mg, 1 mmol) and [Ir(dddppm)(COD)]BF<sub>4</sub> (9 mg, 0.01mmol) and these solids were degassed and dissolved in dry CH<sub>2</sub>Cl<sub>2</sub> (5 ml). The reaction mixture was stirred for 24 h at room temperature under 1 bar H<sub>2</sub>. After evaporation of the solvent, the product was purified by a chromatographic column with 100% of hexane affording **(R)-N-phenyl-1-phenylethylamine, 10<sub>v</sub>**; % *ee*'s were calculated based on chiral HPLC (Daicel Chiralcel OD, 250 x 4.6 mm, 220nm, 0.5ml/min, hexane/2-propanol 90:10; t<sub>R</sub> = 11.59 (S), t<sub>R</sub> = 13.43 (R) min: <sup>1</sup>H NMR (300 MHz, CDCl<sub>3</sub>) δ 1.51 (d, J = 6.7 Hz, 3H, CH<sub>3</sub>), 4.01 (brs, 1H, NH), 4.48 (q, J = 6.7 Hz, 1H, CH), 6.49-6.52 (m, 2H, arom. CH),

6.61-6.66 (m, 1H, CH), 7.05-7.11 (m, 2H, arom. CH), 7.18-7.38 (m, 5H, arom. CH);  $^{13}\text{C}$  NMR (75 MHz,  $\text{CDCl}_3$ )  $\delta$  25.0 ( $\text{CH}_3$ ), 53.4 (CH), 113.3, 117.2, 125.8, 126.8, 128.6, 129.1 (arom. CH), 145.2, 147.3 (arom. C); IR ( $\text{CHCl}_3$ )  $3431\text{ cm}^{-1}$  (N-H); m/z (%): 197 (46) [ $\text{M}^+$ ], 182 (100) [ $(\text{M} - \text{CH}_3)^+$ ], 105 (69) [ $\text{C}_8\text{H}_9^+$ ], 77 (40) [ $\text{C}_6\text{H}_5^+$ ].

**N-benzyl-1-phenylethylamine:** This was prepared by following the same hydrogenation protocol.  $\text{C}_{15}\text{H}_{17}\text{N}$  (211.31): colourless oil: b.p  $85^\circ\text{C}/0.1\text{ mbar}$ ;  $^1\text{H}$  NMR (300 MHz,  $\text{CDCl}_3$ )  $\delta$  1.36 (d,  $J = 6.6\text{ Hz}$ , 3H,  $\text{CH}_3$ ), 1.60 (s, 1H, NH), 3.59 (d,  $J = 13.2\text{ Hz}$ , 1H,  $\text{H}_2\text{CPh}$ ), 3.66 (d,  $J = 13.2\text{ Hz}$ , 1H,  $\text{H}_2\text{CPh}$ ) 3.80 (q,  $J = 6.6\text{ Hz}$ , 1H, HC), 7.23-7.35 (m, 10H, arom. CH);  $^{13}\text{C}$  NMR (75 MHz,  $\text{CDCl}_3$ )  $\delta$  24.5 ( $\text{CH}_3$ ), 52 ( $\text{CH}_2$ ), 57.8 (CH) 126.7, 126.8, 126.9, 128.1, 128.4, 128.5 (arom. CH), 140.7, 145.6 (arom. C); IR ( $\text{CHCl}_3$ )  $3320\text{ cm}^{-1}$  (N-H); m/z (%): 212 (100) [ $(\text{M}+1)^+$ ], 196 [ $(\text{M} - \text{CH}_3)^+$ ], 91 (11) [ $\text{C}_7\text{H}_7^+$ ].

**General procedure for the preparation of racemic imines:** 0.1g (0.5 mmol) of N-(1-phenylethylidene)aniline (**10v**) were dissolved in THF (1ml) and followed by the addition of zinc borohydride (1 ml, 0.5 M) was added into it. The colour changes from yellow-orange to green. The mixture was stirred for 1 day and after decomposed by careful drop wise addition of water, until no further evolution of gas was observed. Then, it was extracted with ether (3 x 20ml). The organic layers were combined and washed with brine and dried over  $\text{Na}_2\text{SO}_4$ . The pure amine was obtained after Kugelrohr distillation as a colourless oil (0.05 g, 55% yield).

More mild conditions were used for the preparation of the racemic product of N-(1-phenylethylidene)benzylamine. 0.5 mmol of the imine was dissolved in MeOH and

1mmol of NaBH<sub>4</sub> was added into it. The mixture was stirred for 1 h and then filtered through silica to obtain the crude product.

**Reaction of 18b with H<sub>2</sub>:** A solution of [Ir(COD)(ddppm)]PF<sub>6</sub> (45 mg, 0.05 mmol) and NH<sub>4</sub>PF<sub>6</sub> (163 mg, 1.00 mmol) in 2 ml of dry methanol was stirred under an atmospheric pressure of hydrogen for one hour. Subsequently the vessel was isolated and left stirring further for one day. During the course of the reaction a yellow microcrystalline powder precipitated. The formed solid was collected via filtration, washed with Et<sub>2</sub>O (2 x 5 mL) and dried under vacuum. NMR analyses showed the formation of complexes **19** and **20**. Data for complex **19**: <sup>1</sup>NMR (500MHz, CDCl<sub>3</sub>):  $\delta$  = -24.42 (m, <sup>2</sup>J(P,H)  $\approx$  25 Hz, 2H; H<sub>t</sub>), -8.48 (t, <sup>2</sup>J(P,H) = 67.1 Hz, 1H; H<sub>b</sub>), -6.54 (d, <sup>2</sup>J(P,H) = 83.6 Hz, 2H; H<sub>b</sub>), 3.0-4.1 (m, 6H), 5.24 (m, 2H; CCH), 6.4-8.5 (m, 20H, ArH); <sup>13</sup>C NMR (125 MHz, CDCl<sub>3</sub>)  $\delta$  = 43.7 (m, 2C; CH<sub>2</sub>), 73.8 (m, 2C; CHP), 84.2 (m, 2C; CHP), 128.5 (m, 4C; Ar), 131.1 (m, 2C; Ar), 133.4 – 134.5 (m, 6C; Ar); <sup>31</sup>P NMR (121MHz, CDCl<sub>3</sub>):  $\delta$  = 9.9 (m), 17.6 (m); IR (KBr)  $\nu$  = 2215 cm<sup>-1</sup> br, m (Ir-H); 1966, 1889, 1810 br, w (Ir-H); MS (ES<sup>+</sup>) *m/z* (%), [M-PF<sub>6</sub>]<sup>+</sup>: 1353.58 (100.0%); MS (accurate mass, ES<sup>+</sup>) *m/z* (%), calculated mass for [M-(H+PF<sub>6</sub>)]<sup>2+</sup>: 676.1339; measured: 676.1325. Data for complex **20**: <sup>1</sup>NMR (500MHz, CDCl<sub>3</sub>):  $\delta$  = -23.71 (m, <sup>2</sup>J(P,H)  $\approx$  20 Hz, 3H; H<sub>t</sub>), -7.12 (qt, <sup>2</sup>J(P,H) = 35 Hz, 1H; H<sub>b</sub>), -6.88 (d, <sup>2</sup>J(P,H) = 92.4 Hz, 3H; H<sub>b</sub>), 3.0-4.1 (m, 6H), 5.24 (m, 2H; CCH), 6.4-8.5 (m, 20H, ArH); <sup>31</sup>P NMR (121MHz, CDCl<sub>3</sub>):  $\delta$  = 9.9 (m), 20.3 (m).

<sup>1</sup> A. Hirao, S. Itsuno, S. Nakaham, N. Yamazaki, *J. Chem. Soc. Chem. Commun*, 1981, 315.

- <sup>2</sup> E.N. Jacobsen, A. Pfaltz, H. Yamamoto, *Comprehensive Asymmetric Catalysis I*, Ed. Springer, 1999, pg. 260-261.
- <sup>3</sup> (a) S. Vargas, M. Rubio, A. Suarez, A. Pizzano, *Tetrahedron Lett.*, 2005, 46 (12) 2049-2052; (b) P. Maire, S. Deblon, F. Breher, J. Geier, C. Bohler, H. Ruegger, H. Schonberg, H. Grutzmacher, *Chem. Eur. J.*, 2004, 10 (17), 4198-4205; (c) C. Blanc, F. Agbossou-Niedercorna, G. Nowogrocki, *Tetrahedron: Asymmetry*, 2004, 15, 2159-2163; (d) K. Fujita, T. Fujii, R. Yamaguchi, *Org. Lett.*, 2004, 6, 3525-3528; (e) W. B. Wang, S. M. Lu, P. Y. Yang, *J. Am. Chem. Soc.*, 2003, 125 (35), 10536-10537; (f) M. T. Reetz, T. Sell; R. Goddard, *Chimia*, 2003, 57 (5), 290-292; (g) X. B. Jiang, A. J. Minnaard, B. Hessen, B. N. Feringa, A. L. L. Duchateau, J. G. O. Andrien, J. A. F. Boogers and J. G. de Vries, *Org. Lett.*, 5 (9), 1503-1506, 2003. (h) D. Xiao, X. Zhang, *Angew. Chem. Int. Ed.*, 2001, 40 (18), 3425; (i) A. Martorell, C. Claver, E. Fernandez, *Inorg. Chem. Comm.* 2000, 3 (3), 132-135; (j) K. Satoh, M. Inenaga, K. Kanai, *Tetrahedron: Asymmetry*, 1998, 9 (15), 2657-2662; (k) P. Schnider, G. Koch, R. Prétôt, G. Wang, F. M. Bohnen, C. Krüger and A. Pfaltz, *Chem. Eur. J.*, 1997, 3 (6), 887-892; (l) K. Tani, J. Onouchi, T. Yamagata, Y. Kataoka, *Chem. Lett.*, 1995, 10, 955-956.
- <sup>4</sup> a) M.T. Reetz, E.W. Bottenmuller, R. Goddard, M. Pasto, *Tetrahedron Lett.*, 1999, 40, 4977; b) R. B. Bedford, P. A. Chaloner, P. B. Hitchcock, G. Lopez, F. Momblona, J. L. Serrano, *An. Quim.*, 1996, 92, 354.
- <sup>5</sup> (a) C. Carcedo, A. Dervisi, I.A. Fallis, *Chem. Comm*, 2004, 1236. (b) The largest bite angle observed within the ddppm complexes is 103.52 (9)° for Pt (ddppm)Cl<sub>2</sub>; unpublised results.
- <sup>6</sup> X-Seed – A software tool for supramolecular crystallography. *J. Supramol. Chem.*, 2001, 1, 189-191.
- <sup>7</sup> (a) S. P. Smidt, N. Zimmermann, M. Studer, A. Pfaltz, *Chem. Eur. J.*, 2004, 10, 4685-4693; (b) D. G. Blackmond, A. Lightfoot, A. Pfaltz, T. Rosner, P. Schnider, N.



---

Zimmermann, *Chirality*, 2000, 12, 442-449; (c) Pfaltz A; Blankenstein J; Hilgraf R; Hormann E; McIntyre S; Menges F; Schonleber M; Smidt SP; Wustenberg B; Zimmermann N, *Adv. Synth. Catal.*, 2003, 345 (1-2), 33-43; (d) G. P. Xu, S.R. Gilbertson, *Tetrahedron Lett.*, 2003, 44, 953-955; (e) F. Menges, A. Pfaltz, *Adv. Synth. Catal.*, 2002, 344 (1), 40-44.

<sup>8</sup> S. M. Joseph Samec, J.-E. Bäckvall, *Chem. Eur. J.*, 2002, 8, 13, 2955-2961.

<sup>9</sup> V. Herrera, B. Muñoz, V. Landaeta, N. Canudas, *J. Mol. Catal. A-Chem*, 2001, 174 (1-2), 141-149.

<sup>10</sup> (a) H-U. Blaser, W. Brieden, B. Pugin, F. Spindler, M. Suder, A. Togni, *Top. Catal.*, 2002, 19 (1), 3-16; (b) H.-U. Blaser, F. Spindler, *Top. Catal.*, 1997, 4 (3-4), 275-282.

<sup>11</sup> H.-U. Blaser, H.-P. Buser, R. Häusel, H.-P. Jalett and F. Spindler, *J. Organomet. Chem.*, 2001, 621 (1-2), 34-38.

<sup>12</sup> R. Sablong, J.A.Osborn, *Tetrahedron: Asymmetry*, 1996, 7 (11), 3059-3062.

<sup>13</sup> (a) Sturm T, Weissensteiner W, Spindler F, *Organometallics* 21 (9), 1766-1774, 2002; (b) Cahill JP; Lightfoot AP; Goddard R; Rust J; Guiry PJ, *Tetrahedron: Asymmetry*, 1998, 9 (24), 4307-4312.

<sup>14</sup> (a) G.X. Zhu, XM Zhang, *Tetrahedron: Asymmetry*, 9 (14), 2415-2418, 1998; (b).

<sup>15</sup> R. Dorta, D. Broggini, R. Stoop, H. Ruegger, F. Spindler, A. Togni, *Chem. Eur. J.*, 2004, 10, 267-278.

<sup>16</sup> a) S. P. Smidt, A. Pfaltz, E. Martínez-Viviente, P.S. Pregosin, A. Albinati, *Organometallics*, 2003, 22(5), 1000-1009; b) H. H. Wang, A. L. Cassalnuovo, B. J.

Johnson, A. M. Muetting, L. H. Pignolet, *Inorg.Chem.*, 1988, 27, 325 - 331; c) A. L. Casalnuovo, L. H. Pignolet, J. W. A. van der Velden, J. J. Bour, J. J. Steggerda, *J. Am. Chem. Soc.*, 1983, 105, 5957-5958; d) H. H. Wang, L. H. Pignolet, *Inorg.Chem.*, 1980, 19, 1470 - 1480; e) D. F. Chodosh, R. H. Crabtree, *J. Organomet. Chem.*, 1978, 161, C67 - C70; f) R. H. Crabtree, H. Felkin, G. E. Morris, T. J. King, J. A. Richards, *J. Organomet. Chem.*, 1976, 113, C7 - C9.

<sup>17</sup> K. Tani, A. Iseki, T. Yamagata, *Angew. Chem., Int. Ed.*, 1998, 37, 3381-3383.

<sup>18</sup> a) M. A. Esteruelas, M. P. Garcia, F. J. Lahoz, M. Martin, J. Modrego, E. Oflate, L. A. Oro, *Inorg. Chem.*, 1994, 33, 3473-3480; b) J. D. Feldman, J. C. Peters, T. D. Tilley, *Organometallics*, 2002, 21, 4050-4064.

<sup>19</sup> D. D. Perrin and W. F. A. Amarego, *Purification of Laboratory Chemicals*, Pergamon, Oxford, 1988.

<sup>20</sup> J. L. Herde, J.C. Lambert, C.V. Senoff, *Inorg. Synth.* 15 (1974), 18.

